ZooKeys 725: 1–15 (2017)
doi: 10.3897/zookeys.725.15059
http://zookeys.pensoft.net

RESEARCH ARTICLE

A peer-reviewed open-access journal
ZooKeys
Launched to accelerate biodiversity research

The first record of Telemidae from Kenya, with the description of two new species (Arachnida, Araneae)

Yang Song[1], Huifeng Zhao[2], Yufa Luo[1], Grace M. Kioko[3], Esther N. Kioko[3], Shuqiang Li[2,4]

1 *School of Life and Environment Sciences, Gannan Normal University, Ganzhou, Jiangxi 341000, China* **2** *Institute of Zoology, Chinese Academy of Sciences, Beijing 100101, China* **3** *Zoology Department, National Museums of Kenya, Box 40658-00100, Nairobi, Kenya* **4** *University of the Chinese Academy of Sciences, Beijing 100049, China*

Corresponding authors: *Yufa Luo* (lyf223@126.com); *Esther N. Kioko* (ekioko@museums.or.ke); *Shuqiang Li* (lisq@ioz.ac.cn)

Academic editor: *Cor Vink* | Received 14 July 2017 | Accepted 18 November 2017 | Published 29 December 2017

http://zoobank.org/A7963434-A52E-4A2E-9715-2E59C709C0C6

Citation: Song Y, Zhao H, Luo Y, Kioko GM, Kioko EN, Li S (2017) The first record of Telemidae from Kenya, with the description of two new species (Arachnida, Araneae). ZooKeys 725: 1–15. https://doi.org/10.3897/zookeys.725.15059

Abstract

Two new species of Telemidae from Kenya are described: *Guhua kakamegaensis* Zhao & Li, **gen. et sp. n.**, *Apneumonella taitatavetaensis* Zhao & Li, **sp. n.** Holotypes are deposited in the National Museum of Kenya in Nairobi, and all paratypes are deposited in the Institute of Zoology, Chinese Academy of Sciences in Beijing. A distribution map of Telemidae found in Kenya is presented.

Keywords

East Africa, Haplogynae, new record, taxonomy

Introduction

Telemidae Fage, 1913 is a relatively small family consisting of nine genera and 69 species (World Spider Catalog 2017), which are unevenly distributed in rainforest and karst regions of tropical Africa, Europe, East and Southeast Asia and the New World. The majority of the species are reported to occur in Southwest China and Southeast Asia, especially *Telema* Simon, 1882 and *Pinelema* Wang & Li, 2012, but 20 species of

this family are fragmentally distributed in other regions of the world. There are three known genera of Telemidae in Africa: *Apneumonella* Fage, 1921, *Cangoderces* Harington, 1951 and *Seychellia* Saaristo, 1978. *Apneumonella* is composed of two species, the type species is from Tanzania (Fage 1921), and the other described species is found in Sumatra, Indonesia (Brignoli 1977). All five species of *Cangoderces* were discovered in western and southern African countries: Cameroon, Ivory Coast and South Africa (Harington 1951, Baert 1985, Wang and Li 2011). The genus *Seychellia* is composed of five species, which occur in Seychelles, Cameroon, Ivory Coast and China (Saaristo 1978, Brignoli 1980, Baert 1985, Lin and Li 2008, Wang and Li 2011). In this paper, we present the first report of Telemidae in Kenya. The new monotypic genus *Guhua* gen. n. is established based on new well-defined morphological characters.

Materials and methods

All specimens were examined and measured using a Leica M205 C stereomicroscope. The bodies, male palps, and receptacles were photographed using an Olympus C7070 digital camera mounted on an Olympus SZX12 stereomicroscope. Images were combined using Helicon Focus version 6.7.1 image stacking software (http://www.heliconsoft.com). Further morphological details were observed under an Olympus BX41 compound light microscope. The left palps of the male were photographed with a Hitachi SU8010 Scanning Electron Microscope. Female genitalia were removed and treated in lactic acid before being photographed. All measurements are reported in millimeters. Leg measurements are shown as: total length (femur, patella, tibia, metatarsus, and tarsus). The following abbreviations are used in the figures:

Em	embolus;	**SO**	secretory orifice;
Re	receptacle;	**Ta**	tegular apophysis.
Rs	receptacle scape;		

Type specimens were deposited in the National Museum of Kenya (**NMK**) in Nairobi and the Institute of Zoology, Chinese Academy of Sciences (**IZCAS**) in Beijing, China.

Systematics

Family Telemidae Fage, 1913

Genus *Guhua* Zhao & Li, gen. n.
http://zoobank.org/5F7D0378-27F2-47DA-B20A-EAA7449091A7

Type species. *Guhua kakamegaensis* sp. n. from Kakamega County, Kenya.

Etymology. The generic name is taken from the Chinese Pinyin 'gǔhuà' meaning sclerotization, referring to the sclerotized receptacle of females. The gender is feminine.

Diagnosis. The new genus can be diagnosed by the following characters: males can be distinguished by an hourglass-shaped lorum (Fig. 1A), extended lateral plates on the anterodorsal surface of the abdomen, two globular apophyses between the lorum and lateral plates (in contrast to a membranous structure in other genera, except *Jocquella leopoldi* Baert, 1980); the male bulb has no tegular apophysis on the middle-upper part of the bulb (Figs 1C–D, 2C–D) (vs. the tegular apophysis or apophyses present in other African genera), no cymbial apophysis on cymbium (Figs 1C, 2A) (vs. a cymbial apophysis in *Pinelema*) or belt-shaped glands on legs (vs. plate-shaped glands in *Telema*); embolus is nearly cylindrical (Figs 1C–D, 2A–B), arising from the anterior surface of the palpal bulb (in most other genera, the embolus is conical, tube-shaped or shaped otherwise with a broad base and rather narrow apex, arising from the apical side of the bulb). Females can be distinguished by the sclerotized and arched receptacle (Fig. 3C–D), as no sclerotized receptacle have been reported in other genera.

Description. See species description.

Species composition. *Guhua kakamegaensis* sp. n.

Distribution. Known only from Kenya.

Note. It is presumed that this new genus was the first record of a sclerotized receptacle in Telemidae. In *Cangoderces lewisi* Harington, 1951, the receptacle was also described as having a relatively sclerotized tube (Brignoli 1978). However, that description is considered to be inaccurate, because the endogyne is similar to most telemids' receptacle and has usually been described as membranous rather than sclerotized.

***Guhua kakamegaensis* Zhao & Li, sp. n.**

http://zoobank.org/A992EFDF-7514-442E-B881-524A79DD0526

Figs 1–3, 7–8, 10

Type material. Holotype ♂ (NMK): Kenya: Kakamega County: Kakamega Town, Kakamega Forest, N00°21.13', E34°52.65', 1542 m, 5.VIII.2016, G.M. Kioko, Q.Y. Zhao & Z.Y. Yao. **Paratypes:** 1♂ and 3♀ (IZCAS), same data as holotype.

Etymology. The specific name refers to the type locality; adjective.

Diagnosis. See genus diagnosis.

Description. Male (holotype). Total length 1.68. Carapace 0.65 long, 0.58 wide. Abdomen 1.01 long, 0.70 wide. Carapace yellow, with dark spots in the mid-thoracic area and distinct radial stripes around it (Fig. 1A). Chelicerae and legs yellow, with dark brown pattern. Six eyes, all well-developed with black rings around them, clypeus 0.08 long. Cheliceral promargin with two large teeth and four tiny granulous denticles, retromargin with four triangular denticles. Labium, endites, and sternum dark brown. Leg measurements: I 4.56 (1.28, 0.22, 1.41, 1.01, 0.64); II 3.98 (1.18, 0.21, 1.19, 0.85, 0.55); III 3.01 (0.90, 0.20, 0.84, 0.63, 0.44); IV 3.97 (1.20, 0.17, 1.14, 0.90, 0.56). Two trichobothria and one seta on tibia IV (Fig. 8A). Tibial glands distinct and

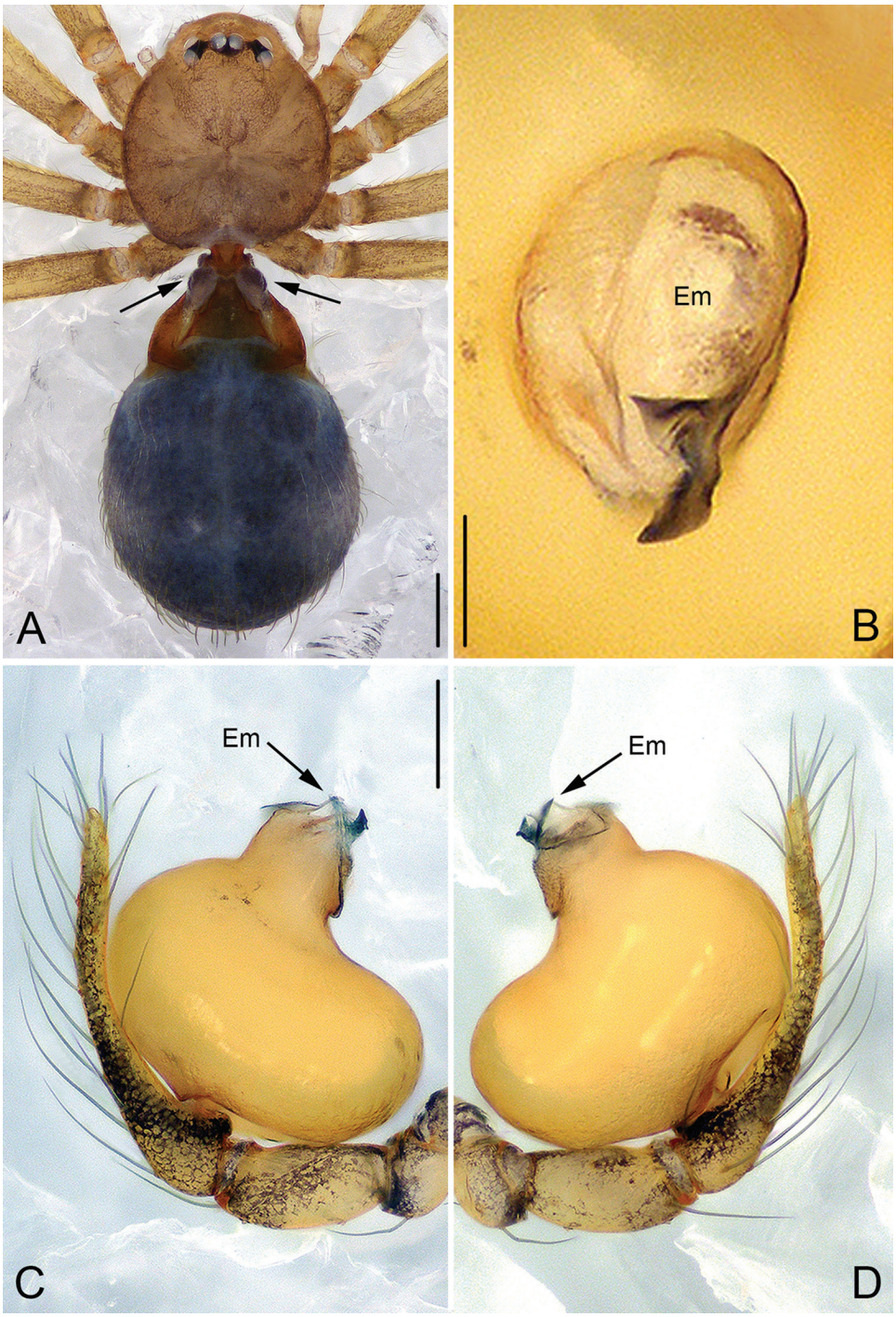

Figure 1. *Guhua kakamegaensis* sp. n., male holotype. **A** Habitus, dorsal view **B** Embolus, apical view **C** Palp, prolateral view **D** Palp, retrolateral view. Scale bars: 0.2 mm (**A**), 0.02 mm (**B**), 0.1 mm (**C, D**). Em, embolus.

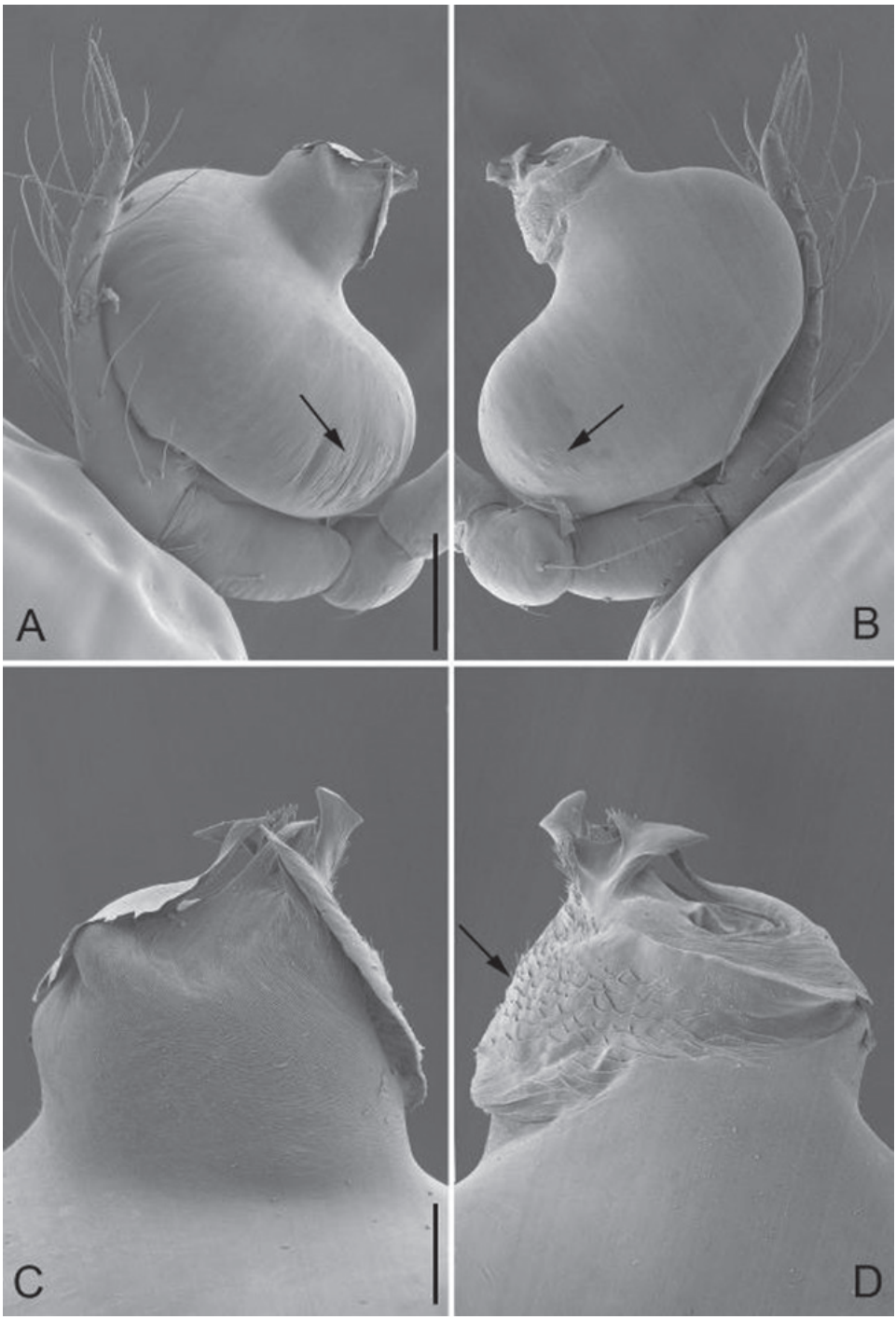

Figure 2. *Guhua kakamegaensis* sp. n., male paratype. **A** Palp, prolateral view **B** Palp, retrolateral view **C** Embolus, prolateral view **D** Embolus, retrolateral view. Scale bars: 0.1 mm (**A, B**), 0.03 mm (**C, D**). Arrows indicate special structures of embolus and bulb.

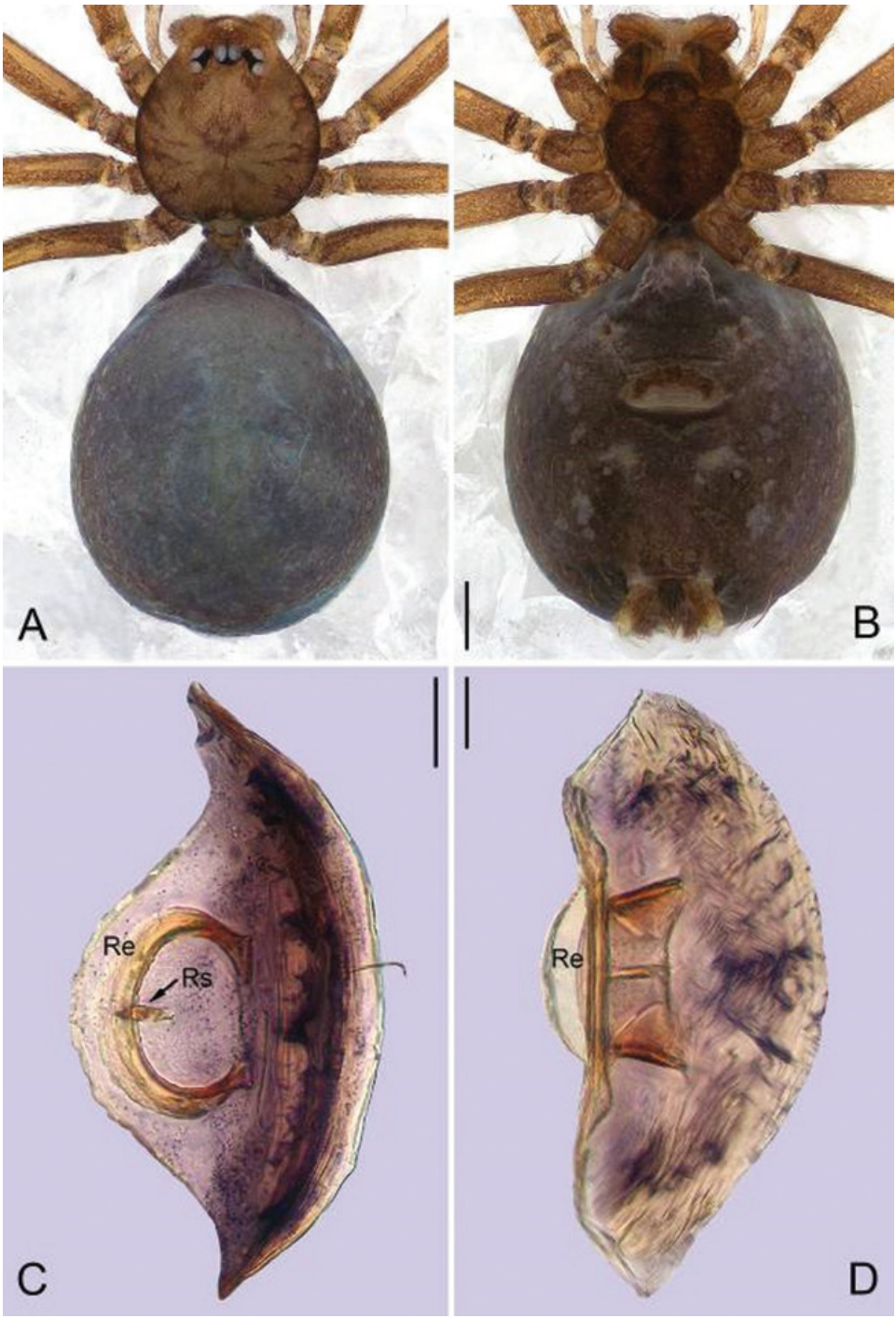

Figure 3. *Guhua kakamegaensis* sp. n., female paratype. **A** Habitus, dorsal view **B** Habitus, ventral view **C** Genitalia, anterior view **D** Genitalia, lateral view. Scale bars: 0.2 mm (**A, B**), 0.05 mm (**C**), 0.02 mm (**D**). Re, receptacle; Rs, receptacle scape.

belt-shaped (Fig. 8B–C), the arrangement of secretory orifices is wave-shaped within a smooth striped tegument (Fig. 8B). Lorum and lateral abdominal plates distinct (Fig. 1A). Abdomen dark green, with dense hairs (Fig. 1A).

Palp: tibia 1.8 times longer than patella, cymbium bent and slender and 2.4 times longer than tibia. Bulb kidney shaped, with a few wrinkles and papillae basally (arrowed on Fig. 2A–B). Embolus cylindrical, with a complex membranous apex (Figs 1B–D, 2A–D), its retrolateral surface rough and covered by many thorn-shaped structures (arrowed on Fig. 2D).

Female. Total length 1.82. Carapace 0.61 long, 0.56 wide. Abdomen 1.14 long, 0.95 wide. Eyes encircled by black rings, clypeus 0.08 long. Other coloration and pattern same as in male (Fig. 3A–B). Abdomen dark brown, with few hairs. Leg measurements: I 3.92 (1.11, 0.19, 1.21, 0.82, 0.59); II 3.44 (0.98, 0.19, 1.05, 0.71, 0.51); III 2.57 (0.75, 0.17, 0.70, 0.53, 0.42); IV 3.62 (1.09, 0.19, 1.06, 0.77, 0.51). Receptacle arch-shaped, sclerotized, with a sclerotized scape arising inward mesally (Fig. 3C–D).

Habitat. Leaf litter in rainforest.

Distribution. Known only from the type locality (Fig. 10).

Genus *Apneumonella* Fage, 1921

Type species. *Apneumonella oculata* Fage, 1921: 528, figs II 1–4.

Apneumonella taitatavetaensis Zhao & Li, sp. n.

http://zoobank.org/2AC0811D-4EBC-494D-917F-0F3ECCB7221E
Figs 4–7, 9, 10

Type material. Holotype ♂(NMK). Kenya: Taita-Taveta County: Wundanyi Town, Ngangao Forest, S03°21.30', E38°20.41', 1821 m, 23.VII.2016, G.M. Kioko, Q.Y. Zhao & Z.Y. Yao. **Paratypes.** 1♂ and 3♀ (IZCAS), same data as holotype.

Etymology. The specific name refers to the type locality; adjective.

Diagnosis. This new species is similar to *A. oculata* but females can be distinguished by their globular abdomen with two outgrowths near the carapace (arrowed on Fig. 6A), which are not present in *A. oculata*. Another difference is that the diameter of the receptacle is four times the diameter of the insemination duct (Fig. 6C) as compared to that of *A. oculata*, whose receptacle is twice the diameter of the insemination duct. The ocular quadrangle width is half of the carapace width while that of *A. oculata* is one-third of the carapace width.

Description. Male (holotype). Total length 1.06. Carapace 0.45 long, 0.41 wide. Abdomen 0.58 long, 0.46 wide. Carapace reddish brown, with dark spots on the mid-thoracic area and obscure radial stripes around it (Fig. 4A). Six eyes, well-developed, encircled by black rings, clypeus 0.05 long. Chelicerae, labium, endites, sternum and legs yellow, with dark brown pattern. Cheliceral promargin with 2 big

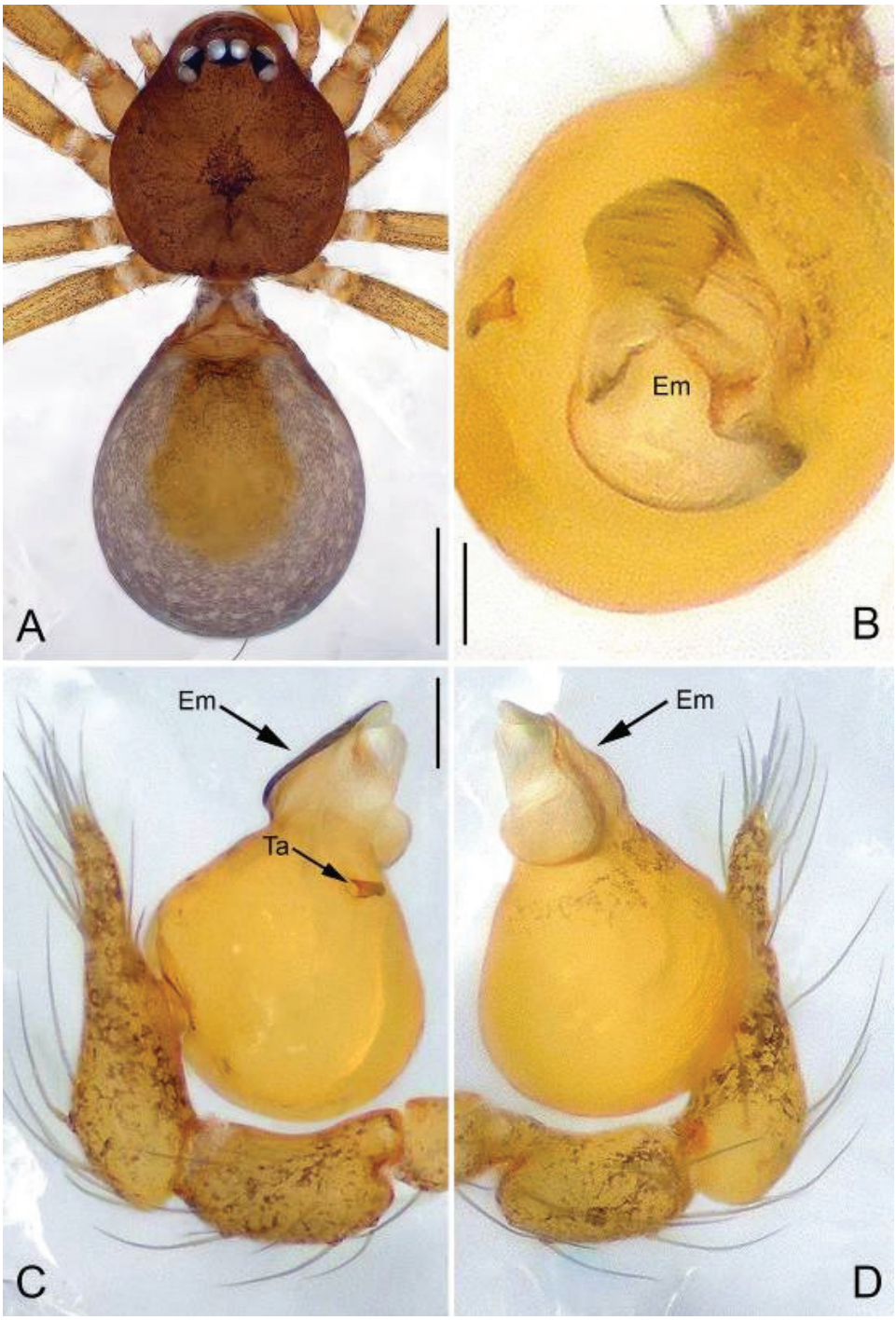

Figure 4. *Apneumonella taitatavetaensis* sp. n., male holotype. **A** Habitus, dorsal view **B** Bulb, apical view **C** Palp, prolateral view **D** Palp, retrolateral view. Scale bars: 0.2 mm (**A**), 0.02 mm (**B**), 0.1 mm (**C, D**). Em, embolus; Ta, Tegular apophysis.

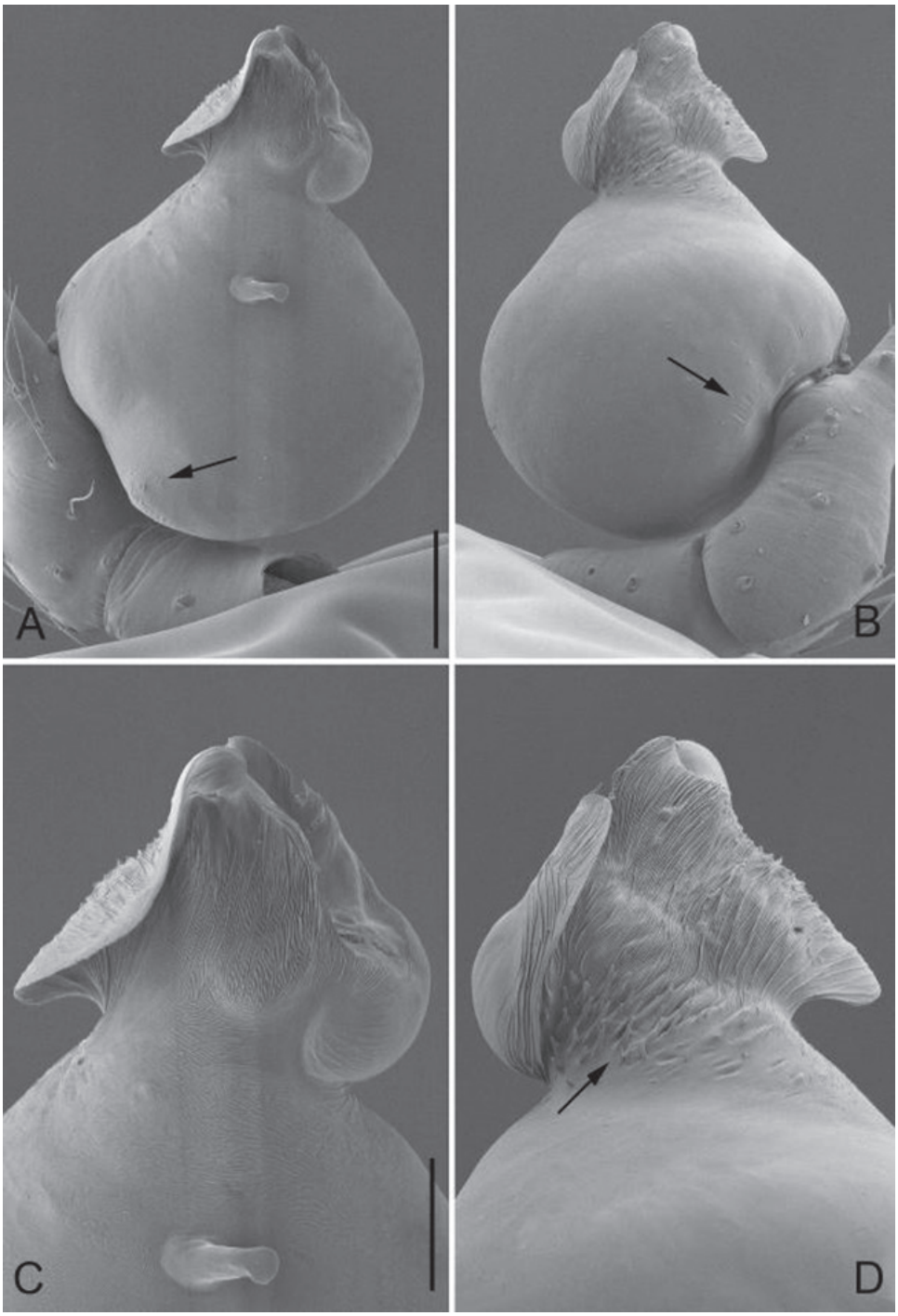

Figure 5. *Apneumonella taitatavetaensis* sp. n., male paratype. **A** Palp, prolateral view **B** Palp, retrolateral view **C** Embolus, prolateral view **D** Embolus, retrolateral view. Scale bars: 0.05 mm (**A, B**), 0.03 mm (**C, D**). Arrows indicate special structures of the embolus and bulb.

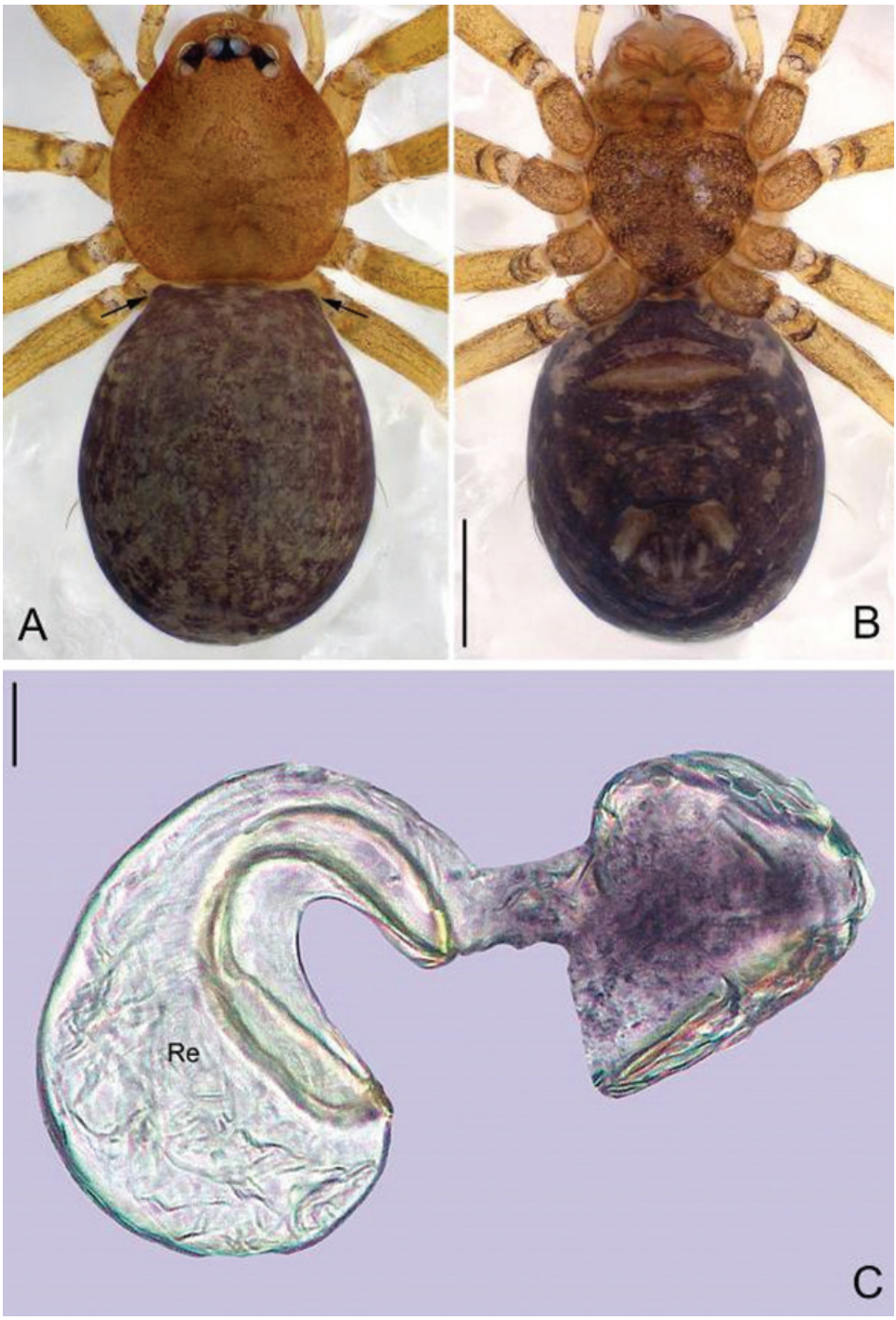

Figure 6. *Apneumonella taitatavetaensis* sp. n., female paratype. **A** Habitus, dorsal view **B** Habitus, ventral view **C** Genitalia, lateral view. Scale bars: 0.2 mm (**A, B**), 0.02 mm (**C**). Re, receptacle. Arrows indicate apophyses of female abdomen.

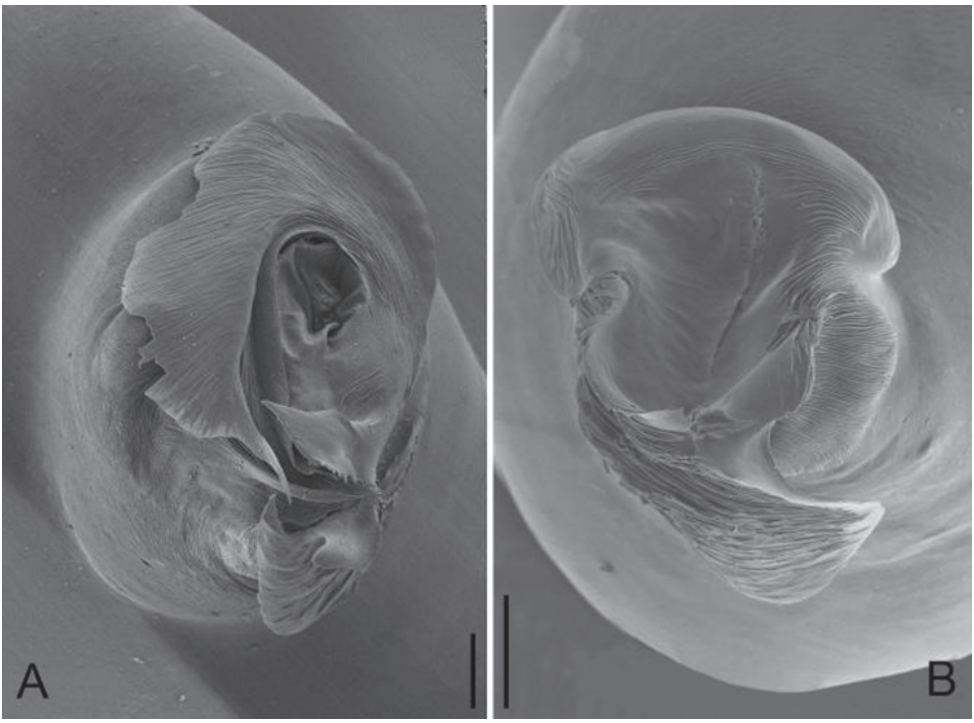

Figure 7. Apical view of embolus. **A** *Guhua kakamegaensis* sp. n. **B** *Apneumonella taitatavetaensis* sp. n. Scale bars: 0.02 mm (**A, B**).

teeth and 5 granulous denticles and retromargin with 4 triangular denticles. Leg measurements: I 2.10 (0.62, 0.16, 0.59, 0.38, 0.35); II 1.75 (0.53, 0.12, 0.46, 0.34, 0.30); III 1.41 (0.40, 0.10, 0.33, 0.34, 0.24); IV 1.83 (0.54, 0.11, 0.50, 0.38, 0.30). Secretory orifices of tibial glands round (Fig. 9B–C). Abdomen light brown with a yellow spot centrally.

Palp: tibia thick, 1.7 times longer than patella; cymbium straight and thick, 1.8 times longer than tibia. Bulb ovoid, with a finger-like tegular apophysis on its middle-upper part and several wrinkles basally (arrowed on Fig. 5A–B). The bulb apex extends into a nearly conical embolus (Figs 4B–D, 5A–D), the surface of the embolus is rough with dense spine-like structures (arrowed on Fig. 5D).

Female. Total length 0.98. Carapace 0.42 long, 0.37 wide. Abdomen 0.55 long, 0.46 wide. Eyes encircled by black rings, clypeus 0.04 long. Carapace light brown, sternum dark brown. Abdomen globular with two outgrowths near carapace (arrowed on Fig. 6A). Other coloration and pattern similar to male (Fig. 6A–B). Leg measurements: I 1.83 (0.54, 0.13, 0.50, 0.34, 0.32); II 1.58 (0.48, 0.11, 0.43, 0.28, 0.28); III 1.34 (0.38, 0.11, 0.35, 0.27, 0.23); IV 1.78 (0.53, 0.11, 0.48, 0.39, 0.27). Insemination duct thin and short, receptacle membranous and baglike with a single tube gradually expanding as a concave sac, and the diameter of receptacle four times larger than that of the insemination duct (Fig. 6C).

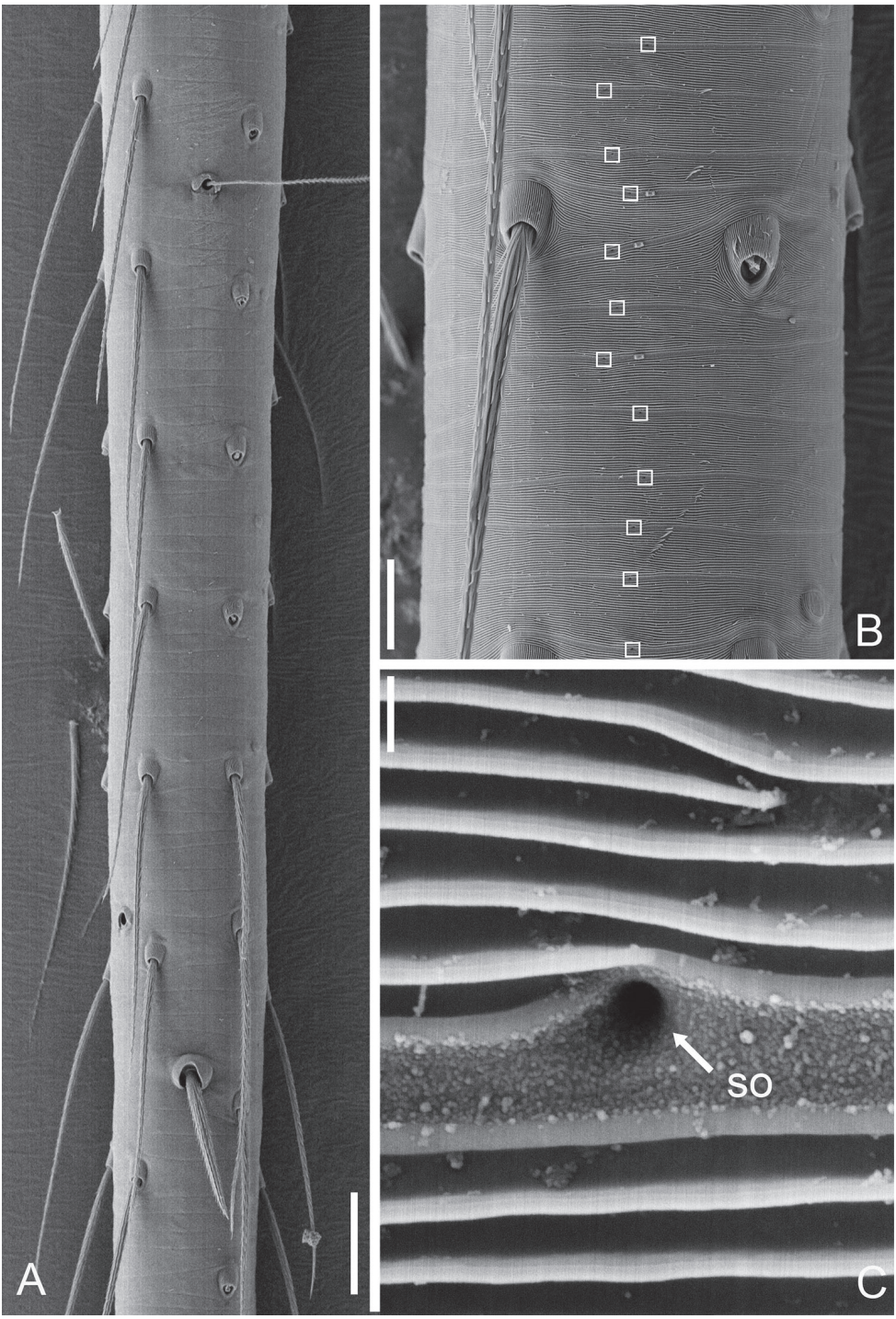

Figure 8. Tibial glands of *Guhua kakamegaensis* sp. n. (**A–C**). **A** Part of tibia **B** Position of tibial glands (white squares) **C** Secretory orifice (SO). Scale bars: 30 μm (**A**), 10 μm (**B**), 0.3 μm (**C**).

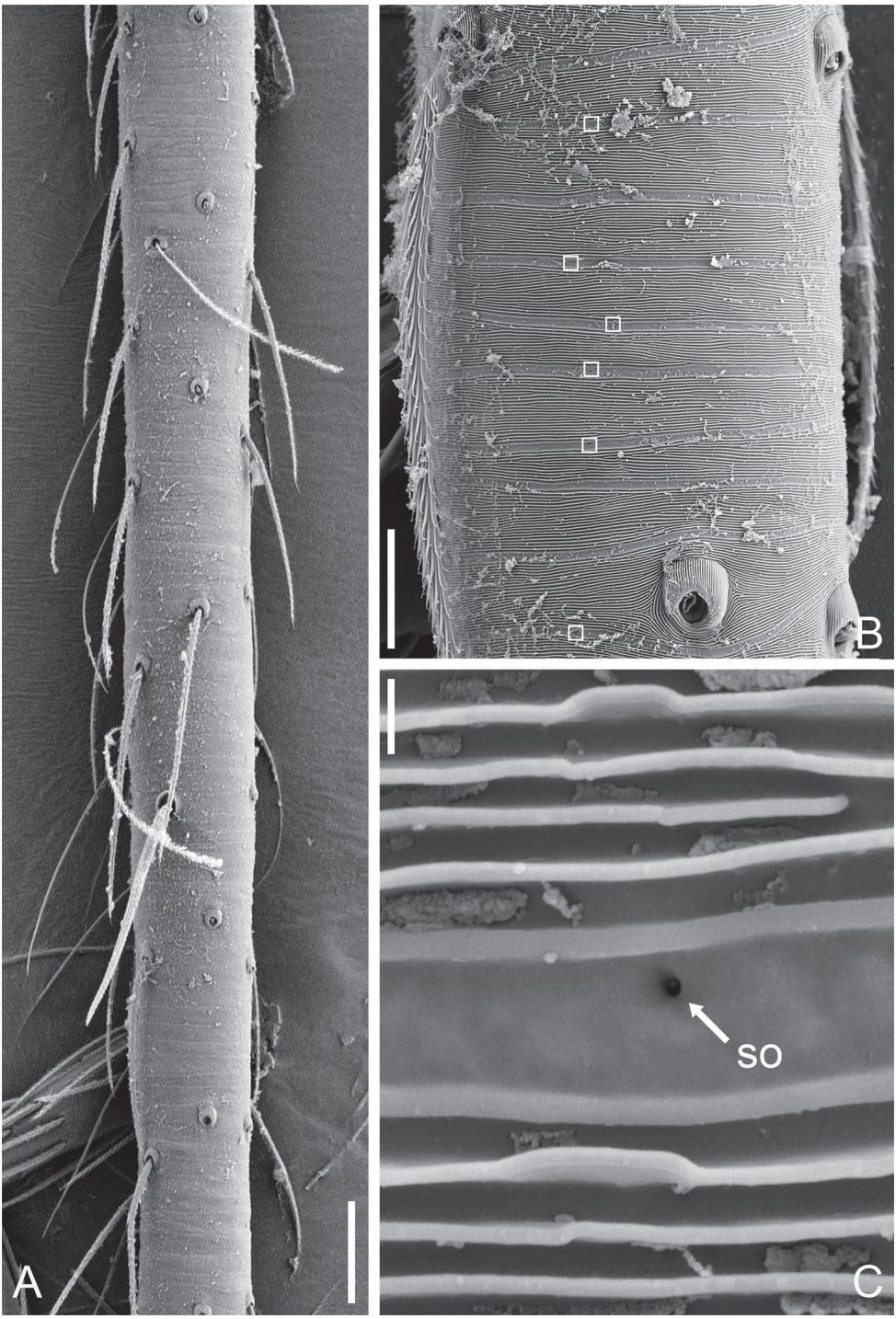

Figure 9 Tibial glands of *Apneumonella taitatavetaensis* sp. n. (**A–C**) **A** Part of tibia **B** Position of tibial glands (white squares) **C** Secretory orifice (SO). Scale bars: 30 μm (**A**), 10 μm (**B**), 0.3 μm (**C**).

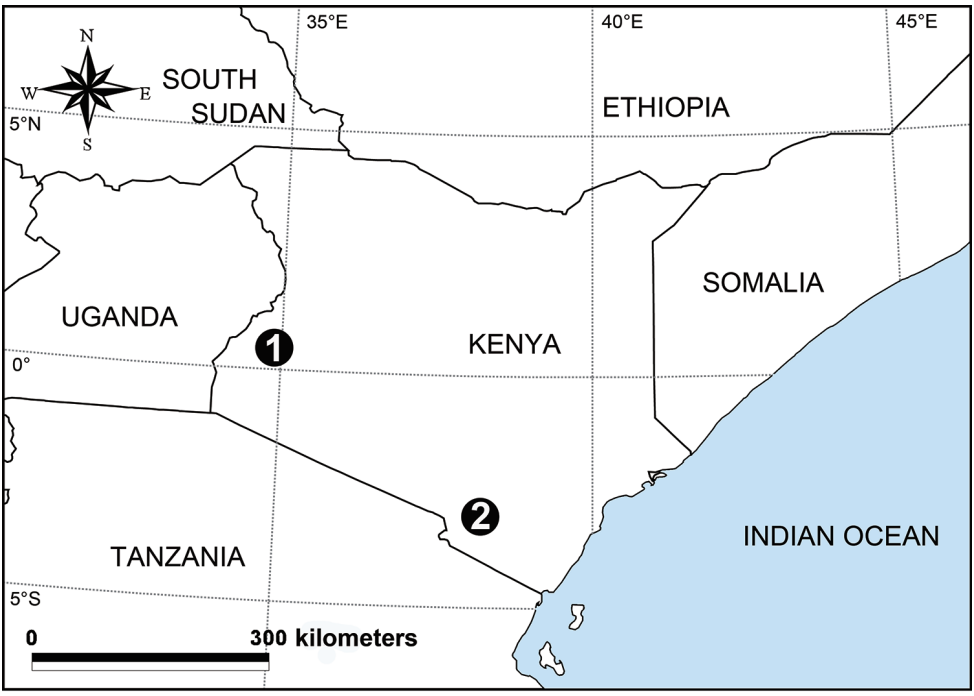

Figure 10. Distribution records of Telemidae in Kenya: **1** *Guhua kakamegaensis* sp. n. **2** *Apneumonella taitatavetaensis* sp. n.

Habitat. Leaf litter in cloud forest.

Comments. *Apneumonella* Fage, 1921 was described with *A. oculata* Fage, 1921 from Tanzania as the type species. The new species shares several characters with *A. oculata*, including the shape of the receptacle and denticulation of the chelicerae. Furthermore, the shape of tibial glands in this species is different from the plate-shaped structure of the tibial glands in *Telema* and *Usofila*, but similar to the lined structure in *Apneumonella* (Emerit 1985). The collection locality of *A. taitatavetaensis* sp. n. is approximately 150 km from the type locality of *A. oculata*.

Distribution. Known only from the type locality (Fig. 10).

Acknowledgements

The manuscript benefitted greatly by comments made by Cor Vink, Nadine Dupérré, and an anonymous referee. English was kindly checked by Sarah C. Crews. The field work in Taita-Taveta and Kakamega was kindly supported by the Kenya Wildlife Service (KWS), the Kenya Forest Service (KFS), the National Environment Management Authority (NEMA) and the National Commission for Science, Technology and Innovation (NACOSTI). This study was supported by the National Natural Sciences Foundation of China (NSFC-31530067, 31471960, 31660611, 31460554) and the South-

east Asia Biodiversity Research Institute, Chinese Academy of Sciences (2015CASE-ABRI005, Y4ZK111B01). Part of the laboratory work was financially supported by the Key Project of Science and Technology of Jiangxi (20161BBF60076), the Landing Project of Science and Technology of Colleges and Universities in Jiangxi Province of China (KJLD14081), and the Science and Technology Foundation of Educational Commission of Jiangxi Province of China (GJJ14663).

References

Baert L (1980) Spiders (Araneae) from Papua New Guinea. I. *Jocquella leopoldi* gen. n., sp. n. (Telemidae). Bulletin of the British Arachnological Society 5: 16–19.

Baert L (1985) Telemidae, Mysmenidae and Ochyroceratidae from Cameroon (Araneae): Scientific report of the Belgian Mount Cameroon Expeditions 1981 and 1983 (no. 13). Biologisch Jaarboek Dodonaea 53: 44–57.

Brignoli PM (1977) Two new spiders from Sumatra (Araneae, Telemidae and Ochyroceratidae). Zoologische Mededelingen 50: 221–229.

Brignoli PM (1978) A few notes on a remarkable South African troglobitic spider, *Cangoderces lewisi* Harington, 1951 (Araneae, Telemidae). Revue Suisse de Zoologie 85: 111–114. https://doi.org/10.5962/bhl.part.82220

Brignoli PM (1980) Contributions à l'étude de la faune terrestre des îles granitiques de l'archipel des Séchelles (Mission P.L.G. Benoit – J.J. Van Mol 1972). Araneae Telemidae et Ochyroceratidae. Revue Zoologique Africaine 94: 380–386.

Emerit M (1985) L'appareil glandulaire tégumentaire de la patte des Telemidae (Araneae): un critère phylogénique? Mém. Biospéol, Université des Sciences et Techniques du Languedoc 12: 91–96.

Fage L (1921) Sur quelques araignées apneumones. Comptes Rendus de l'Académie des Sciences Paris 172: 620–622.

Harington JS (1951) A new leptonetid spider, *Cangoderces lewisi*, n. gen., n. sp., from the Cango Caves, Oudtshoorn. Annals of the Natal Museum 12: 81–90.

Lin Y, Li S (2008) A new species of the family Telemidae (Arachnida, Araneae) from Xishuangbanna rainforest, China. Acta Zootaxonomica Sinica 33: 650–653.

Saaristo MI (1978) Spiders (Arachnida, Araneae) from the Seychelle islands, with notes on taxonomy. Annales Zoologici Fennici 15: 99–126.

Wang C, Li S (2011) Three new species of Telemidae (Araneae) from western Africa. Zootaxa 2902: 44–58.

World Spider Catalog (2017) World spider catalog. Natural History Museum Bern. http://wsc.nmbe.ch, version 18.5 [accessed on October 17, 2017]

ZooKeys 725: 17–29 (2017)
doi: 10.3897/zookeys.725.20010
http://zookeys.pensoft.net

SHORT COMMUNICATION

A peer-reviewed open-access journal
ZooKeys
Launched to accelerate biodiversity research

Seeking quantitative morphological characters for species identification in soldiers of Puerto Rican *Heterotermes* (Dictyoptera, Blattaria, Termitoidae, Rhinotermitidae)

Zachary H. Griebenow[1,2], Susan C. Jones[1], Tyler D. Eaton[1]

1 *Department of Entomology, The Ohio State University, 2501 Carmack Rd., Columbus, OH, 43210-1065, USA* **2** *Department of Entomology & Nematology, University of California-Davis, 381A Briggs Hall, One Shields Ave., Davis, CA, 95616-5270, USA*

Corresponding author: *Zachary H. Griebenow* (zgriebenow@ucdavis.edu)

Academic editor: *P. Stoev* | Received 4 August 2017 | Accepted 21 November 2017 | Published 29 December 2017

http://zoobank.org/E1E422E7-0017-4CD3-8828-7CFCDB672992

Citation: Griebenow ZH, Jones SC, Eaton TD (2017) Seeking quantitative morphological characters for species identification in soldiers of Puerto Rican *Heterotermes* (Dictyoptera, Blattaria, Termitoidae, Rhinotermitidae). ZooKeys 725: 17–29. https://doi.org/10.3897/zookeys.725.20010

Abstract

Subterranean termites in the genus *Heterotermes* Froggatt (Rhinotermitidae: Heterotermitinae) are pantropical wood feeders capable of causing significant structural damage. The aim of this study was to investigate soldier morphological attributes in three Puerto Rican species of *Heterotermes* previously identified by sequencing of two mitochondrial genes and attributed to *Heterotermes tenuis* (Hagen), *H. convexinotatus* (Snyder) and *H. cardini* (Snyder). Soldiers (n = 156) were imaged and measured using the AutoMontage image-stacking program. We demonstrated that Puerto Rican *Heterotermes* soldiers could not be identified to species level based upon seven morphometric indices or any combination thereof. Nor could differences in soldier head pilosity be used to discriminate species, in contrast to previous findings. However, previously described characters of the soldier tergal setae were reported to be useful in discriminating *H. tenuis* from both of its Puerto Rican congeners.

Keywords

Caribbean, *Heterotermes cardini*, *Heterotermes convexinotatus*, *Heterotermes tenuis*, Morphometrics, taxonomy

Introduction

Heterotermes Froggatt, 1897 (Rhinotermitidae: Heterotermitinae) is a pantropical genus of subterranean wood feeding termites (Constantino 2000). Seventeen species have been reported as pests that damage human structures (Scheffrahn and Su 2000). The *Heterotermes* fauna in the Caribbean Region (the Bahamas, Greater Antilles, and Lesser Antilles) is thought to consist exclusively of pest species that have been introduced from the South American mainland (Constantino 1998, Evans et al. 2013). Caribbean *Heterotermes* are consequently of interest in that they are both invasive and economically significant. In the Caribbean Region, the Puerto Rican archipelago is situated at the eastern end of the Greater Antilles and is adjacent to the younger, actively volcanic Lesser Antilles, hence providing a biotic link to the South American mainland.

Our understanding of *Heterotermes* species' identity and distribution in the Caribbean Region has fluctuated over time, with the species composition of the *Heterotermes* fauna in Puerto Rico and its associated islands being quite ambiguous. Snyder (1956) reported *Heterotermes tenuis* (Hagen, 1858) and *Heterotermes convexinotatus* (Snyder, 1924) from the archipelago, while Scheffrahn et al. (2003) left Puerto Rican *Heterotermes* specimens unidentified to species level due to taxonomic uncertainty. Using a phylogenomic approach conjunct with some morphological and biogeographical data, Szalanski et al. (2004) concluded that *Heterotermes cardini* (Snyder, 1924) was present in the Caribbean Region in addition to *H. tenuis* and *H. convexinotatus*, along with one or more undescribed species. Three samples from Puerto Rico were included in their study, all identified as *H. convexinotatus*. In contrast, Eaton et al. (2016) reported *H. tenuis*, *H. convexinotatus*, and *H. cardini* in Puerto Rico based on molecular phylogenies of two mitochondrial loci from 76 Puerto Rican samples, with morphological confirmation of species identification. Furthermore, their phylogenomic data provided strong evidence that the proposed undescribed *Heterotermes* (Szalanski et al. 2004) were consistent with *H. cardini*.

Heterotermes soldiers from the Caribbean remain difficult to reliably distinguish due to non-robust diagnostic morphological characters: Snyder (1924) asserted that soldiers of the three species differed in cephalic and pronotal pilosity, body coloration, and relative size. However, due to morphological ambiguity, Snyder (1924) suggested in his original descriptions of *H. convexinotatus* and *H. cardini* (the latter described from the Bahamas) that they might be synonymous with *H. tenuis*. Consequently, alates (winged reproductives) are essential for reliable species identification of those *Heterotermes* spp. putatively present in Puerto Rico (Snyder 1924; Szalanski et al. 2004; Eaton et al. 2016). Since alates are produced only seasonally, they are difficult to obtain and are seldom properly associated with their parent colonies. Therefore, robust soldier-based identification of Puerto Rican *Heterotermes* is of practical taxonomic interest.

The purpose of our study was to measure morphometric parameters in the soldier caste from a comprehensive sample of the Puerto Rican *Heterotermes* fauna, and to determine what parameters, if any, were most useful in identifying *Heterotermes* to species

level. Additionally, pilosity of the head capsule (Snyder 1924) and abdominal tergites of *Heterotermes* soldiers (Constantino 2000) were examined as diagnostic characters. The possibility of an additional, undescribed species of *Heterotermes* in the Caribbean Region (as per Szalanski et al. 2004) was also herein analyzed.

Materials and methods

Our study is supplementary to that of Eaton et al. (2016) in that it largely uses a subset of the same Puerto Rican *Heterotermes* samples (n = 60 of 76 samples). These were assigned to *H. tenuis*, *H. convexinotatus*, or *H. cardini* on the basis of their 16S rRNA and cytochrome oxidase subunit II (COII) phylogeny. Samples were collected by SCJ from different locales on the main island of Puerto Rico and adjacent Culebra Island in 2002, 2004, 2006, or 2010. Each sample consisted of termites collected from a single access point in a given colony and placed in individual vials filled with absolute alcohol.

In total, 156 individual soldiers were examined morphometrically (see Suppl. material 1), with 3 being selected, when available, from each sample, providing 40 specimens of *H. tenuis*, 55 *H. convexinotatus*, and 61 *H. cardini*. We investigated mandible length in combination with the same axis of the head capsule, along with head width (Figure 1), in order to provide additional commonality with the data presented in Constantino (2000) and Szalanski et al. (2004). In addition, multiple pronotal metrics (Figure 2) were examined, two of them novel to this study (see Suppl. material 1). A total of three morphometric indices recommended by Roonwal (1969) for use in termite taxonomy were derived from a subset of these metrics (see Suppl. material 1). Cephalic setae were surveyed in 79 of the 156 soldiers, plus an additional 7 *H. convexinotatus* soldiers examined without morphometric analysis. Also, setae within a 300-μm radius of the soldier fontanelle were censused in 66 of the 156 soldiers. A subset of 45 of the 156 soldiers was used for characterization of tergal setae.

A Z16 AP0 stereomicroscope (Leica Microsystems, Buffalo Grove, USA) with a KY-570B camera (JVC, Wayne, USA) was used to image specimens for morphometric analysis and examination of tergal setae, with images being stacked into montage microphotographs using Auto-Montage Pro software (ver. 5.01.0005, Synoptics Ltd., Cambridge, UK).

We performed analyses of variance (ANOVA), discriminant analyses, and *k*-means cluster analyses on morphometric data using SPSS Statistics 24 (2016, International Business Machines, Armonk, USA). The level of significance for all analyses was set at α=0.05. Based on the results of ANOVA, a discriminant analysis and three *k*-means cluster analyses were performed using all statistically significant parameters. Discriminant analyses determine the efficacy of any array of variables in assigning group membership (Green et al. 2008).

K-means cluster analyses do not assume *a priori* assignments of specimens to groups, instead attempting to iteratively delineate groups *de novo* from the data given according to the number of groups provided by an *a priori* hypothesis. Our *k*-means

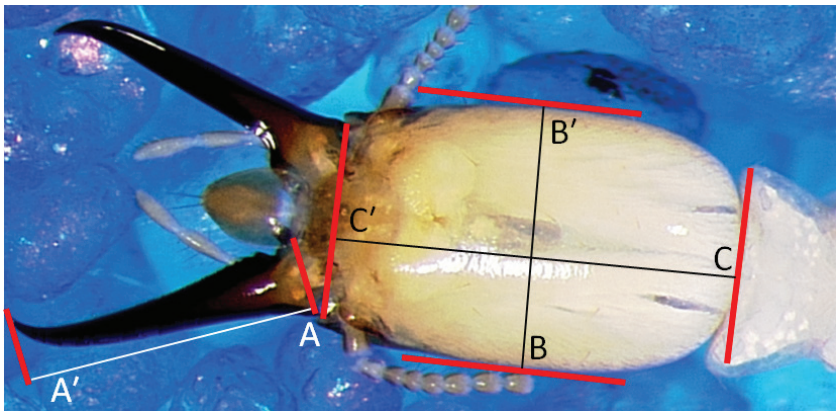

Figure 1. Cephalic metrics: AA' = maximum length of mandible; BB' = maximum width of head; CC' = length of head to lateral base of mandibles. Parallels used to delineate metrics (see Suppl. material 1) are marked in red.

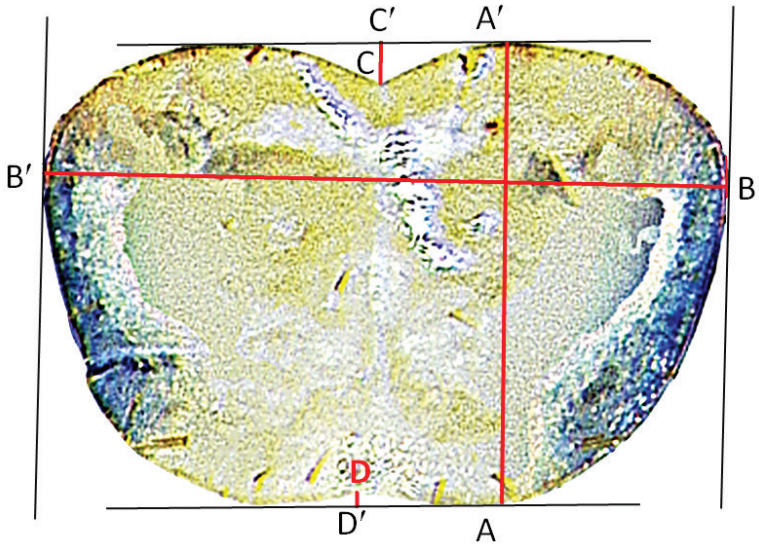

Figure 2. Pronotal metrics: AA'= maximum length of pronotum; BB' = maximum width of pronotum; CC' = depth of anterior pronotal notch; DD' = depth of posterior pronotal notch. Parallels are marked in black.

cluster analyses specified 3, 4, and 2 morphometric-delineated groups within the sampled *Heterotermes* fauna. The first analysis was premised according to the conclusion of Eaton et al. (2016) that there are 3 valid *Heterotermes* spp. in the Puerto Rican archipelago. The second was premised according to the conclusion of Szalanski et al. (2004) that 4 *Heterotermes* spp. occur in the Caribbean Region. The third was premised according to the phylogenetic hypothesis that *H. tenuis* is sister to a clade including *H. convexinotatus* and *H. cardini* (Szalanski et al. 2004; Eaton et al. 2016): if this were

the case, one would expect specimens to group into two clusters. It was not possible to delineate one or more metrics on a total of 40 specimens (5 *H. tenuis*, 8 *H. convexinotatus*, and 27 *H. cardini*), so these were excluded from *k*-means cluster analysis.

Results and discussion

ANOVA concerning all parameters demonstrated that all but one of the metrics surveyed – the depth of the posterior pronotal notch, which was novel to this study – displayed statistically significant variation across all three species (Table 1). Only one of the three morphometric indices we derived – the head-mandible index (Roonwal 1969) – exhibited statistically significant variation across all three species (Table 1).

Discriminant and *k*-means cluster analyses used only statistically significant parameters. Of all 116 specimens with sufficient morphometric data for their inclusion in discriminant analysis, our discriminant analyses correctly classified 87.1% to species. Thus, while the majority of Puerto Rican *Heterotermes* with sufficient morphometric data could be accurately identified to species level using statistically significant morphometric parameters, these data were not invariably reliable for that purpose; nor was this mode of identification concise given that a total of seven parameters was necessary.

The results of morphometric 3- and 4-cluster analyses did not consistently conform to the phylogenetic hypotheses of Eaton et al. (2016) and Szalanski et al. (2004) for Caribbean *Heterotermes*, respectively, nor did any cluster analysis support placement of *H. tenuis* as a sister-group to the remaining two putative species of *Heterotermes*. Furthermore, no morphometric consensus, novel or otherwise, could be made across all three *k*-means cluster analyses (Table 2). These results were likely influenced by the fact that many specimens (n = 40) provided insufficient data to be included in cluster analyses.

We found short to medium-length (uniformly <100 μm) setae on the head capsules of all *H. convexinotatus* specimens examined with respect to this character, but pilosity of this species and *H. tenuis* was comparable (Table 3). Furthermore, there was considerable overlap in head capsule pilosity among all three species (Table 4). Likewise, the area within a 300-μm radius of the fontanelle of a subset of the 156 specimens displayed considerable overlap in seta quantity and no apparent pattern among all three species (Table 5). We therefore conclude that soldier head pilosity is not a reliable character for discriminating among Puerto Rican *Heterotermes* species, contrary to Snyder (1924).

Although soldiers of all three *Heterotermes* species bore a distinct line of bristles (setae noticeably longer than surrounding setae) along the posterior margins of abdominal tergites (excluding the epiproct), only *H. tenuis* soldiers had a distinct row of long hairs on central tergal surfaces (Figure 3). In contrast, short setae (often <10 μm long) not arranged in distinct rows predominated on the central tergal surfaces of *H. convexinotatus* and *H. cardini* soldiers. These correspond to the "numerous microscopic hairs" described by Constantino (2000) on *H. convexinotatus* tergites. Whereas Constantino (2000) did not compare the tergal pilosity of *H. cardini* to *H. tenuis*, we make a novel report that tergal seta distribution also can be used to distinguish *H. tenuis* soldiers from those of *H. cardini*.

Table 1. Results of an ANOVA assessing variation of select morphometric parameters. Parameters exhibited statistically significant differentiation if $P<0.05$.

Parameter	df	*F* value	*P* value
Head capsule length	127	36.089**	0.000
Mandible length	124	36.089**	0.000
Head width	126	50.033**	0.000
Pronotum width	150	46.723**	0.000
Pronotum length	150	15.759**	0.042
Depth of anterior pronotal notch	146	3.242**	0.000
Depth of posterior pronotal notch	122	42.885	0.826
Pronotal index	150	0.575	0.564
Head-mandible index	124	6.732**	0.002
Head index	127	1.434	0.242

Table 2. Cluster membership under respective phylogenetic hypotheses. Insufficient morphometric data precluded analysis of 40 specimens. Cluster numeration was arbitrary. Distance was measured relative to computed cluster center.

Species	2-Cluster Hypothesis		3-Cluster Hypothesis		4-Cluster Hypothesis	
	Cluster	Distance	Cluster	Distance	Cluster	Distance
H. tenuis	2	253.54143	3	32.20008	3	46.50913
H. tenuis	2	326.77099	3	74.86261	3	53.2888
H. tenuis	2	354.21671	3	117.6952	3	93.6614
H. tenuis	2	85.55526	2	84.16529	2	81.85684
H. tenuis	2	312.57804	3	87.58546	3	83.58083
H. tenuis	2	309.6662	3	84.9422	3	85.65045
H. tenuis	2	256.37002	3	39.99476	3	57.39513
H. tenuis	2	234.62472	3	81.46453	3	100.08422
H. tenuis	2	121.91754	2	103.66997	2	106.89786
H. tenuis	2	251.06997	3	52.89946	3	68.95685
H. tenuis	2	314.68978	3	61.76796	3	41.12887
H. tenuis	1	160.0722	1	163.05486	1	163.73504
H. tenuis	2	229.03476	3	62.02824	3	85.69223
H. tenuis	2	340.18453	3	86.72816	3	58.86668
H. tenuis	2	347.37142	3	86.32921	3	62.79373
H. tenuis	2	165.30565	2	233.59069	2	169.00256
H. tenuis	2	113.2921	2	132.59409	2	102.7966
H. tenuis	2	314.97147	3	66.84973	3	43.15213
H. tenuis	2	108.07079	2	186.68133	2	125.18157
H. tenuis	2	208.05716	3	109.93034	3	128.41514
H. tenuis	2	310.24474	3	73.71241	3	55.89708
H. tenuis	2	124.9129	3	142.88123	2	146.78559
H. tenuis	2	380.73388	3	124.49842	3	99.2555
H. tenuis	2	166.58084	3	234.09751	2	177.17161
H. tenuis	2	326.48907	3	68.58936	3	46.22216
H. tenuis	2	151.22401	2	67.91019	4	91.83434

Species	2-Cluster Hypothesis		3-Cluster Hypothesis		4-Cluster Hypothesis	
	Cluster	Distance	Cluster	Distance	Cluster	Distance
H. tenuis	2	193.01248	2	85.87651	4	43.17484
H. tenuis	1	282.70386	2	194.37339	4	102.57221
H. tenuis	2	264.30373	2	154.32751	4	69.74912
H. tenuis	2	230.22493	2	126.27088	4	65.41226
H. tenuis	1	301.11995	2	209.09383	4	124.68136
H. tenuis	2	267.73784	2	157.77828	4	82.99303
H. tenuis	1	301.10911	2	206.37768	4	120.70212
H. tenuis	2	280.63396	2	180.37562	4	113.16429
H. tenuis	2	57.2989	2	166.99186	2	76.70921
H. convexinotatus	2	66.64623	2	162.67921	2	76.51109
H. convexinotatus	2	100.58655	2	74.61512	2	87.54042
H. convexinotatus	2	45.53643	2	73.81509	2	30.55171
H. convexinotatus	1	92.8697	1	106.97731	1	109.89883
H. convexinotatus	1	42.58346	1	61.12458	1	66.23971
H. convexinotatus	1	48.37568	1	68.29212	1	72.47772
H. convexinotatus	1	170.71652	1	197.58664	1	201.95907
H. convexinotatus	1	100.92468	1	129.95624	1	134.78135
H. convexinotatus	1	195.08743	1	171.49698	1	168.40471
H. convexinotatus	1	143.58385	1	159.21383	1	161.85759
H. convexinotatus	1	39.48472	1	61.0434	1	65.59095
H. convexinotatus	2	190.79254	2	87.65711	4	74.07688
H. convexinotatus	1	131.65924	1	160.45317	1	165.14755
H. convexinotatus	1	147.95901	1	173.5811	1	177.67905
H. convexinotatus	2	100.109	2	88.36581	2	85.5312
H. convexinotatus	2	256.96346	2	159.35016	4	111.01812
H. convexinotatus	1	63.17991	1	65.26824	1	67.17037
H. convexinotatus	1	172.68076	1	197.98883	1	201.96107
H. convexinotatus	1	89.89609	1	79.38557	1	79.56232
H. convexinotatus	2	219.01414	2	121.76263	4	78.87236
H. convexinotatus	1	115.93995	1	116.1732	1	117.93494
H. convexinotatus	1	61.6565	1	39.65379	1	39.16278
H. convexinotatus	2	161.9857	2	71.84719	4	93.15414
H. convexinotatus	2	168.94894	2	67.60631	4	72.92106
H. convexinotatus	2	72.73062	2	96.75358	2	55.58775
H. convexinotatus	2	98.61692	2	51.1218	2	75.0215
H. convexinotatus	2	76.54337	2	152.03536	2	76.50752
H. convexinotatus	2	109.20261	2	40.35267	2	86.98483
H. convexinotatus	2	73.69146	2	144.78302	2	80.01889
H. convexinotatus	2	230.57425	2	133.95943	4	100.72459
H. convexinotatus	2	107.73092	2	119.16952	2	90.72008
H. convexinotatus	2	146.14797	3	189.50569	2	156.36624
H. convexinotatus	2	130.50162	2	169.64244	2	130.77036
H. convexinotatus	2	239.38575	2	139.56988	4	99.8207
H. convexinotatus	2	92.55724	2	120.63307	2	77.22261
H. convexinotatus	2	116.67981	2	53.59368	2	94.82665

Species	2-Cluster Hypothesis		3-Cluster Hypothesis		4-Cluster Hypothesis	
	Cluster	Distance	Cluster	Distance	Cluster	Distance
H. convexinotatus	2	143.72191	2	63.84648	4	102.7939
H. convexinotatus	2	55.07361	2	164.29003	2	72.06005
H. convexinotatus	2	100.55303	2	135.18375	2	88.91133
H. convexinotatus	2	116.60445	2	73.3531	2	94.07228
H. convexinotatus	2	82.23475	2	103.79059	2	65.28595
H. convexinotatus	2	160.4155	2	85.86284	4	111.32346
H. convexinotatus	2	89.50309	2	187.87274	2	101.76863
H. convexinotatus	2	167.55718	2	109.25237	4	137.91008
H. convexinotatus	2	79.39547	2	121.25412	2	71.32581
H. convexinotatus	2	124.51904	2	119.70772	2	123.62927
H. convexinotatus	2	101.38499	2	44.47996	2	80.3574
H. cardini	1	50.62172	1	49.4603	1	52.54455
H. cardini	2	156.96056	2	72.06053	4	92.09658
H. cardini	2	116.3222	2	68.96384	2	105.05938
H. cardini	2	133.27853	2	58.6334	4	107.50376
H. cardini	1	69.85903	1	50.30866	1	49.75939
H. cardini	1	63.33121	1	60.63669	1	62.57799
H. cardini	1	228.32884	2	242.53297	4	151.5971
H. cardini	1	233.92987	2	224.04711	4	131.26097
H. cardini	1	152.27189	1	122.78914	1	118.84265
H. cardini	1	156.08061	1	133.17036	1	130.72768
H. cardini	1	127.96476	1	98.93537	1	95.34782
H. cardini	1	186.62386	1	223.11212	4	204.59382
H. cardini	1	187.26549	1	157.73427	1	153.65728
H. cardini	1	183.74985	1	157.39755	1	154.03872
H. cardini	1	233.73398	1	198.98527	1	193.37452
H. cardini	1	74.31731	1	92.99662	1	96.63796
H. cardini	1	103.83294	1	105.39398	1	107.29047
H. cardini	1	217.06493	1	192.74338	1	189.6661
H. cardini	1	201.84888	1	171.83761	1	167.68972
H. cardini	1	238.91474	1	207.60536	1	203.09527
H. cardini	1	195.04476	1	163.03509	1	158.21636
H. cardini	2	150.4453	2	93.68494	4	126.39925
H. cardini	2	135.8617	2	70.67088	4	111.95337
H. cardini	2	164.19757	2	112.11675	4	137.5087
H. cardini	2	279.99234	2	196.786	4	155.38894
H. cardini	1	215.87616	1	214.5414	1	214.2815
H. cardini	1	289.80952	1	272.98807	1	269.8637
H. cardini	2	141.99891	2	98.41767	2	134.63763
H. cardini	2	178.27138	2	79.26567	4	61.65641
H. cardini	2	156.7643	2	92.67277	4	116.96033
H. cardini	2	106.70269	2	86.74184	2	103.08692
H. cardini	2	93.76761	2	142.89509	2	106.73515
H. cardini	1	66.89762	1	65.16361	1	66.45667
H. cardini	1	178.07806	1	183.42556	1	185.36444

Table 3. Summary statistics for cephalic seta counts.

Species	Number of soldiers	Number of samples	Average	Standard error
H. tenuis	13	2	18.6923	2.48427
H. convexinotatus	36	15	16.6111	0.9818
H. cardini	37	13	14.1081	0.85053

Table 4. Cephalic setae counts. Identifiers are as follows: sample #_year of collection_replicate_species.

Identifier	# of cephalic setae
67_10_01_tenuis	27
84_06_01_tenuis	26
84_06_02_tenuis	25
84_06_03_tenuis	25
84_06_04_tenuis	29
84_06_05_tenuis	2
84_06_06_tenuis	10
84_06_07_tenuis	16
84_06_08_tenuis	22
84_06_09_tenuis	19
84_06_10_tenuis	26
84_06_11_tenuis	8
84_06_12_tenuis	8
235_04_01_convexinotatus	19
34_06_01_convexinotatus	13
66_06_01_convexinotatus	15
226_04_01_convexinotatus	20
226_04_02_convexinotatus	13
226_04_03_convexinotatus	21
233_04_01_convexinotatus	27
233_04_02_convexinotatus	17
233_04_03_convexinotatus	26
74_02_01_convexinotatus	18
74_02_02_convexinotatus	17
74_02_03_convexinotatus	21
64_02_01_convexinotatus	12
64_02_02_convexinotatus	19
64_02_03_convexinotatus	15
257_04_01_convexinotatus	10
257_04_02_convexinotatus	23
257_04_03_convexinotatus	16
267_04_01_convexinotatus	16
267_04_02_convexinotatus	25
267_04_03_convexinotatus	25
258_04_01_convexinotatus	17
258_04_02_convexinotatus	24
258_04_03_convexinotatus	17
427_04_01_convexinotatus	11

Identifier	# of cephalic setae
427_04_02_convexinotatus	14
427_04_03_convexinotatus	20
414_04_02_convexinotatus	2
404_04_01_convexinotatus	14
407_04_01_convexinotatus	7
407_04_02_convexinotatus	14
407_04_03_convexinotatus	5
407_04_04_convexinotatus	8
428_04_01_convexinotatus	18
428_04_02_convexinotatus	16
428_04_03_convexinotatus	23
10_02_01_cardini	18
10_02_02_cardini	13
218_04_01_cardini	9
218_04_02_cardini	11
218_04_03_cardini	6
22_02_01_cardini	15
22_02_02_cardini	19
22_02_03_cardini	19
222_04_01_cardini	15
222_04_02_cardini	14
222_04_03_cardini	15
25_06_01_cardini	13
25_06_02_cardini	13
25_06_03_cardini	8
31_06_01_cardini	4
32_02_01_cardini	16
32_02_02_cardini	20
32_02_03_cardini	18
44_02_01_cardini	6
44_02_02_cardini	14
44_02_03_cardini	5
65_02_01_cardini	10
65_02_02_cardini	20
65_02_03_cardini	20
66_02_01_cardini	14
66_02_02_cardini	8
66_02_03_cardini	11
67_02_01_cardini	16
67_02_02_cardini	21
67_02_03_cardini	14
78_02_01_cardini	17
78_02_02_cardini	18
78_02_03_cardini	9
79_02_01_cardini	9
79_02_02_cardini	20
79_02_03_cardini	26
79_02_04_cardini	18

Table 5. Summary statistics for seta counts within a 300-μm radius of the soldier fontanelle.

Species	Number of soldiers	Number of samples	Average	Standard error
H. tenuis	13	2	3.184211	0.190053
H. convexinotatus	15	7	5.666667	0.214214
H. cardini	38	14	4.230769	0.405096

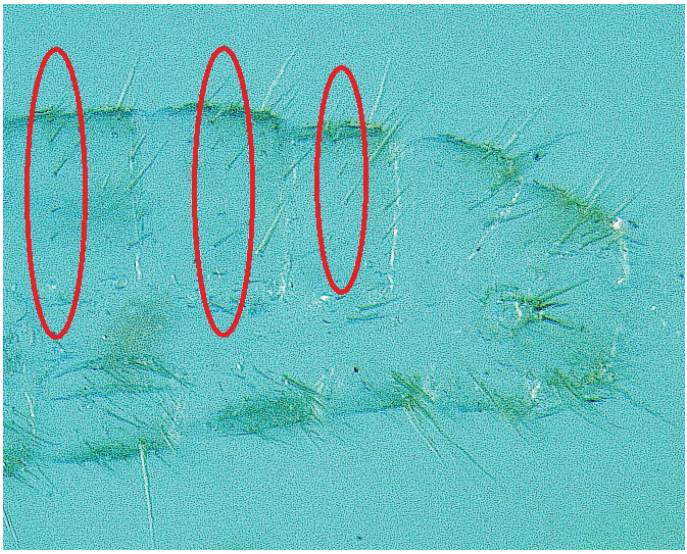

Figure 3. Posterior abdominal tergites of *H. tenuis*. Rows of long setae on central tergal surfaces are circled.

Conclusions

Our findings demonstrated that examined morphometric characters of the soldier pronotum and head could not reliably differentiate *Heterotermes* species in the Puerto Rican archipelago. These data did not provide any well-resolved distinction between the three putative species in question, such as is supported by rigorous phylogenomic investigation (Eaton et al. 2016). We also found that *H. convexinotatus* and *H. cardini* soldiers could not be unequivocally discriminated by cephalic seta counts, contrary to Snyder (1924). However, *H. tenuis* soldiers could be readily identified by means of tergal setal distribution, as reported by Constantino (2000). We furthermore report that soldier tergal seta distribution is useful to distinguish *H. tenuis* from *H. cardini*.

Acknowledgements

This research was supported in part by State and Federal funds appropriated to the Ohio Agricultural Research and Development Center, by USDA NIFA Hatch Project OHO01170,

and by Research Scholar Award funds disbursed by the Undergraduate Research Office of The Ohio State University. The authors would like to thank Abhijoy Saha for his statistical consulting services; Dr David Shetlar for his assistance proofreading application materials for the Research Scholar Award; Huayan Chen and Dr Hans Klompen for their assistance in the imaging process; and Alex Tyrpak, Kara Baker and Nina Bogart for their past and present aid and support at the Jones Laboratory.

References

Constantino R (1998) Catalog of the living termites of the New World (Insecta: Isoptera). Arquivos de Zoologia 35: 135–231. http://dx.doi.org/10.11606/issn.2176-7793.v35i2p135-230

Constantino R (2000) Key to the soldiers of South American *Heterotermes* with a new species from Brazil (Isoptera: Rhinotermitidae). Insect Systematics and Evolution 31: 463–472. http://dx.doi.org/10.1163/187631200X00499

Eaton TD, Jones SC, Jenkins TM (2016) Genetic diversity of Puerto Rican *Heterotermes* (Isoptera: Rhinotermitidae) revealed by phylogenetic analysis of two mitochondrial genes. Journal of Insect Science 16: 111. https://doi.org/10.1093/jisesa/iew099

Evans TA, Forschler BT, Grace JK (2013) Biology of invasive termites: a worldwide review. Annual Review of Entomology 58: 455–474. https://doi.org/10.1146/annurev-ento-120811-153554

Froggatt WW (1897) Australian Termitidae. Part II. Proceedings of the Linnaean Society of New South Wales, 21(4) [1896]: 510–552. [2 plates]

Green SB, Salkind NJ, Akey TM (2008) Using SPSS for Windows and Macintosh: Analyzing and understanding data. Prentice Hall, Upper Saddle River, New Jersey, 458 pp.

Hagen HA (1858) Monographie der Termiten. Linnaea Entomologica 12: i-iii, 4–342, 459. [3 plates]

Roonwal ML (1969) Measurement of termites (Isoptera) for taxonomic purposes. Journal of the Zoological Society of India 21: 9–66.

Scheffrahn RH, Su N-Y (2000) Featured creatures – West Indian subterranean termite. University of Florida – IFAS. http://entnemdept.ufl.edu/creatures/urban/termites/heterotermes.htm

Scheffrahn RH, Jones SC, Kreček J, Chase JA, Mangold JR, Su N-Y (2003) Taxonomy, distribution, and notes on the termites (Isoptera: Kalotermitidae, Rhinotermitidae, Termitidae) of Puerto Rico and the U.S. Virgin Islands. Annals of the Entomological Society of America 96: 181–201. https://doi.org/10.1603/0013-8746(2003)096[0181:TDANOT]2.0.CO;2

Snyder TE (1924) Descriptions of new species and hitherto unknown castes of termites from America and Hawaii. Proceedings of the U. S. National Museum 64: 1–40. [5 plates] https://doi.org/10.5479/si.00963801.64-2496.1

Snyder TE (1956) Termites of the West Indies, the Bahamas and Bermuda. Journal of Agriculture of the University of Puerto Rico 40: 189–202.

Szalanski AL, Scheffrahn RH, Austin JW, Kreček J, Su N-Y (2004) Molecular phylogeny and biogeography of *Heterotermes* (Isoptera: Rhinotermitidae) in the West Indies. Annals of the Entomological Society of America 97: 556–566. https://doi.org/10.1603/0013-8746(2004)097[0556:MPABOH]2.0.CO;2

Supplementary material 1

Definitions of soldier morphometric parameters

Authors: Zachary H. Griebenow, Susan C. Jones, Tyler D. Eaton

Data type: taxonomic metrics and indices.

Explanation note: Definitions of all morphometric parameters utilized in this study, *sensu* Roonwal (1969).

Link: https://doi.org/10.3897/zookeys.725.20010.suppl1

ZooKeys 725: 31–36 (2017)
doi: 10.3897/zookeys.725.20777
http://zookeys.pensoft.net

RESEARCH ARTICLE

A peer-reviewed open-access journal
ZooKeys
Launched to accelerate biodiversity research

New contributions to the leafhopper genus *Gladkara* from Thailand (Hemiptera, Cicadellidae, Typhlocybinae, Erythroneurini)

Yuehua Song[1,2], Zizhong Li[3], Christopher H. Dietrich[2], Can Li[4]

1 *School of Karst Science, Guizhou Normal University/ State Eniineering Technology Institute for karst Desertfication controal, Guiyang, Guizhou 550001, China* **2** *Illinois Natural History Survey, Prairie Research Institute, University of Illinois, 1816 S. Oak St., Champaign, IL 61820, USA* **3** *Institute of Entomology, Guizhou University, Guiyang, Guizhou 550025, China* **4** *Guizhou Provincial Key Laboratory for Rare Animal and Economic Insect of the Mountainous Region, Guiyang University, Guiyang, China*

Corresponding author: *Can Li* (lican790108@163.com)

Academic editor: *J. Zahniser* | Received 4 September 2017 | Accepted 31 October 2017 | Published 29 December 2017

http://zoobank.org/EA1E898B-79CB-4B31-BE1F-AE50646005D8

Citation: Song Y, Li Z, Dietrich CH, Li C (2017) New contributions to the leafhopper genus *Gladkara* from Thailand (Hemiptera, Cicadellidae, Typhlocybinae, Erythroneurini). ZooKeys 725: 31–36. https://doi.org/10.3897/zookeys.725.20777

Abstract

General characteristics of *Gladkara* Dworakowska and a checklist to all the known species of this genus are provided. A new species *Gladkara klongensis* Song & Dietrich, **sp. n.** from Thailand is added.

Keywords

Auchenorrhyncha, Homoptera, morphology, new species, taxonomy

Introduction

The leafhopper genus *Gladkara* was established by Dworakowska (1995) with *G. albida* Dworakowska as its type species. The genus previously contained 13 species, all of which were distributed in the Oriental Region. In this work, one more new species from Thailand is described and illustrated and a checklist of all known species of this genus worldwide is provided.

Materials and methods

Morphological terminology used in this work follows Dietrich (2005). Habitus photos were taken using a Canon EOS 5D Mark II camera and the Camlift V2.7.0 software. Multiple photographs of each specimen were compressed into final images with Zerene Stacker (64-bit) software. Body length was measured from the apex of crown to the tip of forewings. Abdomens were removed from specimens and cleared in cold 10% KOH solution overnight. The cleared material was rinsed with water and stored in glycerine. An Olympus SZX12 dissecting microscope was used for specimen study and Olympus BX41 and BX53 stereoscopic microscopes were used alternately for drawing of the dissected male genitalia and wings. The holotype of the new species is deposited at the Queen Sirikit Botanical Garden (**QSBG**), Chiang Mai, Thailand and additional specimens examined are deposited at the Illinois Natural History Survey (**INHS**), Prairie Research Institute, University of Illinois at Urbana-Champaign, USA (**UIUC**) and the School of Karst Science (**SKS**), Guizhou Normal University, Guiyang, China.

Results

Gladkara Dworakowska, 1995

Gladkara Dworakowska, 1995: 4; Dworakowska 2011: 10

Type species. *Gladkara albida* Dworakowska, 1995

Diagnosis. Dorsum beige or white. Color pattern absent or brown. Head narrower than pronotum, crown produced in midline anteriorly. Face convex. Pronotum with large impressions medially. Forewing with AA vein prominent, all known species with dark patch in 3rd apical cell except the type species. Hind wing venation usual for Erythroneurini.

Male 2S abdominal apodemes broad, reaching 3S posterior margin.

Male genitalia. Genital capsule cylindrical, slightly laterally compressed. Pygofer side broad, with caudal margin oval to square, with numerous sparse long fine setae, with or without enlarged macrosetae scattered at ventrolateral angle; dorsal appendage moveably articulated to the lobe, simple or bifurcate far from base, extended to pygofer apex or extended beyond pygofer apex; ventral appendage absent; segment X appendage present. Subgenital plate lamellate, with small latero-basal articulation with style, about 4–5 macrosetae in single or double row, setae of basal group in an oblique or longitudinal row, intergrading into marginal microsetae. Style long and slim, apical part tapering, smooth or adorned with sculpture; preapical lobe small. Connective lamellate, lateral arms long, stem reduced and central lobe desclerotized to various degree. Aedeagus with or without processes, aedeagal shaft tubular; dorsal apodeme with distinct V-shaped ligaments, connected to anal tube and/or pygofer

dorsal appendages; preatrium about as long as or shorter than shaft; gonopore apical or subapical on ventral surface.

Distribution. India; Brunei; Vietnam and Thailand.

***Gladkara klongensis* Song & Dietrich, sp. n.**
http://zoobank.org/EB8889D7-9CAA-4A8B-BAF0-58520703DE72
Figs 1–18

Specimens examined. Holotype: ♂, THAILAND, Surat Thani, Khao Sok NP Klong Morg Unit, 8°53.725'N, 98°39.025'E, 87 m, Malaise trap, 16-23.xii.2008, coll. Pongphan (QSBG). Paratypes: 3♀♀, same data as holotype (INHS, SKS).

Diagnosis. This species has its own salient characteristics as follows: pygofer with a bifurcate dorsal appendage (Fig. 10), segment X appendage twisted medially and hook-like apically (Fig. 11); style extremely elongated, with many cellular sculpturing apically (Fig. 14); aedeagus with long and tubular shaft, and a single short tooth-like process arising from preatrium (Fig. 18).

Description. Ground color pale beige. Eyes grey (Figs 1-3). Face pale beige; apex of frontoclypeus slightly darker in male; coloration extremely pale in female (Figs 4, 8). Pronotum pale anterolaterally, blackish beige medially and posteriorly (Figs 1, 3). Scutellum beige, with prominent scutellar suture (Figs 1, 3). Fore wing beige, with an irregular big dark brown spot at 3rd apical cell (Figs 1, 2).

Male abdominal apodemes broad, extending to the hind margin of third sternite (Fig. 9).

Male genitalia. Pygofer with dorsal appendage movably articulated (Fig. 10), segment X appendage elongated, twisted medially, and hook-like apically (Figs 11, 12). Pygofer lobe broadened, with two long fine setae arising from dorso-caudal margin and several long fine setae scattered near caudal margin medially (Fig. 10). Subgenital plate solid, much longer than hind margin of pygofer lobe, with four macrosetae on lateral surface and numerous stout setae along upper margin from sub-base to apex of plate, several microsetae scattered apically (Figs 10, 13). Style extremely elongated, with many cellular sculptures apically; preapical lobe small (Figs 14, 16). Connective V-shaped with lateral arms long and slim, widely divergent; stem short; central lobe absent (Fig. 15). Aedeagus with a single short toothlike process arising from preatrium; preatrium little shorter than length of shaft in lateral view, expanded in ventral view; shaft slender, tubular, slightly tapered distally in lateral view; gonopore apical (Figs 17, 18).

Measurements. Body length, male 3.7 mm; females 3.5–3.6 mm.

Remarks. This species is similar to *G. lisiogon* Dworakowska, 1995 from Brunei (Ulu Temburong) in the form of the aedeagus, but differs in having the dorsal pygofer appendage bifurcate apically (Fig. 12); the single short tooth-like process arising from aedeagal preatrium (Fig. 18); and the aedeagus dorsal apodeme not strongly expanded in caudal view (Fig. 18).

Etymology. The specific name is derived from a part of the type locality name in which all examined species were collected.

Figures 1–8. *Gladkara klongensis* Song & Dietrich, sp. n. Male (♂): **1** Habitus, dorsal view **2** Habitus, lateral view **3** Head and thorax, dorsal view **4** Face; Female (♀): **5** Habitus, dorsal view **6** Habitus, lateral view **7** Head and thorax, dorsal view **8** Face.

The species of the genus *Gladkara* worldwide and their distributions

1. *Gladkara albida* Dworakowska, 1995 Distribution: India.
2. *Gladkara bramka* Dworakowska, 1995 Distribution: Brunei.
3. *Gladkara cellularis* Dworakowska, 1995 Distribution: Brunei.
4. *Gladkara hirsuta* Dworakowska, 1995 Distribution: Brunei.
5. *Gladkara interrupta* Dworakowska, 1995 Distribution: Brunei.
6. *Gladkara klara* Dworakowska, 1995 Distribution: Brunei.
7. *Gladkara klongensis* Song & Dietrich, sp. n. Distribution: Thailand.
8. *Gladkara lisiogon* Dworakowska, 1995 Distribution: Brunei.
9. *Gladkara obligata* Dworakowska, 1995 Distribution: Brunei.
10. *Gladkara pulchra* Dworakowska, 1995 Distribution: Brunei.
11. *Gladkara quadrata* Dworakowska, 1995 Distribution: Brunei.

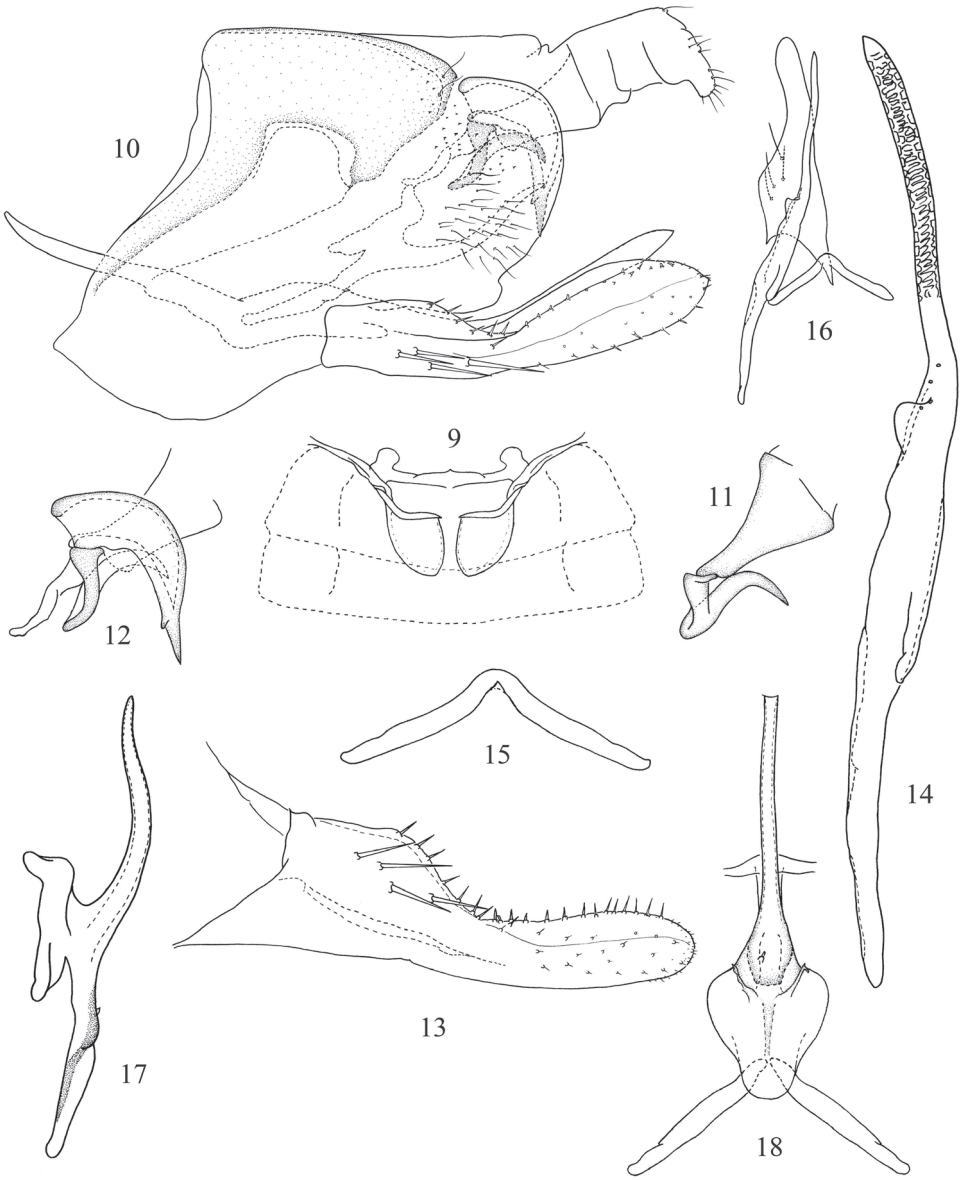

Figures 9–18. *Gladkara klongensis* Song & Dietrich, sp. n. **9** Abdominal apodemes **10** Genital capsule **11** Segment X appendage **12** Details of connections between segment X, dorsal pygofer appendage and dorsal ligament of aedeagus **13** Subgenital plate **14** Style **15** Connective **16** Subgenital plate, style and connective **17** Aedeagus, lateral view **18** Aedeagus and connective, caudal view.

12. *Gladkara sclerosa* Dworakowska, 1995 Distribution: Brunei.
13. *Gladkara vietnamica* Dworakowska, 2011 Distribution: Vietnam.
14. *Gladkara zavijka* Dworakowska, 1995 Distribution: Brunei.

Acknowledgements

The study was partly supported by the National First Class Discipline Construction Project of Guizhou province "geography of Guizhou Normal University" (Qian Jiao Keyan Fa [2017]85) the Graduate Education Innovation Project of Guizhou Province (Qian Jiao Yan He GZS Zi, No. [2016] 04), the Special Foundation for the Excellent Youth Science and Technology Scholars of Guizhou Province (Qian Ke He Ren Zi, No. [2015] 17), the Natural Science Research Project of Education Department of Guizhou Province (Qian Jiao He KY Zi, No. [2015] 357), the Science and Technology Planning Project of Guizhou Province (Qian Ke He Ren Cai [2016] 4020) and the National First Class Discipline Construction Project of Guizhou province "Ecology of Guizhou Normal University" (Qian Jiao Keyan Fa [2017]85).

References

Dietrich CH (2005) Keys to the families of Cicadomorpha and subfamilies and tribes of Cicadellidae (Hemiptera: Auchenorrhyncha). Florida Entomologist 88: 502–517. http://dx.doi.org/10.1653/0015-4040(2005)88[502:KTTFOC]2.0.CO;2

Dworakowska I (1995) *Yeia* gen. nov. and some other Typhlocybinae (Insecta: Auchenorrhyncha: Cicadellidae). Entomologische Abhandlungen Staatliches Museum für Tierkunde Dresden 57(1/5): 1–35.

Dworakowska I (2011) On several genera of leafhoppers of the tribe Erythroneurini from the Pacific rim (Hemiptera: Auchenorrhyncha: Cicadellidae: Typhlocybinae). Nova Supplementa Entomologica 22: 1–90.

ZooKeys 725: 37–47 (2017)
doi: 10.3897/zookeys.725.21040
http://zookeys.pensoft.net

RESEARCH ARTICLE

A peer-reviewed open-access journal
ZooKeys
Launched to accelerate biodiversity research

Discovery of a most remarkable cave-specialized trechine beetle from southern China (Coleoptera, Carabidae, Trechinae)

Mingyi Tian[1], Sunbin Huang[1], Dianmei Wang[1]

1 *Department of Entomology, College of Agriculture, South China Agricultural University, Wushan, Guangzhou, Guangdong, 510640, China*

Corresponding author: *Mingyi Tian* (mytian@scau.edu.cn)

Academic editor: *A. Casale* | Received 17 September 2017 | Accepted 1 November 2017 | Published 29 December 2017

http://zoobank.org/078BF7E1-BA6A-409E-B045-21591F7F82E4

Citation: Tian M, Huang S, Wang D (2017) Discovery of a most remarkable cave-specialized trechine beetle from southern China (Coleoptera: Carabidae: Trechinae). ZooKeys 725: 37–47. https://doi.org/10.3897/zookeys.725.21040

Abstract

Xuedytes bellus Tian & Huang, **gen. et sp. n.** is described from a limestone cave in Du'an Karst of Guangxi, a kingdom of cavernicolous trechine beetles in southern China. From a morphological point of view, *Xuedytes* Tian & Huang, **gen. n.** seems to be the most extremely cave-adapted trechines in the world. Superficially, it looks much like *Giraffaphaenops* Deuve, 2002 in general body shape, in particular the structure of the prothorax, but simultaneously it is similar to *Dongodytes* (*s. str.*) Deuve, 1993, based on elytral characters, including chaetotaxy. Hence the new genus seems to represent a lineage intermediate between *Giraffaphaenops* and *Dongodytes* (*s. str.*).

Keywords

aphaenopsian, Guangxi, ground beetle, troglobite

Introduction

The globe's largest and highly varied karst landscapes that blanket nearly the entire area of southern China (Deharveng and Bedos 2012) are long known to host the richest diversity of cave-dwelling trechine beetles in the world. To date, 48 genera of cavernicolous trechines containing over 130 species have been recorded there (Deuve and Tian 2016, Tian et al. 2016, Zhao and Tian 2016, Fang et al. 2017, Huang et al.

2017). Many of them are morphologically highly cave-adapted, such as *Giraffaphaenops* Deuve, 2002, *Dongodytes* Deuve, 1993, *Uenotrechus* Deuve & Tian, 1999, *Pilosaphaenops* Deuve & Tian, 2008, *Sinaphaenops* Uéno & Wang, 1991 and *Shuangheaphaenops* Tian, 2017. As the cave beetle fauna of China is still poorly-known, it is hardly surprising that another highly peculiar species representing another new genus has been revealed in the country (Tian 2017).

In early August 2017, a cave biological survey carried out in Du'an Karst of northern Guangxi, southern China led to the discovery of a very peculiar species belonging to the subfamily Trechinae, family Carabidae. Moreover, it shows a number of most remarkable troglomorphic features amongst subterranean trechines generally. Superficially, its strongly elongated and slender body looks very much like that of a *Giraffaphaenops* species, especially due to the extremely elongated prothorax. However, *Giraffaphaenops* species are known from the Leye-Tianlin karsts of northwestern Guangxi, about 200 km away from Du'an Karst (Deuve 2002, Tian and Luo 2015). In contrast, the elytra in the new species are quite similar to those observed in *Dongodytes* (*s. str.*) Deuve, 1993, yet being much more strongly elongated. In addition, it has many other particular morphological characteristics, such as: (1) Head comparatively short, but sufficiently long and aphaenopsian, bearing multisetiferous pores in frontal areas; (2) Right mandible edentate; (3) Prothorax extremely elongated; (4) Lateral margins of pronotum visible in fore part from above, while long erect setae on disc and two pairs of latero-marginal setae in middle portion present; and (5) Elytra extremely elongated, smooth and glabrous, with striae completely obliterated.

Materials and methods

The beetles were collected in the cave using an aspirator, and kept in vials with 50% ethanol before study, except for a specimen put in a vial with 95% ethanol for molecular analysis.

Techniques and terminology are the same as in Tian (2017).

Taxonomic treatment

***Xuedytes* Tian & Huang, gen. n.**
http://zoobank.org/C8AACC92-F265-45CD-9F50-09DAB01ADFD0

Type species. *Xuedytes bellus* Tian & Huang, sp. n.

Generic characteristics. Highly modified aphaenopsian trechines, body shape, in particular prothorax, similar to that in *Giraffaphaenops*, but elytra generally like in *Dongodytes* (*s. str.*) (Fig. 1); large-sized, with body (especially prothorax and elytra) and appendages thin and extremely elongated, eyeless and unpigmented; fore body part (head including mandibles, plus prothorax) much longer than, or as long as (excluding mandibles) elytra, respectively; body smooth; three pairs of frontal setiferous pores present

on head; mandibles thin and elongated, feebly curved apically, longer than head width, right mandible edentate; labial suture completely missing; mentum bisetose on either side of tooth at base, base broadly concave; mental tooth simple, short and blunt at tip; submentum 8-setose; ligula bisetose at apex (Fig. 2); antennae very long, antennomeres 10 and 11 extending beyond elytral apices. Prothorax similar to that of *Giraffaphaenops*, wider than head, very strongly elongated, much longer than head including mandibles, propleura distinctly tumid in basal 1/3, visible from above; pronotum barrel-shaped, thin and distinctly elongated, lateral margins visible throughout from above, slightly narrower than head; hind latero-marginal setae absent, but two long latero-marginal setae plus two or three additional short setae present from middle to front. Elytra similar to those in *Dongodytes* (*s. str.*), narrow anteriorly and dilated posteriorly, side margins narrowly bordered throughout, shoulders lacking; striae virtually missing, only weakly traceable; two dorsal and the pre-apical setiferous pores present, each with a very long seta; chaetotaxy similar to that in *Dongodytes* (*s. str.*). Protibia smooth, without longitudinal sulcus; protarsomeres not modified in male. Ventrites VII bisetose apically in male, but quadrisetose in female. Male genitalia moderately sclerotized, small, strongly curved ventrally in lateral view, with a quite large and thin sagittal aileron; apical lobe wide and broad in dorsal view; parameres much shorter than median lobe, yet well-developed.

Discussion. *Xuedytes* Tian & Huang, gen. n. is undoubtedly the most remarkable cavernicolous trechine genera as regards the extremely elongated prothorax and elytra. It may be considered as a lineage intermediate between *Giraffaphaenops* and *Dongodytes* (Fig. 3). Superficially it resembles *Giraffaphaenops* because of the similarly thin and strongly elongated body, especially the prothorax. Its elytra, however, are quite similar to those of *Dongodytes* (*s. str.*). The most striking character states of *Xuedytes* are as follows: (1) Prothorax much longer than head; (2) Elytra very narrow and strongly elongated; (3) Three pairs of frontal pores present on head; and (4) Right mandibular tooth obsolete.

Although *Xuedytes* is similar to *Giraffaphaenops*, there are several important differences: (1) Prothorax and elytra much more strongly elongated in *Xuedytes* than in *Giraffaphaenops*; (2) Head subquadrate, slightly convex laterally, not contracted posteriad in *Xuedytes* (vs. inversed triangular, with a well-marked neck constriction in *Giraffaphaenops*); (3) Entire lateral margins of pronotum visible from above in *Xuedytes* (vs. invisible from above in front half in *Giraffaphaenops*); and (4) Two pairs of latero-marginal setae present behind middle of pronotum in *Xuedytes* (vs. absent in *Giraffaphaenops*) (Fig. 3).

Apart from the differences in prothoracic features, *Xuedytes* is easily distinguished from *Dongodytes* (*s. str.*) by the following characteristics: (1) Head thicker and broader, not narrowed posteriad in *Xuedytes* (vs. thinner and evidently narrowed posteriad, forming a long and distinct neck constriction in *Dongodytes*); (2) Three pairs of frontal pores present in *Xuedytes*, instead of only one pair in *Dongodytes*; (3) Elytral striae completely obliterated in *Xuedytes* (vs. partially visible in *Dongodytes*) (Fig. 3).

Furthermore, differences between the new genus and both *Giraffaphaenops* and *Dongodytes* are also evident regarding the structure of the male genitalia (Fig. 4). The median lobe of the aedeagus is shorter in *Xuedytes*, but thicker, especially so at the base, with a thinner, almost transparent sagittal aileron.

Etymology. "Xue + dytes". "Xue" in Chinese means "cave", to indicate that the beetles are cavernicolous. Gender masculine.

Generic range. China (Guangxi Zhuang Autonomous Region).

***Xuedytes bellus* Tian & Huang, sp. n.**
http://zoobank.org/13622878-92B3-43B7-B253-426CE076E37F
Figs 1–5

Holotype. Male, Cave II, southeastern Du'an Yao Autonomous County, Hechi Shi (=Prefecture), northern Guangxi Zhuang Autonomous Region, southern China, VIII-08-2017, leg. Mingyi Tian, Sunbin Huang, Dianmei Wang and Mengzhen Chen; paratypes: 2 males and 1 female, IBID. All type material is deposited in the insect collection of South China Agricultural University, Guangzhou.

Diagnosis. A large-sized, blind, cave-adapted trechine, remarkably modified morphologically, with both prothorax and elytra highly elongated and slender so that body five times longer than wide, antennae slightly shorter than body including mandibles, extending beyond elytral apices; head, pronotum and base of elytra covered with sparse erect setae. Habitus as in Figs 1 and 3.

Description. Length: 8.3–9.0 mm (from apex of right mandible to elytral apex) or 7.5–8.6 mm (from labrum to elytral apex); width: 1.4–1.5 mm.

Body yellowish brown, but antennae, palps and tarsi pale; strongly shining; head, pronotum and base of elytra covered with rather long and sparse setae, other parts of elytra glabrous, underside of fore body excluding pleurae, meso- and metasterna pubescent, abdominal ventrites densely pubescent; microsculptural engraved meshes transverse striate on head, pronotum and elytra; fore body very strongly elongated, much longer than elytra, (HLm+PrL)/EL = 1.55–1.60.

Head oblong subquadrate, much longer than wide, HLm/HW = 3.02–3.03, HLl/HW = 2.02–2.04; genae fairly well developed, broadly dilated on sides, widest at about middle of head from neck to clypeal margin, gradually tapered posteriorly; frons and vertex moderately convex, frontal furrows moderately defined, strongly diverging posteriorly, ending level with middle frontal pores; clypeus transverse, 6-setose; labrum transverse, frontal margin nearly truncate, 6-setose; three pairs of frontal setiferous pores present; mentum and submentum completely fused, mentum bisetose on either side of tooth at base, mental tooth short and blunt at apex, basal fovea broadly concave; submentum 8-setose; palps thin and very slender, glabrous except for labial palpomere 2 which is bisetose on inner margin; 2nd labial palpomere 1.40 times longer than 3rd; 3rd maxillary palpomere 1.25 times longer than 4th; suborbital pore much closer to base than to submentum (Fig. 2). Antennae thin and very long, 1st antennomere shortest and stoutest, 4th longest, 11th longer than 10th, length ratios of antennomere 1 to 11 as 1.00 / 1.36 / 3.07 / 3.55 / 2.77 / 2.81 / 2.52 / 2.10 / 1.94 / 1.65 / 1.94.

Prothorax (Fig. 3a) much longer than head including mandibles, PrL/HLm = 1.15–1.17, PrL/HLl = 1.70–1.72, widest at about 1/5 off base, nearly 3 times as long as wide,

Figure 1. Habitus of *Xuedytes bellus* Tian & Huang, gen. et sp. n., holotype male.

Figure 2. Head (ventral) of *Xuedytes bellus*, a paratype female.

PrL/PrW = 2.94–2.95, slightly wider than head, PrW/HW = 1.18–1.19, evidently wider than pronotum, PrW/PnW = 1.27–1.30. Pronotum very strongly elongated, tube-like in front half which is narrow and nearly parallel-sided; convex at about basal 1/5 where the widest point lies, then gently sinuate before hind angles which are obtuse and rectangular, fore angles rounded; nearly four times longer than wide, PnL/PnW = 3.84, slightly narrower than head, PnW/HW = 0.91–0.92, base slightly concave, wider than front, PbW/PfW = 1.27, front convex; lateral sides finely bordered throughout, base and front unbordered;

Figure 3. Habitus of three highly modified aphaenopsian beetles (chaetotaxy indicated by white points) **a** *Xuedytes bellus*, holotype male **b** *Giraffaphaenops clarkei* Deuve, 2002, male **c** *Dongodytes grandis* Uéno, 1998, male.

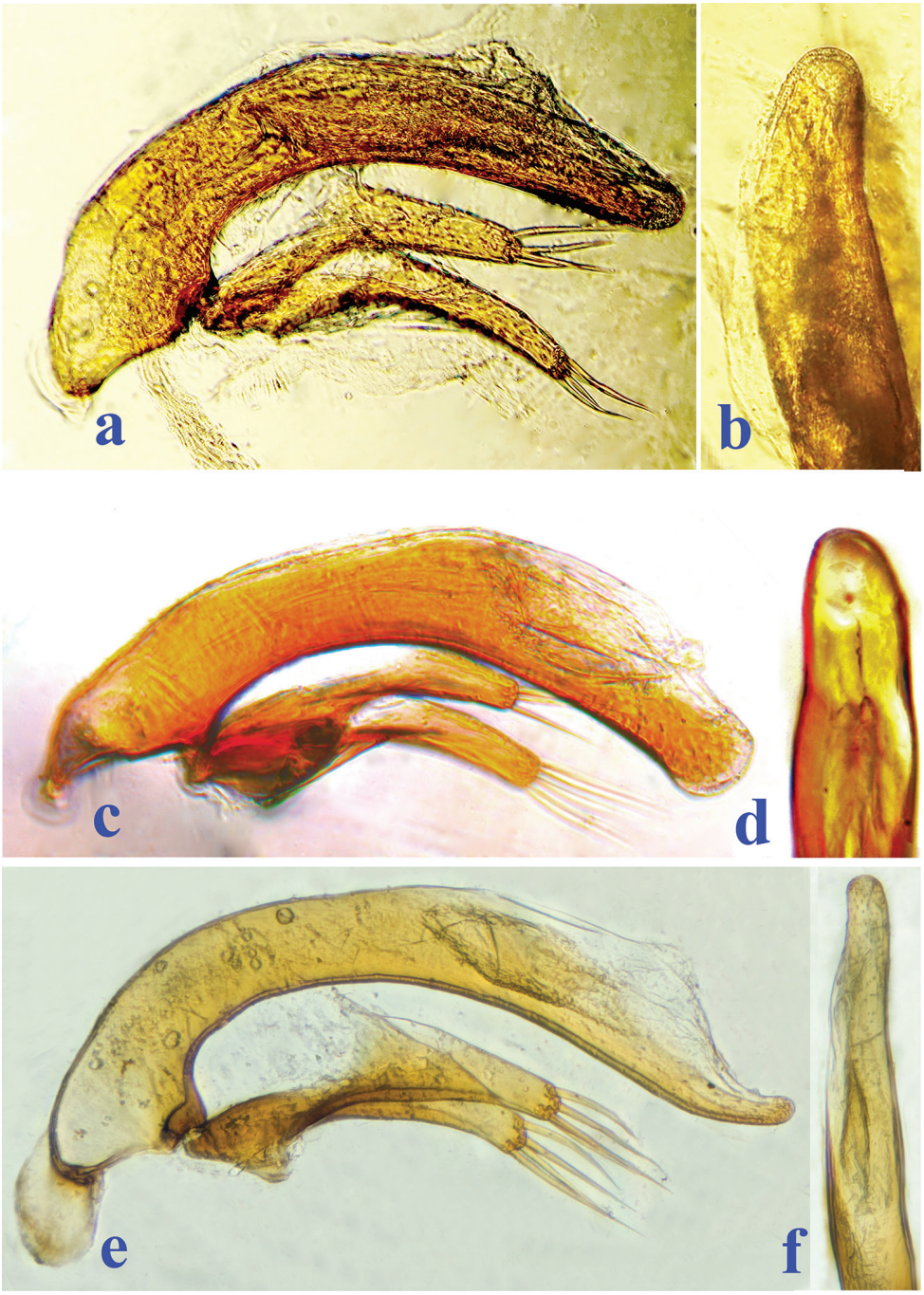

Figure 4. Male genitalia of three highly modified aphaenopsian beetles, median lobe and parameres in lateral, and apical lobe in dorsal views, respectively **a, b** *Xuedytes bellus* **c, d** *Giraffaphaenops yangi* Tian & Luo, 2015 **e** *Dongodytes grandis* Uéno, 1998.

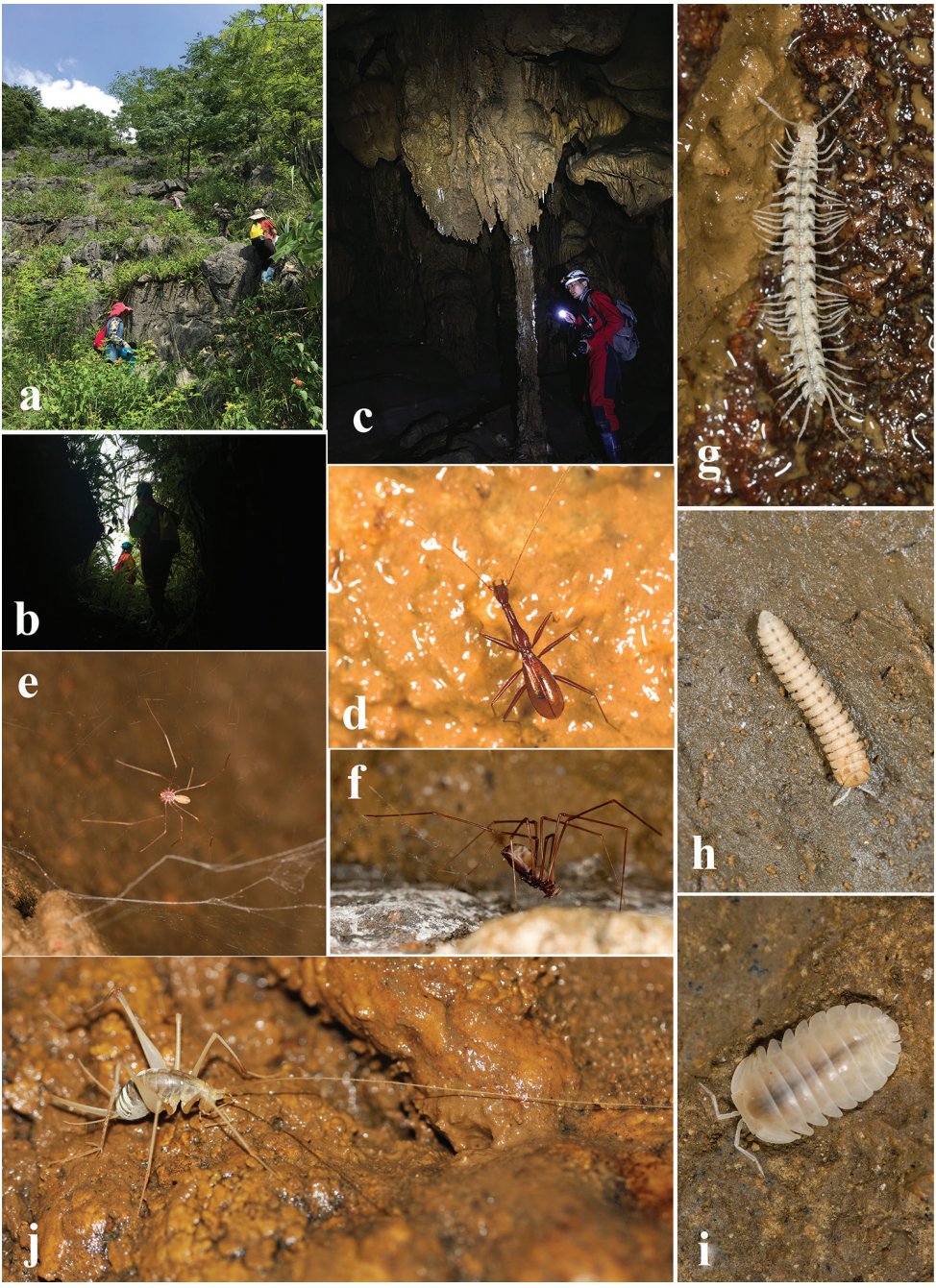

Figure 5. Cave II, southeastern Du'an, the type locality of *Xuedytes bellus*, and sympatric cave animals **a, b** cave environs and opening **c** a chamber in the cave where the beetles were collected **d** a running beetle in cave **e, f** cave spiders **g, h** cave millipedes **i** a cave woodlouse **j** a cave cricket.

basal latero-marginal setae absent, two latero-marginal setae present in about middle portion, with three or four additional short setae in fore part; disc strongly convex in front and moderately convex in basal half, deeply concave a little before middle; median line clear, but shallow, basal transverse impression well-marked, short; scutellum fairly large.

Elytra (Fig. 3a) very strongly elongated ovate, much longer than wide, EL/EW = 2.46; longer than prothorax, EL/PrL = 1.58–1.59, almost twice as wide as prothorax, EW/PrW = 1.90–1.91; distinctly dilated posteriorly, widest at about 3/5 of elytra off base, lateral sides smooth, not ciliate, finely bordered throughout, marginal gutters well-marked; disc distinctly convex, but evidently concave near base; striae virtually missing, yet more or less traceable, intervals moderately convex. Chaetotaxy (Fig. 3a): dorsal pores with stout and long setae, two dorsal setiferous pores present on 3rd stria at about 1/3 and 3/5 of elytra off base, respectively; pre-apical pore at about apical 1/6 of elytra, much closer to elytral suture than to apical margin; basal pore located between scutellum and marginal gutter; marginal umbilicate pores not aggregated, pores 1–3 and 10 near marginal gutter, other pores distant from gutter; humeral groups with pores 1 and 4 widely isolated, 2 and 3 close to each other, distance from pore 4 to 3 subequal to 5; middle group closely spaced, distance of pore 5 and 4 subequal to that of pore 5 and 6; apical group composed of four pores.

Legs slender and long, bearing short pubescence; fore and middle femora sparsely setose; fore tibia smooth, with neither a longitudinal furrow nor a sulcus; 1st tarsomere shorter than, slightly longer than, and much longer than 2nd–4th tarsomeres combined in fore, middle, and hind legs, respectively.

Male genitalia (Fig. 4a, b). Aedeagus quite small and short, distinctly curved ventrally in middle portion in lateral view, then broad at apex; inner sac with a fairly large copulatory piece, the latter about 1/3 as long as median lobe; base quite large, open ventrally, with a hyaline sagittal aileron; in dorsal view, apical lobe fairly stout, slightly sinuate on right side, rounded at apex. Parameres short and quite elongated, each bearing four long apical setae.

Etymology. "*Bellus*", in Latin meaning "beautiful", to refer to this beautiful aphaenopsian beetle.

Distribution. China (Guangxi: Du'an). Known only from Cave II.

This cave maintains a natural condition, opening on a small hill on the northern bank of the Hongshui River. The entrance is surrounded by dense bushes and not readily accessible (Fig. 5a, b). The total length of the cave is still unknown, but said to be about 200 m, according to local people. It is sufficiently wet inside the gallery and is good for cave fauna. The beetles were found running on walls and stalactites (Fig. 5c, d), sympatric with spiders (Fig. 5e, f), millipedes (Fig. 5g, h), woodlice (Fig. 5i) and crickets (Fig. 5j).

Acknowledgements

We are most grateful to Dr. Thierry Deuve (National Museum of Natural History, Paris) for his comments and suggestions that proved to be helpful in improving an early draft of this manuscript. Our particular thanks go to Dr. Sergei Golovatch (Russian Academy of Sciences, Moscow) for checking the English. This study is sponsored by

the Nanjing Institute of Environmental Sciences, Ministry of Environmental Protection, through a biodiversity conservation project which focused on cave biodiversity, and a project of the Specialized Research Fund for the Doctoral Program of Higher Education of China (Grant no. 20134404110026).

References

Deharveng L, Bedos A (2012) Diversity patterns in the tropics. In: White WB, Culver DC (Eds) Encyclopedia of Caves. Academic Press, Chennai, 238–250. https://doi.org/10.1016/B978-0-12-383832-2.00032-3

Deuve T (1993) Description de *Dongodytes fowleri* gen. n., sp. n., Coléoptère troglobie des karsts du Guangxi, Chine (Adephaga, Trechidae). Bulletin de la Société entomologique de France 98: 291–296.

Deuve T (2002) Deux remarquables Trechinae anophthalmes des cavités souterraines du Guangxi nord-occidental, Chine (Coleoptera, Trechidae). Bulletin de la Société entomologique de France 107: 515–523.

Deuve T, Tian MY (2016) Descriptions de sept nouveaux Trechini cavernicoles de la Chine continentale (Coleoptera, Caraboidea). Bulletin de la Société entomologique de France 121(3): 343–354.

Fang J, Li WB, Tian MY (2016) Occurrence of cavernicolous ground beetles in Anhui Province, eastern China (Coleoptera, Carabidae, Trechinae). ZooKeys 625: 99–110. https://doi.org/10.3897/zookeys.625.9846

Huang SB, Cen YJ, Tian MY (2017) A new genus and a new subgenus of cavernicolous beetles from Furong Jiang valley, southwestern China (Coleoptera: Carabidae: Trechinae). Annales de la Société entomologique de France (N.S.) 53(4): 286–295. https://doi.org/10.1080/00379271.2017.1344566

Tian MY (2017) A new highly cave-adapted trechine genus and species from northern Guizhou Province, China (Coleoptera, Carabidae, Trechinae). ZooKeys 643: 97–108. https://doi.org/10.3897/zookeys.643.11050

Tian MY, Huang SB, Wang XH, Tang MR (2016) Contributions to the knowledge of subterranean trechine beetles in southern China's karsts: five new genera (Insecta: Coleoptera: Carabidae: Trechini). ZooKeys 564: 121–156. https://doi.org/10.3897/zookeys.564.6819

Tian MY, Luo XZ (2015) A new species of the highly modified hypogean genus *Giraffaphaenops* Deuve, 2002 (Coleoptera: Carabidae: Trechinae). Zootaxa 3911: 581–588. https://doi.org/10.11646/zootaxa.3911.4.7

Zhao DY, Tian MY (2016) A new genus and species of troglobitic ground beetle from eastern Guizhou, Southwest China (Coleoptera: Carabidae: Trechinae). Zootaxa 4097(3): 434–441. https://doi.org/10.11646/zootaxa.4097.3.11

ZooKeys 725: 49–69 (2017)
doi: 10.3897/zookeys.725.13675
http://zookeys.pensoft.net

DATA PAPER

A peer-reviewed open-access journal
ZooKeys
Launched to accelerate biodiversity research

Whitefly predation and extensive mesonotum color polymorphism in an *Acletoxenus* population from Singapore (Diptera, Drosophilidae)

Wong Jinfa[1], Foo Maosheng[2], Hugh T. W. Tan[1], Rudolf Meier[1,2]

1 *Department of Biological Sciences, National University of Singapore, Singapore 117543* **2** *Lee Kong Chian Natural History Museum, National University of Singapore, Singapore 117377*

Corresponding author: *Rudolf Meier* (meier@nus.edu.sg)

Academic editor: *V. Silva* | Received 14 May 2017 | Accepted 12 September 2017 | Published 29 December 2017

http://zoobank.org/A3484B14-F925-4CA8-8577-9ABDDACB5715

Citation: Wong, J, Foo, M, Tan HTW, Meier R (2017) Whitefly predation and extensive mesonotum color polymorphism in an *Acletoxenus* population from Singapore (Diptera, Drosophilidae). ZooKeys 725: 49–69. https://doi.org/10.3897/zookeys.725.13675

Abstract

Acletoxenus is a small genus of Drosophilidae with only four described species that are closely associated with whiteflies (adults and larvae). Here, the first video recordings of larvae feeding on whiteflies (*Aleurotrachelus trachoides*) are presented. Typical morphological adaptations for predation by schizophoran larvae are also described: the larval pseudocephalon lacks a facial mask and the cephaloskeleton is devoid of cibarial ridges that could be used for saprophagy via filtration. Despite being a predator, *Acletoxenus* is unlikely to be a good candidate for biological control of whiteflies because the life cycle is fairly long (24 days), lab cultures could not be established, and the puparia have high parasitization rates by a pteromalid wasp (*Pachyneuron leucopiscida*). Unfortunately, a confident identification of the Singapore *Acletoxenus* population to species was not possible because species identification and description in the genus overemphasize coloration characters of the mesonotum which are shown to be unsuitable because the Singapore population has flies with coloration patterns matching three of the four described species. Based on morphology and DNA sequences, the population from Singapore is tentatively assigned to *Acletoxenus indicus* or a closely related species.

Keywords

Acletoxenus, Diptera, Drosophilidae, predatory maggot, Singapore, whitefly

Introduction

Drosophilidae contains >3950 described species in 77 genera and two subfamilies (Bächli 2015). The best-known species is *Drosophila melanogaster* which is typical for most in the family in that it has saprophagous larvae. However, the larvae of many other drosophilid species utilize a wide variety of substrates and the natural history of the family is full of surprising convergence. For example, associations between drosophilid larvae and spittlebugs have evolved at least three times (Thompson and Mohd-Saleh 1995) and gave rise to a species-rich clade with more than 100 species (*Cladochaeta*: (Wheeler and Patterson 1952, Grimaldi and Nguyen 1999). Many other drosophilid species have larvae that prey on eggs, including the species in the *Drosophila simulivora* species group whose aquatic larvae feed on the eggs and larvae of Simuliidae, Chironomidae, and Odonata (Aubertin 1937, Tsacas and Disney 1974). Another case of surprising convergence is found in Steganinae. *Rhinoleucophenga* (Steganinae) and *Acletoxenus* have larvae that are predators of Sternorrhyncha (Malloch 1929, Clausen and Berry 1932, Ashburner 1981, Parchami-Araghi and Farrokhi 1995, Culik and Ventura 2009, Lambkin and Zalucki 2010, Yu et al. 2012). Yet, *Rhinoleucophenga* and *Acletoxenus* are distantly related; i.e., larval predation of Sternorrhyncha by steganine larvae likely evolved twice.

Recently, an *Acletoxenus* population was discovered in Singapore that was associated with whiteflies feeding on chilli plants, *Capsicum annuum* L. (Solanaceae). The population was studied in greater detail and we present the first video recordings documenting larval predation , provide a larval description, and determine the length of the life cycle. Lastly, we comment on the inappropriateness of using mesonotum coloration for species identification and description in *Acletoxenus*. The color patterns of the mesonotum are shown to be very variable within a single population. Yet, the description and identification of the four currently accepted species rely quite heavily on color pattern and chaetotaxy characters (Table 1, Fig. 1). This is partially due to the fact that the type of one of the species is female (*Acletoxenus indicus* Malloch, 1929) so that a comparison of male genitalia with the remaining species cannot be carried out. Fortunately, male type material is available for *Acletoxenus formosus* (Leow, 1864) (see Bächli 1984), *Acletoxenus quadristriatus* Duda, 1936, and *Acletoxenus meijerei*. The latter has syntypes in Berlin (Bächli 1984: sex not specified) and a male syntype in Amsterdam (Bächli 1987: now Leiden), but the location of the latter is currently unknown (Pasquale Cliliberti, pers. comm.).

Materials and methods

Acletoxenus recruitment, collection, and identification

Chili (*Capsicum annuum* 'Yang Jiao') were grown along a building corridor of Block S2 of the Kent Ridge campus of the National University of Singapore (1°17'45.01"N, 103°46'41.08"E). Whiteflies naturally appeared on the chilli plants which in turn attracted

Table 1. Morphological differences between the described species of *Acletoxenus*.

Acletoxenus formosus (Leow, 1864)	Proclinate orbital bristles not noticeably shorter than the anterior reclinate bristles (Malloch 1929)	Mesonotum almost entirely black with yellowish tan lateral margins (Malloch 1929, Bock 1982)
	Proclinate orbital bristles noticeably shorter than anterior reclinate bristles (Bächli et al. 2004)	
Acletoxenus indicus Malloch, 1929	Proclinate orbital bristles noticeably shorter than anterior reclinate bristles (Malloch 1929)	Mesonotum with central black vitta and two vittas on each side that are interrupted at suture and extend sublaterally (Malloch 1929)
Acletoxenus meijerei Duda, 1924	Proclinate orbital bristles not noticeably shorter than anterior reclinate bristles (Duda 1924, Malloch 1929)	Mesonotum with two broad dark vittas which are more or less confluent behind the suture and do not extend to the hind margin margin (Duda 1924, Malloch 1929, Bock 1982)
Acletoxenus quadristriatus Duda, 1936	Proclinate orbital bristles noticeably shorter than the anterior reclinate bristles (Malloch 1929)	Mesonotum with four broad dark longitudinal vittas coalescing or slightly separated, with the medial vittas reaching to rear third while the lateral ones almost to the posterior dorsocentral (Malloch 1929, McEvey 2016)

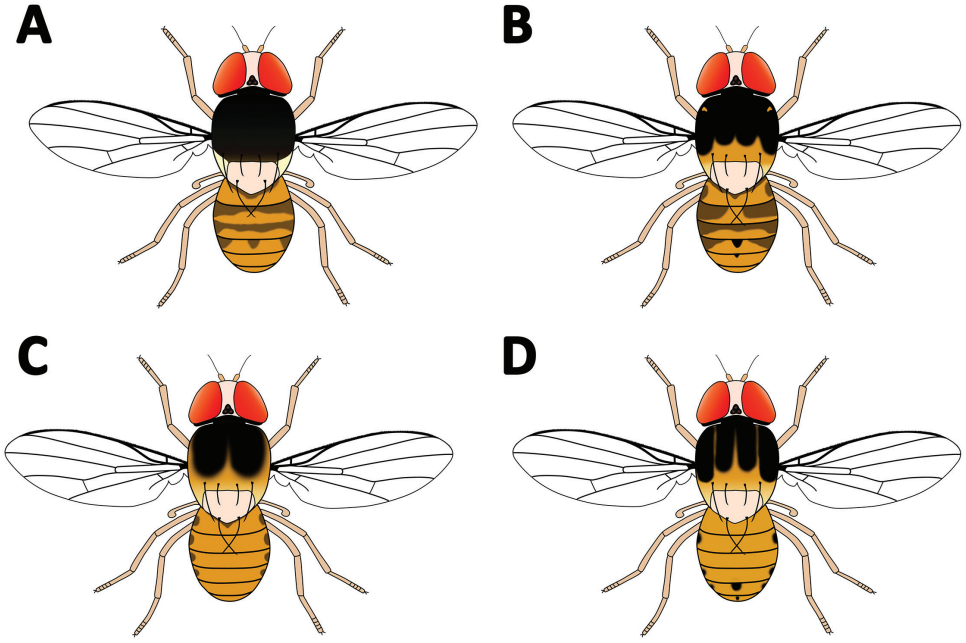

Figure 1. Morphology of **A** *Acletoxenus formosus* **B** *A. indicus* **C** *A. meijerei,* and **D** *A. quadristriatus.*

Acletoxenus. Adult flies were captured and either stored in 100% ethanol or flash frozen with liquid nitrogen before being stored in a freezer at –80 °C. Three morphotypes were identified based on the pigmentation pattern of the mesonotum. These morphotypes corresponded to the descriptions and figures (see McEvey 2016) of *Acletoxenus formosus,*

Acletoxenus indicus, and *Acletoxenus quadristriatus* (Malloch 1929, Duda 1936, Bock 1982). The relative abundance of the three morphotypes was determined, and Fisher's exact probability 2 × 3 test was used to test whether the differences were significant. Samples were also sent to Dr. Gerhard Bächli from the Zoological Museum of the University of Zurich and Dr. Shane McEvey from the Australian Museum for identification. Samples of the whiteflies' fourth instars were sent to Dr. Paul De Barro (CSIRO).

DNA barcoding

Genomic DNA was extracted from whole specimens of using QIAGEN DNeasy Blood & Tissue Kits. Polymerase chain reaction (PCR) was used to amplify the target mitochondrial cytochrome c oxidase, subunit I (COI) gene using primer pairs (Table 2). The PCR mixture (20 μL) contained 2.5 μL of buffer, 2 μL of dNTP, 1 μL of each primer of a primer pair, 0.15 μL of Ex Taq and 5 μL of template DNA. The program consisted of 40 cycles of amplification (30 sec of denaturation at 94 °C, 30 sec of annealing at 52 °C and 1 min of extension at 72 °C). The PCR products were then purified using BIOLINE SureClean according to the manufacturer's protocol before cycle sequenced using BigDye Terminator ver. 3.1 Cycle Sequencing Kit. The cycle sequencing mixture (10 μL) contained 2 μL of buffer, 0.5 μL of BigDye, 1.75 μL of each primer and 2 μL of template DNA. The program consisted of 1 min of initial denaturation at 95 °C, followed by 25 cycles of amplification (30 sec of denaturation at 94 °C, 30 sec of annealing at 52 °C and 4 min of extension at 60 °C). An ABI 3730xl sequencer was used for sequencing. Reference COI sequences for *Acletoxenus formosus* (700 base pairs) and *Acletoxenus indicus* (1536 base pairs) were downloaded from GenBank (accession numbers EF576933, HQ701131). The sequences for the different *Acletoxenus* morphotypes from Singapore were then aligned against the reference sequences from GenBank using MAFFT ver. 7 using the default settings (Katoh and Standley 2013). Afterwards, MEGA6 was used to add the new sequences for *Acletoxenus* in order to determine pairwise distances (Tamura et al. 2013)

Are *Acletoxenus* predators?

Behavioral observations of *Acletoxenus* larvae and adults were made in the field and ex-situ. The ex-situ observations were based on individuals that were placed on whitefly infested leaves under a dissection microscope. Behavior was video-taped using a Canon LEGRIA HF S30 video camera. In addition, the morphology of the larvae and adults was studied in order to determine whether the species has features that are known to be typical of predatory larvae. For comparative purposes, the larvae of a known saprophage, *Drosophila melanogaster*, were also studied. All larvae were killed in hot soapy water before dehydration via a graded ethanol series (see Meier 1995, 1996). In order

Table 2. Primer pairs used in PCR reaction.

Species	Primer name	Primer sequence
Acletoxenus (2 individuals from each sex and morphotype)	LCO1490	5'-GTCAACAAATCATAAAGATAT TGG-3'
	HCO2198	5'-TAAACTTCAGGGTGACCAAAAAATCA-3'
	s2183	5'-CAACATTTATTTTGATTTTTTGG-3'
	a3014	5'-TCCAAT GCACTAATCTGCCATATTA-3'
Whitefly prey	mlCOIintF	5'-GGWACWGGWTGAACWGTWTAYCCYCC-3'
	jgHCO2198	5'-TAIA CYTCIGGRTGICCRAARAAYCA-3'
Parasitoid wasp	LepF	5'-ATTCAACCAATCATAAAGATATTGG-3'
	LepR	5'-TAAACTTCTGGATGTCCAAAAAATCA-3'

to study the cephaloskeleton, the larvae were cut at the mid-section and soaked in potassium hydroxide for 15 minutes (light microscopy with Olympus BX51) or three days (confocal microscopy: mounted on glass slide with Euparal; imaging with a Zeiss LSM 510 META at 20× using 488 nm wavelength with LP505 filter). The confocal images were rendered into a three-dimensional model with Amira 5.3.3.

Life cycle of *Acletoxenus*

Field observations were used for determining the length of the life cycle of *Acletoxenus* because attempts to rear the species under laboratory conditions failed. Individual larvae on chili plant leaves infected with whiteflies were regularly tracked. Upon discovery of an *Acletoxenus* egg, larva, or puparium, its length was measured with Vernier calipers and the leaf was labelled. On the following day, all labelled leaves were checked for the presence of the same individual as determined by stage and size. If a larva was no longer present, the leaves in closest proximity were checked until a larva was located. The larva was deemed to be the same individual if its length was the same or slightly longer. All larvae that could no longer be located were excluded from determining the duration of the larval stage. If there were multiple larvae on a leaf, data were only collected if the lengths of the larvae were sufficiently different to distinguish individuals.

In order to determine adult longevity, adult emergence was documented by collecting puparia (n= 34) and placing them on moist tissue paper in an enclosed plastic container. Emergence was recorded with a Canon LEGRIA HF S30 video camera (see above). Newly emerged *Acletoxenus* were then used to determine the life span of adults by maintaining them in Petri dishes in an air-conditioned laboratory at 25 °C. The Petri dishes contained a piece of whitefly-infested leaf placed on a moist piece of tissue paper and a cotton ball soaked in honey. The leaves were changed every other day and the cotton ball weekly to ensure an adequate supply of food. The lifespan of each adult was calculated by counting the number of days from emergence to death.

Parasitism

In the last four months of the experiment, the population of *Acletoxenus* declined and many *Acletoxenus* puparia were black instead of green. Parasitization was suspected and a few dark puparia were subsequently placed on wet tissue paper in a plastic container. Parasitoids emerged and were killed in 100% ethanol before identifying them using taxonomic keys (Mani 1939, Gupta and Poorani 2009). Photographs of the parasitoid wasp were also taken with a Nikon EOS-1 camera (Visionary Digital). Only empty parasitized puparial cases retained some dark brown pigments, which allowed for determining of the monthly rate of parasitism based on empty puparia (May–July 2014).

Results and discussion

No confident species identification despite a wealth of knowledge

The flies were confirmed to belong to *Acletoxenus* by S McEvey (pers. comm.) and G. Bächli (pers. comm.). Specimens representing the Singapore *Acletoxenus* population have proclinate orbital setae that are noticeably shorter than the anterior reclinate setae (Fig. 3). According to the identification key in Malloch (1929; see couplet 1), only two of the four described species of *Acletoxenus* have this trait (*A. indicus*; *A. quadristriatus*), but note that Bächli et al.'s (2004) redescription of *A. formosus* mentions that this species also has noticeably shorter anterior reclinate setae. This means that the bristle character observed in the Singapore specimens only excludes *A. meijerei*. It was hoped that species identification would be possible based on the mesonotum coloration patterns that feature prominently in the taxonomic literature on *Acletoxenus*. However, the Singapore population includes specimens that match the patterns of three of the four described species of *Acletoxenus* (Fig 2): the *A. quadristriatus* morphotype is only present in males while the other two morphotypes are found in both sexes (Fig. 2). Gender and morphotypes were significantly co-dependant (Fisher's exact probability test, p-value < 0.01) with the *A. formosus* morphotype being more common in females. An additional character system that is discussed in the literature is the coloration patterns of the abdomen. However, the dorsocentral black mark on the fourth tergite and a much smaller mark of similar shape on the fifth tergite are found in all morphotypes (Fig. 2). The coloration patterns on the remaining tergites are also variable in the Singapore population and range from broadly blackened tergites (Fig. 2A) to reduced spots (Fig. 2B, C). Note that such intraspecific variability has previously been noted for *A. formosus* (Collin 1902, Malloch 1929, Bock 1982) but it is here confirmed for yet another *Acletoxenus* species.

For two reasons, we are confident that this morphological variability in the Singapore population was indeed intraspecific. Firstly, it appears unlikely that more than one species was found on the same hallway of a building on NUS campus. Secondly, COI barcodes were sequenced for two individuals of each sex and morphotype. When these

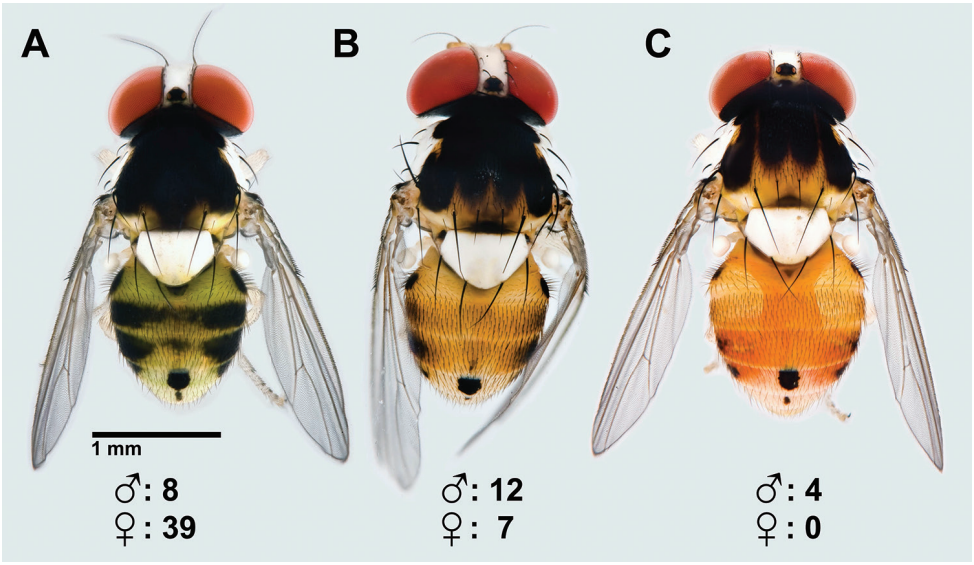

Figure 2. Mesonotum color patterns **A** entirely black **B** with central black vitta that is split and connected to two other vittas on each side, and **C** four dark longitudinal stripes; all three morphotypes were bred from larvae collected together on the same host plant in Singapore.

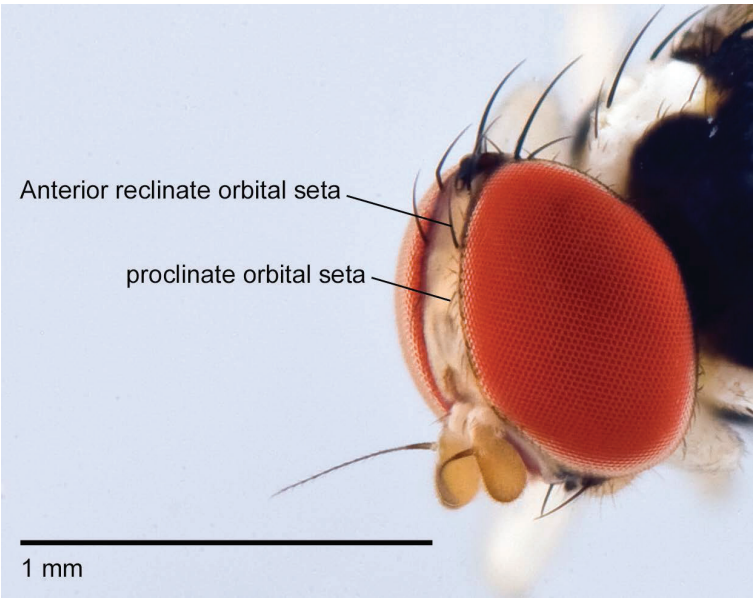

Figure 3. *Acletoxenus* sp. proclinate orbital setae noticeably shorter than the anterior reclinate setae.

sequences were aligned and compared, the average pairwise distance between the 12 individuals from Singapore was 0.06% which is compatible with intraspecific variability and rarely observed between species of Diptera (Meier 2008, Meier et al. 2008).

When the sequences were compared with those in Genbank, the best uncorrected pairwise match was 1.69% (Srivathsan and Meier 2012) and the matching sequence belonged to a specimen from China that was identified as *Acletoxenus indicus* (Accession number: HQ701131.1). The match to a sequence for *A. formosus* (Accession number EF576933.1) was much poorer (11.14%) and is consistent with being interspecific (Meier et al. 2008). No sequences are known for *Acletoxenus quadristriatus* which is only known from Thursday island and was described after *A. indicus*. Overall, there is no described feature that distinguishes the Singapore population from *A. quadristriatus* or *A. indicus* but the latter is hypothesized to have a wide distribution that is compatible with the occurrence of the species in Singapore; i.e., based on overall evidence, we believe that the Singapore population either belongs to *A. indicus* or represents a closely related species because a barcode distance of 1.69% is reasonably common within but also between species given that COI is not directly involved in speciation and only measures time of divergence (Kwong et al. 2012). If *A. indicus* is indeed polymorphic and widespread, it raises the possibility that *A. quadristriatus* could be a junior synonym of *A. indicus*. However, this issue can only be addressed by detailed study of all types. A stumbling block will be the fact that *A. indicus* was described based on a female; i.e., one would have to find a species-specific character in a female that can distinguish this species from all others.

Overall, it is frustrating that despite having obtained considerable amounts of morphological and molecular data, the specimens could not be identified confidently to species. In the case of *Acletoxenus*, it was the widespread use of color pattern characters and a species description based on a female that caused this problem. But identification problems are so common that they play a major role in the decline of natural history research (Tewksbury et al. 2014). Many observations on insects and other animals are made but they are difficult to communicate because the species involved cannot be identified even if a voucher is collected. This problem is particularly severe in the tropics where the species diversity is high (e.g., Basset et al. 2012), most species are undescribed (e.g., Riedel et al. 2010), and many old descriptions are so superficial that they cannot be used for species identification (Meier 2017). Arguably, the best way forward will be higher quality (re)descriptions (Tan et al. 2010, Ang et al. 2013b, Rohner et al. 2014), digital reference collections including types and specimens identified by taxonomic experts (Ang et al. 2013a), and DNA barcodes (Hebert et al. 2003). The latter are becoming sufficiently cost-effective (Wong et al. 2014, Meier et al 2016) that they can become widely available. They can be used to obtain approximate species identifications once more of the fauna is barcoded (Kwong et al. 2012). This can now happen rapidly through low-cost "NGS barcoding" (Meier et al. 2016). Hopefully biologists will start collecting vouchers associated with interesting natural history observations that can be published in journals such as the Biodiversity Data Journal (Smith et al. 2013). The natural history observations can be included in such publications where the video evidence can be embedded in the publication (e.g., Ang et al. 2013b).

Are *Acletoxenus* Predators?

The first video evidence that the larvae are indeed predators of whiteflies is presented here (Movie 1). The larvae move on infected leaves by raising and swinging their anterior end ("pseudocephalons") from side to side (Movie 2). If no prey is touched, the mouth hooks are used to anchor the anterior end of the larva. After anchoring, the abdominal segments move forward via contraction (Movie 3). However, if prey is touched, the larva uses its mouth hooks to stab a whitefly puparium whose content is then imbibed (Fig. 4A, Movie 2). When a whitefly puparium is empty and gets dislodged from the leaf, it is often glued to the body of the *Acletoxenus* larva using a mucus secreted by the larva (Clausen and Berry 1932, Ashburner 1981). Similarly, whitefly eggs and wax are often found glued to the larva. Overall, the larvae move little and slowly (see Movie 3) and Clausen and Berry (1932) even stated that *Acletoxenus indicus* larvae are largely inactive and never leave the leaf upon which they were born. However, this is not the case for the *Acletoxenus* population in Singapore. Larvae did move to other leaves in order to locate prey, albeit at a very slow speed. All movements (forward or backward) were via peristaltic contractions of the abdominal segments (Movie 3).

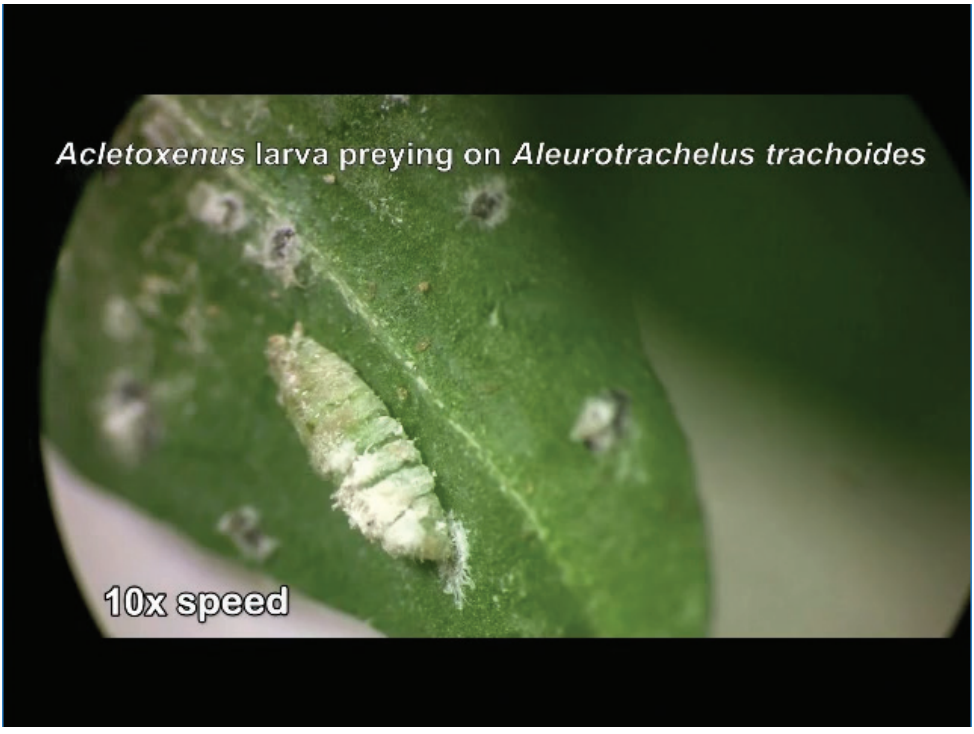

Movie 1. *Acletoxenus* cf. *indicus*: larval predation behavior.

Movie 2. *Acletoxenus* cf. *indicus*: larval feeding behavior and camouflage.

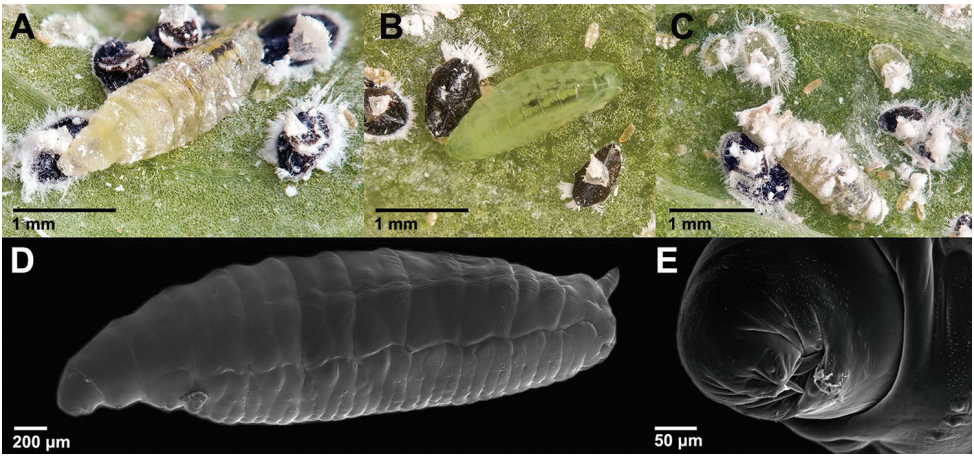

Figure 4. *Acletoxenus* cf. *indicus* larvae **A** feeding on whitefly **B** have a green colored body, and **C** are usually covered in whitefly wax and instars **D** SEM Lateral view, and **E** SEM of pseudocephalon with strongly reduced facial mask.

As discussed in Courtney et al. (2000), most predatory cyclorrhaphan larvae have strongly reduced facial masks that often lack the cirri and oral ridges that are present in saprophagous Cyclorrhapha larvae for rasping and directing bacteria into the mouth

Movie 3. *Acletoxenus* cf. *indicus*: larval movements.

opening (Dowding 1967, Roberts 1971). This is also the case for saprophagous ephydroid larvae (Ferrar 1987, Kirk-Spriggs et al. 2002, Wipfler et al. 2013). The pseudocephalon of *Acletoxenus* fits the pattern of a predatory cyclorrhaphan larva. The preoral cavity on the ventral side of the pseudocephalon has few oral ridges flanking the mouth and lacks a well-developed facial mask (absence of cirri; Fig. 4E). The cephaloskeleton of *Acletoxenus* is furthermore semi-translucent and less sclerotized than that of *Drosophila melanogaster* and lacks a pharyngeal filter (Fig. 5) while it was clearly visible for *D. melanogaster* larvae (Fig. 6). Additional adaptations for being a diurnal predator are found on the remaining larval body segments. The larvae are so weakly sclerotized that the internal fat body is visible. It turns from cream-colored in early instars to greenish in third instars (3–4 mm long, 1mm wide; Fig. 4) and thus provides camouflage on leaves (Movie 1 and 2). Camouflage is also the most likely explanation for why the larva collects and glues whitefly wax, egg and puparium onto its body (Fig. 3C; Clausen and Berry 1932, Ashburner 1981). Because pupation of schizophoran flies takes place within the last larval skin, this camouflage extends to the pupal stage of *Acletoxenus* (Fig. 10; ca. 3.3 mm long, 1.3 mm wide) (Fig. 10); the pupal integument remains translucent and reveals the green color of the fat body and later the red eyes of the developing adult (Fig. 10C). The puparia are glued via a flattened ventral surface to leaf surfaces (Clausen and Berry 1932) and the ability to adhere to surfaces is retained

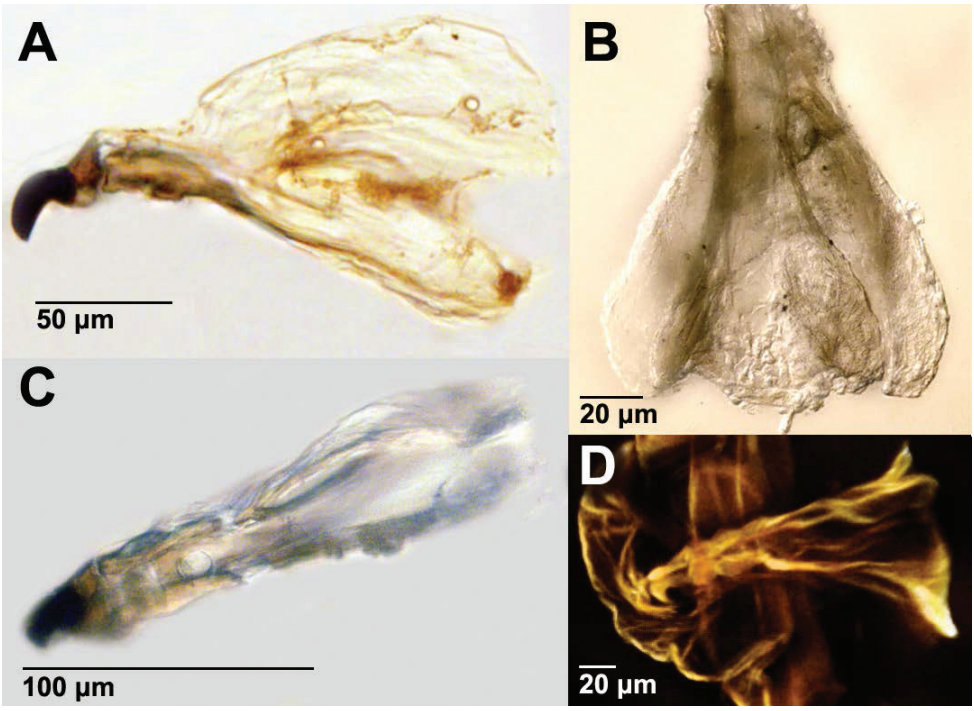

Figure 5. *Acletoxenus* cf. *indicus* larval cephaloskeleton **A** lateral view with light microscope **B** ventral view close-up with light microscope **C** ventral view with light microscope, and **D** ventral view with confocal microscope, showing a lack of pharyngeal filter.

even when the puparia are dislodged and placed on moist tissue. The adults emerge by breaking open the distinct lid at the anterior end and leave behind a translucent empty puparium (Clausen and Berry 1932).

In contrast to the larvae that have obvious adaptations for predation, the adults are apparently not predatory. This conclusion is mostly based on observations, but the adults also lack obvious morphological adaptations for predation. For example, the adults have a typical schizophoran proboscis (Colless and McAlpine 1991) with two sponge-like labellar lobes (Fig. 7). Each labellar lobe has six pseudotrachea with likely capillary function (Fig. 7) (Elzinga and Broce 1986).

Prey: *Acletoxenus* larvae belonging to the Singapore population preyed on *Aleurotrachelus trachoides* (Back, 1912) (Fig. 8A) which has fourth instars with dentate margin and a large, setose lingual that expands apically and protrudes beyond the vasiform orifice. These features were used for a preliminary identification but the identity of the prey was also confirmed by D Barro (pers. comm.) and DNA barcodes (99% match to sequence for *Aleurotrachelus trachoides*; accession number KF059957) (Hodges and Evans 2005, Walker 2008). Note that *Aleurotrachelus trachoides*, is a major cosmopolitan pest of commercial plants (Hodges and Evans 2005, Malumphy 2005, Martin 2005, Forest Health 2013 highlights 2014). Thus,

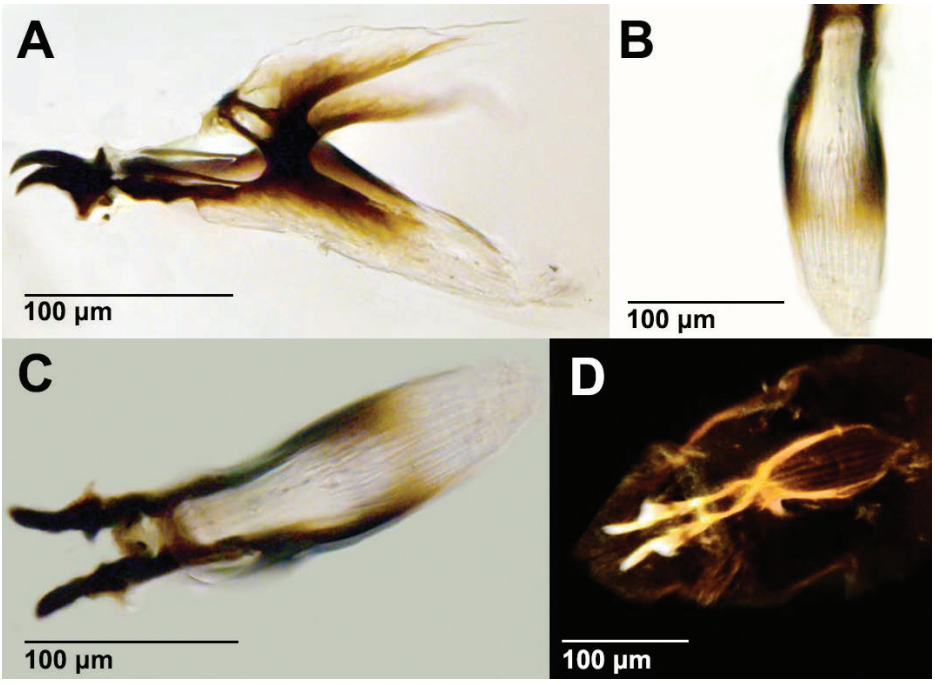

Figure 6. *Drosophila melanogaster* larval cephaloskeleton **A** lateral view with light microscope **B** ventral view close-up with light microscope **C** ventral view with light microscope, and **D** ventral view with confocal microscope, showing a pharyngeal filter.

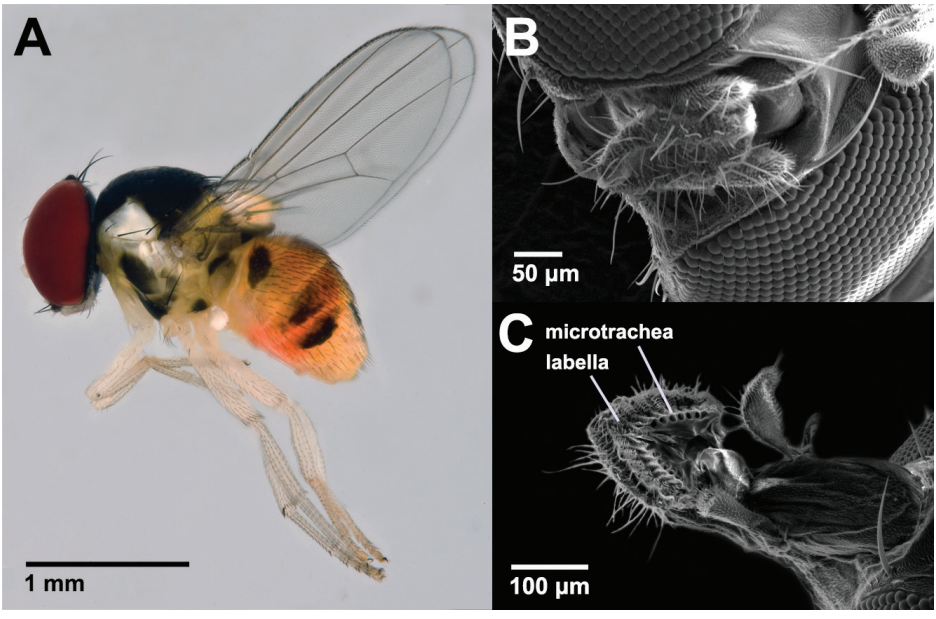

Figure 7. *Acletoxenus* cf. *indicus* adult **A** lateral view **B** SEM with proboscis folded in, and **C** SEM showing a typical extended schizophoran proboscis.

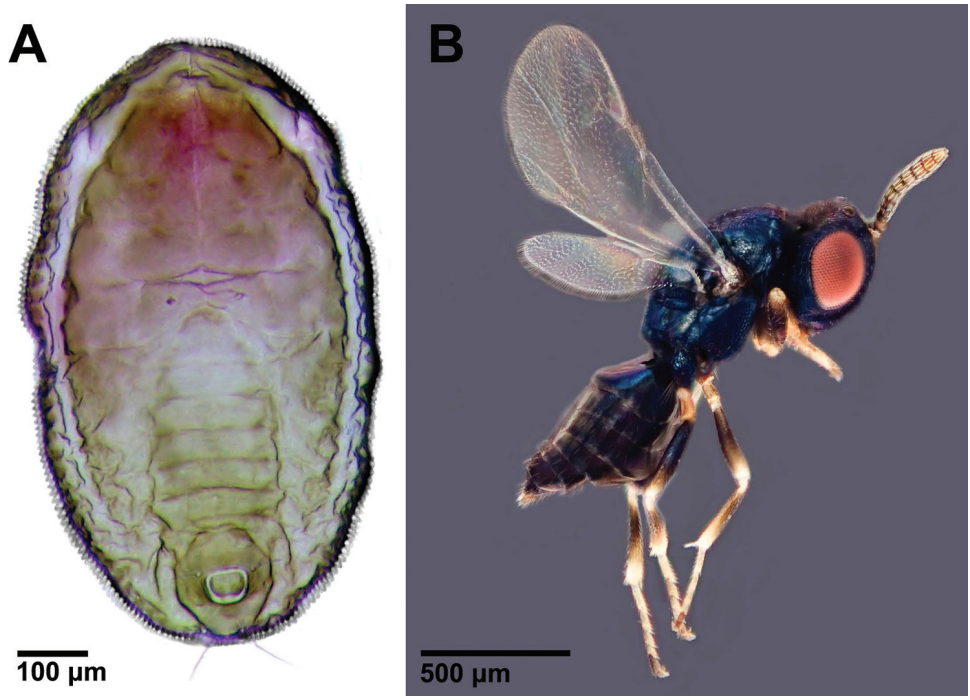

Figure 8. A Fourth instar of *Aleurotrachelus trachoides*, the prey of *Acletoxenus* cf. *indicus* and **B** adult *Pachyneuron leucopiscida*, the parasite of *Acletoxenus* cf. *indicus*.

Figure 9. *Acletoxenus* sp. egg (left) found next to whitefly first instars (right).

Acletoxenus cf. *indicus* could be considered a potential biological control agent for white flies given that the larvae consume 30 to 40 whitefly puparia during development (Pelov and Trenchev 1973). However, past attempts at using *Acletoxenus* for

Table 3. Monthly parasitism rates.

Month	Number of parasitized puparium found	Number of non-parasitized puparium found	Percentage of Parasitized Puparium
May 2014	18	21	46.2%
June 2014	16	13	55.2%
July 2014	4	10	28.6%

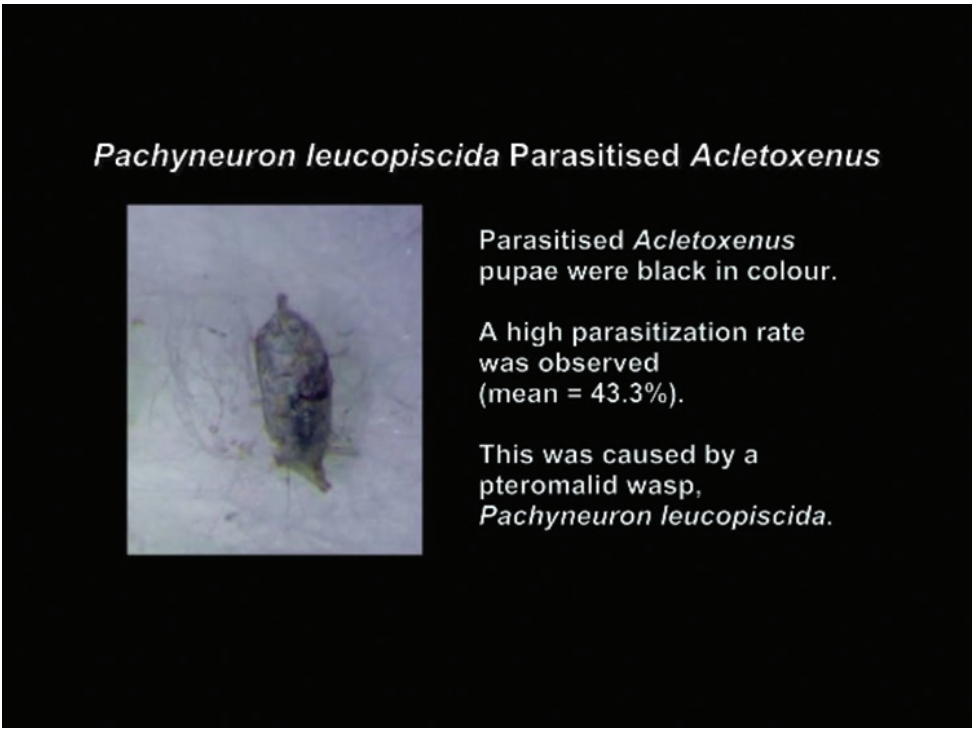

Movie 4. *Pachyneuron leucopiscida* emerging from parasitized *Acletoxenus* cf. *indicus* pupa.

this purpose have failed (Clausen and Berry 1932, Vayssière 1953) and although the reasons were never fully resolved, it has been suggested that extensive parasitism by Hymenoptera could be a contributing factor (Clausen and Berry 1932, Mentzelos 1967, Pelov and Trenchev 1973). This explanation is partially supported by our data. A high parasitization rate was observed (mean = 43.3%; Table 3) that was caused by a pteromalid wasp (Fig. 8B; Movie 4). This wasp was identified as *Pachyneuron leucopiscida* Mani, 1939. The same species had previously been recorded as a parasitoid of *Acletoxenus indicus* (Gupta & Poorani, 2009). The highest rate of parasitism in the Singapore population was in June while July saw a decrease in both the number of *Acletoxenus* that successfully emerged and the rate of parasitism. As the parasitism rates increased, the population of *Acletoxenus* cf. *indicus* declined and it crashed by August.

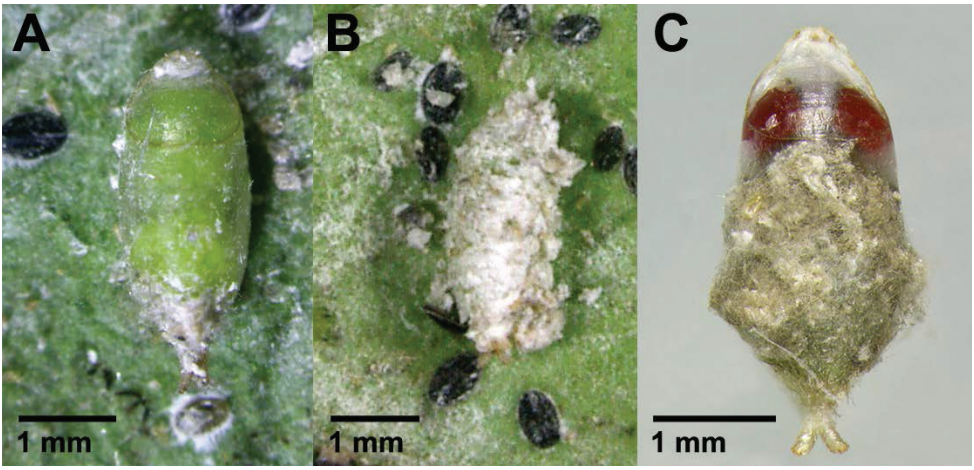

Figure 10. *Acletoxenus* cf. *indicus* puparium **A** with green body, is usually **B** covered in whitefly wax and instars, and **C** translucent integument revealing red eyes of the developing adult at later stages.

Life cycle of *Acletoxenus* cf. *indicus*

Acletoxenus cf. *indicus*' mean development time in Singapore was 24 days (Table 4). This is similar to the life cycle duration of European *Acletoxenus formosus* whose development time varies from 12 (Frauenfeld 1868) to 27 days (Pelov and Trenchev 1973). The mean lifespan of the adult flies was 12 days (Table 4). The Singapore population of *Acletoxenus* cf. *indicus* oviposits in the morning and afternoon and early instars of whiteflies are the initial prey while Clausen and Berry's (1932) described oviposition by *Acletoxenus indicus* during midday. In Singapore, the eggs were laid singly and the number of eggs oviposited on one leaf varied from one to four. All eggs were white and firmly attached to the abaxial surface of the leaves (Clausen and Berry 1932; Fig. 9). The eggs are approximately 0.45 mm in length and 0.2 mm in width with somewhat indistinct reticulate markings; The eggs of the Singapore population are thus slightly bigger compared to the eggs of *Acletoxenus indicus* in Clausen and Berry (1932; 0.4 mm length).

Table 4. Time spent in each life cycle stage of *Acletoxenus* cf. *indicus*.

Stage	Mean number of days	Standard deviation
Egg	3.5	1.1
Larva	12.4	2.8
Puparium	8.6	2.4
Adult	12.0	4.8

Acknowledgements

We thank Mr. Ng Soon Hwee and Dr. Diego Pitta de Araujo who provided us advice and help with the microscopy work. The project was supported by a MOE tier 2 grant (R-154-000-A22-112).

References

Ang Y, Puniamoorthy J, Pont AC, Bartak M, Blanckenhorn WU, Eberhard WG, Puniamoorthy N, Silva VC, Munari L, Meier R (2013a) A plea for digital reference collections and other science-based digitization initiatives in taxonomy: Sepsidnet as exemplar. Systematic Entomology 38: 637–644. https://doi.org/10.1111/syen.12015

Ang Y, Wong LJ, Meier R (2013b) Using seemingly unnecessary illustrations to improve the diagnostic usefulness of descriptions in taxonomy-a case study *on Perochaeta orientalis* (Diptera, Sepsidae). ZooKeys 9–27.

Ashburner M (1981) Entomophagous and other bizarre Drosophilidae. The Genetics and Biology of *Drosophila* 3a: 375–429.

Aubertin D (1937) A new species of *Drosophila*, *D. gibbinsi* sp. N., from Uganda (Diptera). Proceedings of the Royal Entomological Society of London, Series B, Taxonomy 6: 169. https://doi.org/10.1111/j.1365-3113.1937.tb01681.x

Bächli G, Vilela CR, Escher SA, Saura A (2004) The Drosophilidae (Diptera) of Fennoscandia and Denmark. Brill Academic Publishers.

Bächli G (1984) Die Drosophiliden-Typen der Dipterensammlung des Zoologischen Museums in Berlin. Mitteilungen aus dem Zoologischen Museum in Berlin 60: 229–261.

Bächli G (1987) List of type specimens of Drosophilidae (Diptera) in the collections of the Zoölogical Museum Amsterdam. Bulletin Zoologische Museum 11: 81–93.

Bächli G (2015) TaxoDros: Classification. http://www.taxodros.uzh.ch [accessed: 12 April 2015]

Basset Y, Cizek L, Cuénoud P, Didham RK, Guilhaumon F, Missa O, Novotny V, Ødegaard F, Roslin T, Schmidl J, Tishechkin AK, Winchester NN, Roubik DW, Aberlenc H-P, Bail J, Barrios H, Bridle JR, Castaño-Meneses G, Corbara B, Curletti G, Duarte da Rocha W, De Bakker D, Delabie JHC, Dejean A, Fagan LL, Floren A, Kitching RL, Medianero E, Miller SE, Gama de Oliveira E, Orivel J, Pollet M, Rapp M, Ribeiro SP, Roisin Y, Schmidt JB, Sørensen L, Leponce M (2012) Arthropod Diversity in a Tropical Forest. Science 338: 1481–1484. https://doi.org/10.1126/science.1226727

Bock IR (1982) Drosophilidae of Australia. V. Remaining genera and synopsis (Insecta: Diptera). Australian Journal of Zoology, Supplementary Series 89: 1–164. https://doi.org/10.1071/AJZS089

Clausen CP, Berry PA (1932) The citrus blackfly in Asia, and the importation of its natural enemies into tropical America. US Department of Agriculture. Washington, 1–22.

Colless DH, McAlpine DK (1991) Diptera (flies). The Insects of Australia 2: 717–786.

Collin JE (1902) Note on *Acletoxenus syrphoides*, Frauenfeld. Entomologist's Monthly Magazine, 2nd Series 38: 1–3.

Courtney GW, Sinclair BJ, Meier R (2000) Morphology and terminology of Diptera larvae. Contributions to a manual of Palaearctic Diptera. Science Herald Press, Budapest, 85–161.

Culik MP, Ventura JA (2009) New species of *Rhinoleucophenga*, a potential predator of pineapple mealybugs. Pesquisa Agropecuária Brasileira 44(4): 417–420. https://doi.org/10.1590/S0100-204X2009000400013

Dowding VM (1967) The function and ecological significance of the pharyngeal ridges occurring in the larvae of some cyclorrhaphous Diptera. Parasitology 57(2): 371–388. https://doi.org/10.1017/S0031182000072164

Duda O (1936) XXXI.—Weitere neue afrikanische und orientalische akalyptrate Musciden (Dipt.) des British Museum. The Annals and Magazine of Natural History 18(105): 337–351. https://doi.org/10.1080/00222933608655200

Elzinga RJ, Broce AB (1986) Labellar modifications of Muscomorpha flies (Diptera). Annals of the Entomological Society of America 79(1): 150–209. https://doi.org/10.1093/aesa/79.1.150

Ferrar P (1987) A Guide to the Breeding Habits and Immature Stages of Diptera Cyclorrhapha (Part 1: Text). Entomonograph. E.J. Brill/Scandinavian Science Press 8, 1–478.

Forest Health 2013 highlights (2014) http://www.fs.fed.us/foresthealth/fhm/fhh/fhh_13/PI_FHH_2013.pdf [accessed: 15 Jun 2015]

Frauenfeld GRV (1868) Zoologische Miscellen. XIV & XV. Verhandlungen Der Zoologisch-Botanischen Gesellschaft in Wien 18: 1885–1899.

Grimaldi DA, Nguyen TC (1999) Monograph on the spittlebug flies, genus *Cladochaeta* (Diptera: Drosophilidae: Cladochaetini). Monografía de las moscas de la baba de culebra o salivazo, género *Cladochaeta* (Diptera: Drosophilidae: Cladochaetini). Bulletin of the American Museum of Natural History 241: 1–326.

Gupta A, Poorani J (2009) Taxonomic studies on a collection of chalcidoid wasps (Hymenoptera: Chalcidoidea) from Sunderbans, West Bengal, India. Records of the Zoological Survey of India 109(1): 300–304.

Hebert PDN, Cywinska A, Ball SL, deWaard JR (2003) Biological identifications through DNA barcodes. Proceedings of the Royal Society Biological Sciences Series B, 270: 313–321. https://doi.org/10.1098/rspb.2002.2218

Hodges GS, Evans GA (2005) An identification guide to the whiteflies (Hemiptera: Aleyrodidae) of the Southeastern United States. Florida Entomologist 88(4): 518–534. https://doi.org/10.1653/0015-4040(2005)88[518:AIGTTW]2.0.CO;2

Katoh K, Standley DM (2013) MAFFT multiple sequence alignment software version 7: improvements in performance and usability. Molecular Biology and Evolution 30(4): 772–780. https://doi.org/10.1093/molbev/mst010

Kirk-Spriggs AH, Barraclough DA, Meier R (2002) The immature stages of Katacamilla cavernicola Papp, the first described for the Camillidae (Diptera: Schizophora), with comparison to other known Ephydroidea larvae, and notes on biology. Journal of Natural History 36(9): 1105–1128. https://doi.org/10.1080/00222930110048936

Kwong S, Srivathsan A, Meier R (2012) An update on DNA barcoding: low species coverage and numerous unidentified sequences. Cladistics 28: 639–644. https://doi.org/10.1111/j.1096-0031.2012.00408.x

Kwong S, Srivathsan A, Vaidya G, Meier R (2012) Is the COI barcoding gene involved in speciation through intergenomic conflict? Molecular phylogenetics and evolution 62(3): 1009–1012. https://doi.org/10.1016/j.ympev.2011.11.034

Lambkin TA, Zalucki MP (2010) Long-term efficacy of *Encarsia dispersa* Polaszek (Hymenoptera: Aphelinidae) for the biological control of *Aleurodicus dispersus* Russell (Hemiptera: Aleyrodidae) in tropical monsoon Australia. Australian Journal of Entomology 49(2): 190–198. https://doi.org/10.1111/j.1440-6055.2009.00742.x

Loew H (1864) *Gitona formosa*, eine neue deutsche Art. Wiener Entomologische Monatschrift 8: 366–368.

Malloch JR (1929) LXVI. Exotic Muscaridæ (Diptera). XXV. Journal of Natural History 3(17): 545–564. https://doi.org/10.1080/00222932908673006

Malumphy C (2005) The Neotropical solanum whitefly, *Aleurotrachelus trachoides* (Back) (Hem., Aleyrodidae), intercepted in the U.K. on sweet potato leaves imported from Gambia. Entomologist's Monthly Magazine 141: 94.

Mani MS (1939) Descriptions of New and Records of some known Chalcidoid and other Hymenopterous Parasites from India. Indian Journal of Entomology 1(pt. 1-2): 69–99.

Martin JH (2005) Whiteflies of Belize (Hemiptera: Aleyrodidae) Part 2-a review of the subfamily Aleyrodinae Westwood. Moscas blancas de Belice (Hemiptera: Aleyrodidae). Parte 2-revisión de la subfamilia Aleyrodinae Westwood. Zootaxa (1098): 1–116. https://doi.org/10.11646/zootaxa.843.1.1

McEvey S (2016) *Acletoxenus formosus* and *A. quadristriatus* from Australia (Diptera: Drosophilidae). figshare. https://doi.org/10.6084/m9.figshare.4468610.v1 [accessed: 04 28 Jun 2017]

Meier R (1995) Cladistic analysis of the Sepsidae (Cyclorrhapha: Diptera) based on a comparative scanning electron microscopic study of larvae. Systematic Entomology 20(2): 99–128. https://doi.org/10.1111/j.1365-3113.1995.tb00086.x

Meier R (1996) Larval morphology of the Sepsidae (Diptera, Sciomyzoidea): with a cladistic analysis using adult and larval characters. Bulletin of the American Museum of Natural History (USA) 228: 3–147.

Meier R (2008) DNA sequences in taxonomy – Opportunities and challenges. In: Wheeler QD (Ed.) New Taxonomy, CRC Press, Taylor and Francis Group, New York, 95–127.

Meier R (2017) Citation of taxonomic publications: the why, when, what and what not. Systematic Entomology, Systematic Entomology 42: 301–304. https://doi.org/10.1111/syen.12215

Meier R, Wong W, Srivathsan A, Foo M (2016) $1 DNA barcodes for reconstructing complex phenomes and finding rare species in specimen-rich samples. Cladistics 32: 100–110. https://doi.org/10.1111/cla.12115

Meier R, Zhang GY, Ali F (2008) The Use of Mean Instead of Smallest Interspecific Distances Exaggerates the Size of the "Barcoding Gap" and Leads to Misidentification. Systematic Biology 57: 809–813. https://doi.org/10.1080/10635150802406343

Mentzelos IA (1967) Contribution to the study of the entomophagous insects of *Siphoninus phillyreae* Halid.(= ineaqualis Gautier)(Aleyrodidae) on pear trees in central Macedonia. Rep. Plant Protection Agriculture Research Station Thessaloniki 3: 92–102.

Parchami-Araghi M, Farrokhi S (1995) *Acletoxenus formosus* Loew (Dip: Drosophilidae), predator of immature stages of whiteflies in Iran. Journal of Entomological Society of Iran 15: 73.

Pelov V, Trenchev G (1973) *Siphoninus phillyreae* Hal. And its entomophages. Rastitelna Zashchita 21(11): 26–27.

Riedel A, Daawia D, Balke M (2010) Deep cox1 divergence and hyperdiversity of *Trigonopterus* weevils in a New Guinea mountain range (Coleoptera, Curculionidae). Zoologica Scripta 39: 63–74. https://doi.org/10.1111/j.1463-6409.2009.00404.x

Roberts MJ (1971) The structure of the mouthparts of some galypterate dipteran larvae in relation to their feeding habits. Acta Zoologica 52(2): 171–188. https://doi.org/10.1111/j.1463-6395.1971.tb00556.x

Rohner PT, Ang Y, Lei Z, Puniamoorthy N, Blanckenhorn WU, Meier R (2014) Genetic data confirm the species status of *Sepsis nigripes* Meigen (Diptera: Sepsidae) and adds one species to the Alpine fauna while questioning the synonymy of *Sepsis helvetica* Munari. Invertebrate Systematics 28(5): 555–563. https://doi.org/10.1071/IS14023

Smith V, Georgiev T, Stoev P, Biserkov J, Miller J, Livermore L, Baker E, Mietchen D, Couvreur T, Mueller G, Dikow T, Helgen K, Frank J, Agosti D, Roberts D, Penev L (2013) Beyond dead trees: integrating the scientific process in the Biodiversity Data Journal. Biodiversity Data Journal 1: e995. https://doi.org/10.3897/BDJ.1.e995

Srivathsan A, Meier R (2012) On the inappropriate use of Kimura-2-parameter (K2P) divergences in the DNA-barcoding literature. Cladistics 28: 190–194. https://doi.org/10.1111/j.1096-0031.2011.00370.x

Tamura K, Stecher G, Peterson D, Filipski A, Kumar S (2013) MEGA6: molecular evolutionary genetics analysis version 6.0. Molecular Biology and Evolution 30(12): 2725–2729. https://doi.org/10.1093/molbev/mst197

Tan DS, Ang Y, Lim GS, Ismail MRB, Meier R (2010) From 'cryptic species' to integrative taxonomy: an iterative process involving DNA sequences, morphology, and behaviour leads to the resurrection of *Sepsis pyrrhosoma* (Sepsidae: Diptera). Zoologica Scripta 39(1): 51–61. https://doi.org/10.1111/j.1463-6409.2009.00408.x

Tewksbury JJ, Anderson JGT, Bakker JD, Billo TJ, Dunwiddie PW, Groom MJ, Hampton SE, Herman SG, Levey DJ, Machnicki NJ, del Rio CM, Power ME, Rowell K, Salomon AK, Stacey L, Trombulak SC, Wheeler TA (2014) Natural History's Place in Science and Society. Bioscience 64: 300–310. https://doi.org/10.1093/biosci/biu032

Thompson V, Mohd-Saleh N (1995) Spittle maggots: studies on *Cladochaeta* fly larvae living in association with Clastoptera spittlebug nymphs. American Midland Naturalist 134: 215–225. https://doi.org/10.2307/2426292

Tsacas L, Disney RHL (1974) Two new African species of *Drosophila* (Diptera, Drosophilidae) whose larvae feed on *Simulium* larvae (Dipt., Simuliidae). Tropenmedizin Und Parasitologie 25(3): 360–377.

Vayssière P (1953) Rapport de la Commission pour les recherches sur la lutte biologique contre les ennemis des cultures. Comptes Rendus de l'Assemblée Générale de l'Union Internationale Des Sciences Biologique, Nice 12: 1–12.

Walker K (2008) Aleurotrachelus whitefly (*Aleurotrachelus trachoides*). http://www.padil.gov.au/pests-and-diseases/pest/main/136164 [accessed: 14 January 2015]

Wheeler MR, Patterson JT (1952) The Drosophilidae of the Nearctic Region, exclusive of the genus *Drosophila*. Studies in the Genetics of *Drosophila*; VII. Further articles on genetics, cytology, and taxonomy. The Drosophilidae of the Nearctic Region, Exclusive of the Genus *Drosophila*. Studies in the Genetics of *Drosophila*; VII. Further Articles on Genetics, Cytology, and Taxonomy.

Wipfler B, Schneeberg K, Löffler A, Hünefeld F, Meier R, Beutel RG (2013) The skeletomuscular system of the larva of Drosophila melanogaster (Drosophilidae, Diptera) – A contribu-

tion to the morphology of a model organism. Arthropod structure & development 42(1): 47–68. https://doi.org/10.1016/j.asd.2012.09.005

Wong WH, Tay YC, Puniamoorthy J, Balke M, Cranston PS, Meier R (2014) 'Direct PCR' optimization yields a rapid, cost-effective, nondestructive and efficient method for obtaining DNA barcodes without DNA extraction. Molecular Ecology Resources 14: 1271–1280. https://doi.org/10.1111/1755-0998.12275

Yu G, Wu L, Lu J, Chen H (2012) Discovery of a predaceous drosophilid *Acletoxenus indicus* Malloch in South China, with descriptions of the taxonomic, ecological and molecular characters (Diptera: Drosophilidae). Journal of Natural History 46(5-6): 349–354. https://doi.org/10.1080/00222933.2011.639466

ZooKeys 725: 71–78 (2017)
doi: 10.3897/zookeys.722.21267
http://zookeys.pensoft.net

RESEARCH ARTICLE

A peer-reviewed open-access journal
ZooKeys
Launched to accelerate biodiversity research

A new species of *Homoneura* (*Euhomoneura*) from northern China (Diptera, Lauxaniidae)

Li Shi[1], Xuefeng Gao[1], Wenliang Li[2]

1 *College of Agronomy, Inner Mongolia Agricultural University, Hohhot 010019, China* **2** *College of Forestry, Henan University of Science and Technology, Luoyang 471003, China*

Corresponding author: *Li Shi* (lirui2003@imau.edu.cn)

Academic editor: *R. Meier* | Received 28 September 2017 | Accepted 10 November 2017 | Published 29 December 2017

http://zoobank.org/3DB9F57F-7D56-4A13-868D-984915DF2294

Citation: Shi L, Gao X, Li W (2017) A new species of *Homoneura* (*Euhomoneura*) from northern China (Diptera, Lauxaniidae). ZooKeys 725: 71–78. https://doi.org/10.3897/zookeys.725.21267

Abstract

Homoneura (*Euhomoneura*) *yanqingensis* **sp. n.** is described as new to science and *Homoneura* (*E.*) *shatalkini* Papp, 1984 is recorded from China for the first time. Photographs and illustrations are provided for both of these species, including genitalia. A key is provided to separate the Chinese species of the subgenus *Euhomoneura*.

Keywords

Euhomoneura, *Homoneura*, new record, new species, Palaearctic region

Introduction

The subgenus *Euhomoneura* Malloch, 1927 is a small subgenus of the genus *Homoneura* (Wulp, 1891), which can be separated from other subgenera by the following key features: the lower margin of the face being about three times as wide as height of the gena and the anteriormost dorsocentral seta being at or before the transverse suture of the mesonotum. It includes 12 described species with three in China (Shiet al. 2012).

One species *Homoneura* (*Euhomoneura*) *yanqingensis* sp. n. is described as new to science and one species *Homoneura* (*E.*) *shatalkini* Papp, 1984 is newly recorded in China. A key is provided to separate the Chinese species of the subgenera *Euhomoneura*.

Materials and methods

General terminology follows Gaimari and Silva (2010) and Shi and Yang (2014). Genitalia preparations were made by removing and macerating the apical portion of the abdomen in cold saturated NaOH for one hour, then rinsing and neutralizing them for dissection and study. After examination in glycerin, genitalia were transferred to fresh glycerine and stored in a microvial pinned below each specimen. Specimens examined were deposited in two collections: entomological collections of China Agricultural University, Beijing (**CAUC**) and Inner Mongolia Agricultural University, Hohhot (**IMAU**).

Taxonomy

***Homoneura* (*Euhomoneura*) *shatalkini* Papp, 1984**
Figures 1–12

Homoneura shatalkini Papp, 1984a: 167. Type locality: Japan. Shatalkin, 2000: 29.

Specimens examined. CHINA: Ningxia Province (IMAU): 1♂, Liupan Mountain, 7–8.vii.2008, Jingxian Liu. **CHINA: Jilin Province** (IMAU): 2♂♂, 2♀♀, Changbai Mountain, South slope, 1520–1720 m, 1.viii.2004, Xingyue Liu. **CHINA: Shaanxi Province** (IMAU): 1♂, Zhouzhi, Houzhenzi, 1235 m, 11.viii.2013, Wencheng Chang; 1♂, Zhouzhi, Laoxiancheng, 1846 m, 19.viii.2014, Xiumei Lu; 2♂♂, 2♀♀, Zhouzhi, Laoxiancheng, 1808 m, 12.viii.2013, Wencheng Chang (2 males, 2 females: IMAU); 1♂, Feng County, Huangniupu, light trap, 1501 m, 21.viii.2013, Yuqiang Xi; 1♂, Zhouzhi, Houzhenzi, 1235 m, 11.viii.2013, Xuankun Li; 2♂♂, Zhouzhi, Taibai Mountains, 1648 m, 17.viii.2014, Xunkun Li.

Distribution. New record to China (Ningxia, Jilin, Shaanxi); Japan, Russia.

***Homoneura* (*Euhomoneura*) *yanqingensis* sp. n.**
http://zoobank.org/EB333015-A744-430C-8448-B06F98ACBB89
Figures 13–24

Type material. Holotype ♂, **CHINA: Beijing** (CAUC): Yanqing County, Songshan, 8.ix.2009, Xiaoyan Liu. Paratypes: **CHINA: Beijing** (CAUC): 7♂♂, 8♀♀, data same as holotype. **CHINA: Shaanxi Province** (IMAU): 1♂, Baoji City, Feng County, Huangniupu, 1501 m, 21.viii.2013, Yuqiang Xi; 1♂, 1♀, Zhouzhi, Houzhenzi, 1235 m, 11.viii.2013, Wencheng Chang; 1♀, Zhouzhi, Laoxiancheng, 1916 m, 19.viii.2014, Xiumei Lu.

Diagnosis. Body yellow. Arista pubescent. Palpus with brown apex. Mesonotum with four strong and long acrostichal setae (two before suture, two after suture). All femora each with a brown irregular apicoventral spot and all tasomeres 3–5 brown. Wing hyaline, with five brown isolated spots.

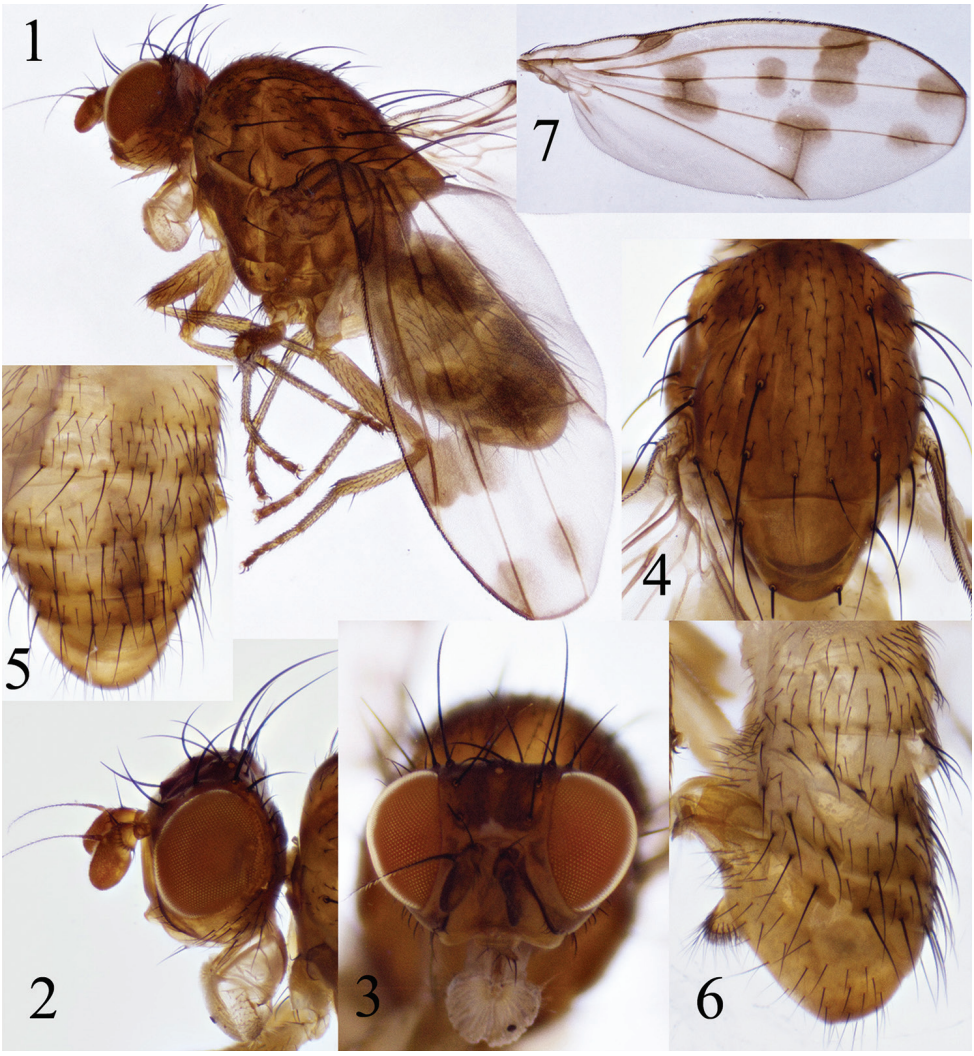

Figures 1–7. *Homoneura* (*Euhomoneura*) *shatalkini* Papp, 1984. Male from Shaanxi. **1** Habitus, lateral view **2, 3** Head, laeral and anterior view **4** Thorax, dorsal view **5, 6** Abdomen, dorsal and lateral view **7** Wing.

Description. Male. Body length 3.8–4.2 mm. Wing length 3.7–4.3 mm. Female. Body length 3.8–4.2 mm.Wing length 3.7–4.3 mm.

Head pale yellow. Frons with sparse grayish white pruinosity, longer than wide and parallel-sided; ocellar triangle brown, ocellar setae well developed, longer than anterior fronto-orbital setae, anterior fronto-orbital setae shorter than length of posterior one; gena about 1/6 height of eye; antenna yellow; 1st flagellomere yellowish brown, 1.5 times longer than high; arista dark brown except for pale brownish base, ray pubescent, with longest ray as long as 1/3 height of 1st flagellomere. Proboscis yellow, palpus yellow except for brown apex.

Thorax yellow. Mesonotum with 1+2 dorsocentral setae; acrostichal setae in irregular six rows, with four strong and long acrostichal setae (two before suture, two after suture); a pair of prescutellar setae shorter than 1st post-sutural dorsocentral setae. Leg mostly

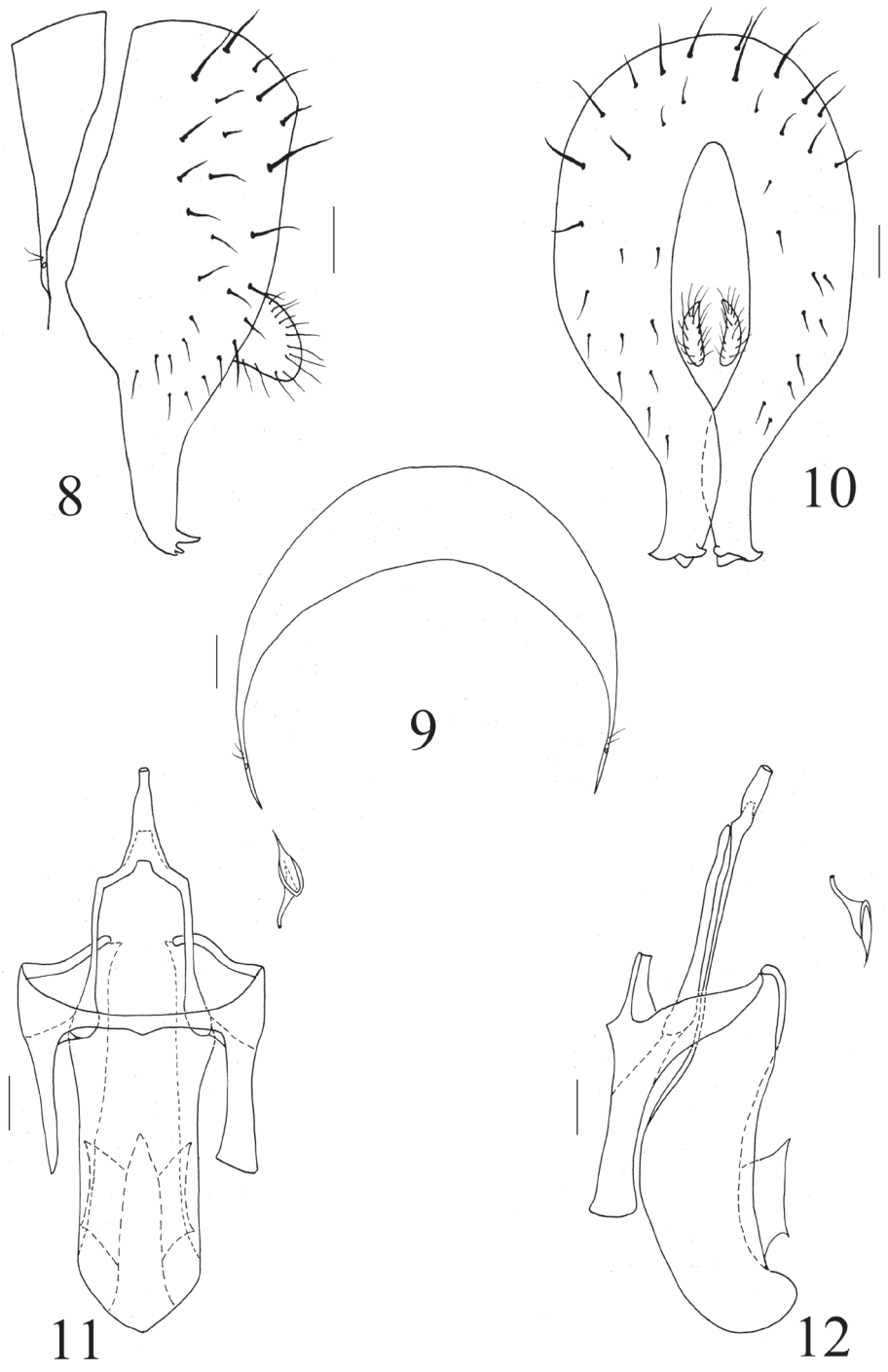

Figures 8–12. *Homoneura* (*Euhomoneura*) *shatalkini* Papp, 1984. Male from Shaanxi. Male genitalia. **8** Syntergosternite and epandrial complex, lateral view **9** Syntergosternite, anterior view **10** Epandrium, posterior view **11** Aedeagal complex, ventral view **12** Aedeagal complex, lateral view. Scale bar: 0.1 mm.

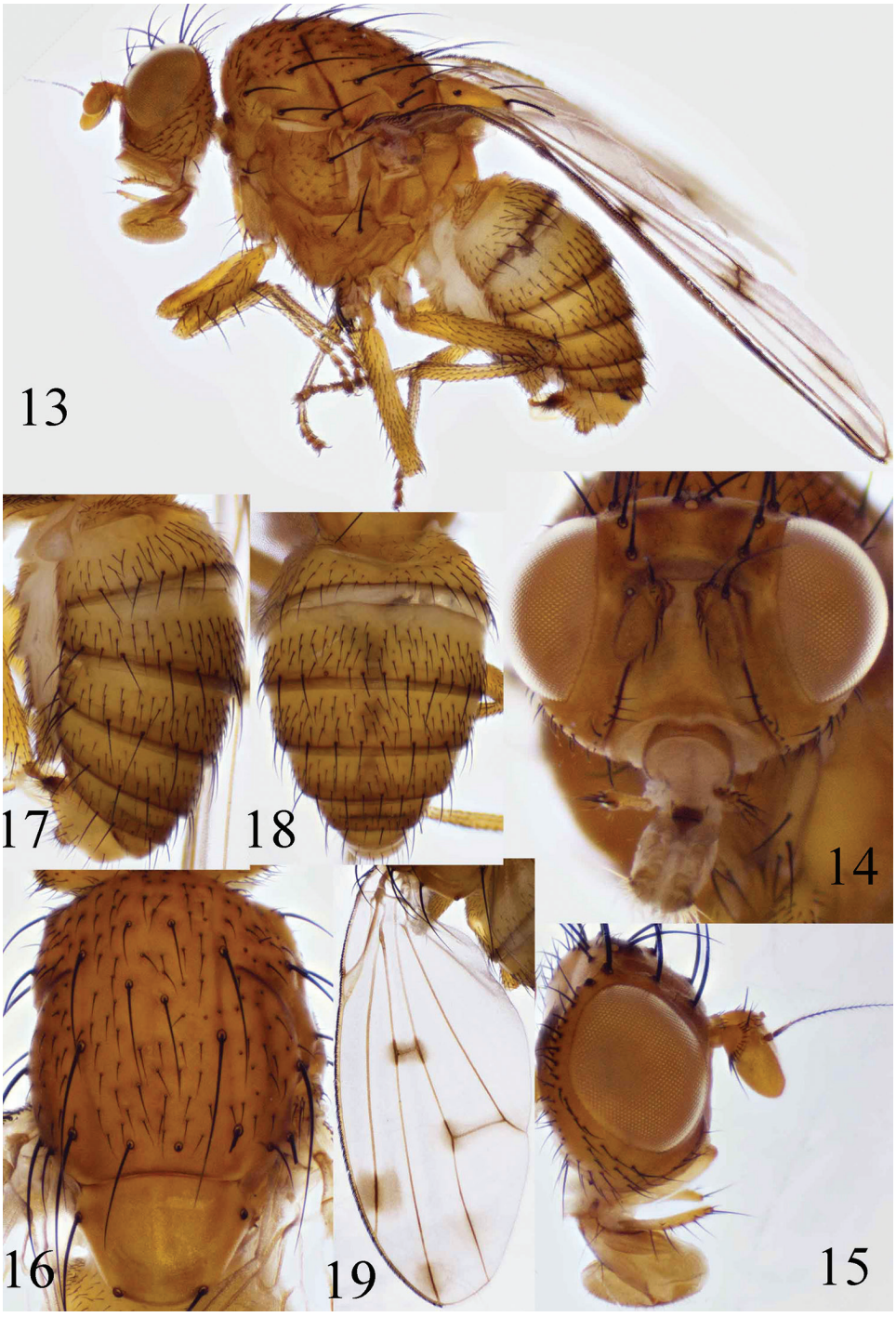

Figures 13–19. *Homoneura* (*Euhomoneura*) *yanqingensis* sp. n. Paratype male from Shaanxi. **13** Habitus, lateral view **14, 15** Head, anterior and lateral view **16** Thorax, dorsal view **17, 18** Abdomen, dorsal and dorsal view **19** Wing.

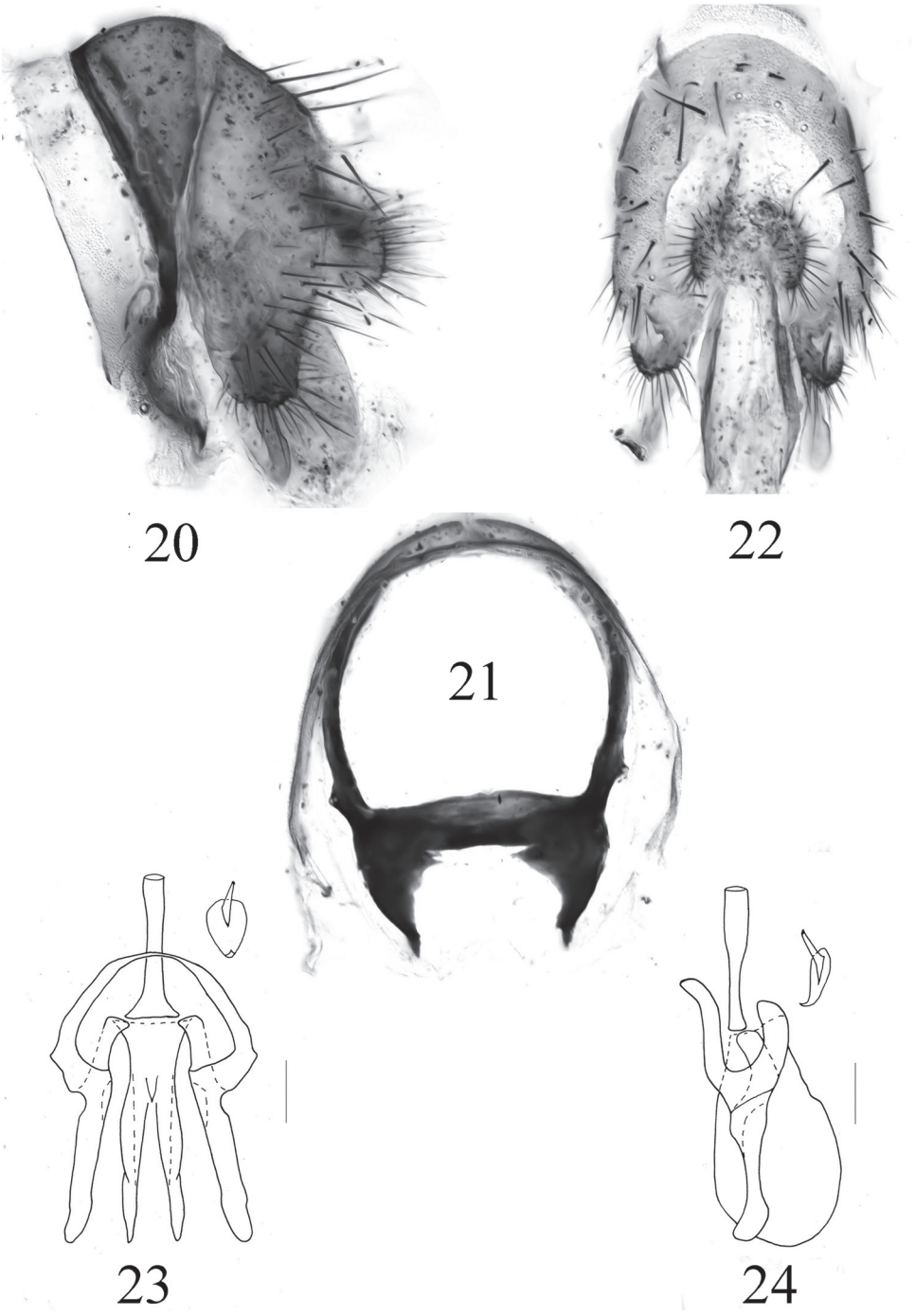

Figure 20–24. *Homoneura* (*Euhomoneura*) *yanqingensis* sp. n. Paratype male from Shaanxi. Male genitalia. **20** Syntergosternite and epandrial complex, lateral view **21** Syntergosternite, anterior view **22** Epandrium, posterior view **23** Aedeagal complex, ventral view **24** Aedeagal complex, lateral view. Scale bar: 0.1 mm.

yellow, all femora each with a brown irregular apicoventral spot and all tasomeres 3–5 brown. Fore femur with 6–7 posterodorsal setae, 4–5 posteroventral seate, and ctenidium with 11–12 short setae; fore tibia with one strong preapical anterodorsal seta and one short apicoventral seta. Mid femur with five anterior setae and one short apical posterior seta; mid tibia with one strong preapical anterodorsal seta and one short apicoventral seta. Hind femur with one preapical anterodorsal seta and three anteroventral setae; hind tibia with one preapical anterodorsal seta and one short apicoventral seta. Wing hyaline, with five brown isolated spots: preapical spot on R_{2+3}, apical spot on R_{4+5}, subapical spot on M_1, a cloud on crossvein r-m, and a narrow stripe-like spot on crossvein dm-cu (anterior margin and posterior margin darker than central area); pale brown along the radial sector; subcostal cell pale brown; costa with 2nd, 3rd and 4th sections in proportion of 4.5:1.8:1; r-m beyond middle of discal cell; ultimate and penultimate sections of M_1 in proportion of 1:1.6; ultimate section of CuA_1 about 1/6 of penultimate. Halter yellow.

Abdomen pale yellow, tergites 2–5 (female 2–6) with narrow brown posterior margin, and tergite 3–5 (female 3–6) brownish median spot or absent. Male genitalia: syntergosternite circular with a pair of ventral processes; epandrium broad with dense apical setae, surstylus narrow but slightly broaden at apex; hypandrium slender U-shaped; postgonite long cylindrical; aedeagus broad at middle and bluntly rounded in lateral view, aedeagal apodeme shorter than length of aedeagus.

Etymology. The new species is named after collection locality.

Distribution. China (Beijing, Shaanxi).

Comments. The new species is similar to *Homoneura* (*Euhomoneura*) *balluca* Sasakawa, 1992 from Malaysia. It can be separated from the latter by the mesonotum having brown stripes, the coxa and femora of legs being brown and the tibiae each having brown rings on both apex, and the abdominal tergite 6 having a pair of brown lateral spots.

A key to the five known species of the subgenus *Euhomoneura* in China

1 Frons black with yellowish grey pruinosity; gena reddish yellow with black spots; male abdominal tergites greyish black without spots, but female abdominal tergites with a pair of reddish brown spots on anterolateral corners ..... ***H.* (*E.*) *variipennis* Czerny**

– Frons yellow; gena yellow; abdomen yellow with pale brown spots or absent **2**

2 Wing with two brown spots on R_{4+5} between vertical level of *r-m* and apical spot **3**

– Wing without brown spots on R_{4+5} between vertical level of *r-m* and apical spot **4**

3 Arista short plumose; male genitalia: surstylus with a sharp and a blunt apical protuberance in lateral view, aedeagus without rectangular dorsal sclerites (see Gao et al. 2003: 194) ..... ***H.* (*E.*) *minuscula* Gao, Yang & Gaimari**

– Arista pubescent; male genitalia: surstylus with three sharp processes, aedeagus with a pair of nearly rectangular dorsal sclerites in lateral view (see Papp, 1984: 167) ..... ***H.* (*E.*) *shatalkini* Papp**

4 Mesonotum with acrostichal setae in irregular six rows, especially four strong and long acrostichal setae (two before suture, two after suture); male genitalia: surstylus blunt without tip and aedeagus separated at apex in posterior view ..... ***H.* (*E.*) *yanqingensis* sp. n.**

– Mesonotum without strong central acrostichal setae; male genitalia: surstylus with tip projecting and upturned and aedeagus crossed at apex in posterior view (see Gao et al. 2003: 195) .... ***H.* (*E.*) *xiaolongmenensis* Gao, Yang & Gaimari**

Acknowledgements

The author Li Shi gives sincere thanks to all collectors and the reviewers for reviewing this manuscript. The research is supported by National Natural Science Fundation of China (No. 31260525) and Inner Mongolia outstanding youth Cultivation Fund (No. 2015JQ03).

References

Czerny L (1932) Lauxaniidae (Sapromyzidae). In: Lindner E (Ed.) Die Fliegen der Palaearktischen Region. Volume 5, part 50. E. Schweizerbart'sche, Stuttgart, 1–76.

Gaimari SD, Silva VC (2010) Lauxaniidae (Lauxaniid flies). In: Brown BV, Borkent A, Cumming JM, Wood DM, Woodley NE (Coords.) Manual of Central American Diptera, Volume 2. NRC Research Press, Ottawa, 971–995.

Gao CX, Yang D, Gaimari SD (2004) The subgenus *Euhomoneura* Malloch (Diptera: Lauxaniidae) in the Palaearctic Realm. Pan-Pacific Entomologist 79(3/4): 192–197.

Malloch JR (1927) Notes on Australian Diptera (No. XIII). Proceedings of the Linnean Society of New South Wales 52: 399–446.

Papp L (1984) Lauxaniidae (Diptera), new Palaearctic species and taxonomical notes. Acta Zoologica Hungarica 30(1/2): 159–177.

Sasakawa M (1992) Lauxaniidae (Diptera) of Malaysia (Part 2): A revision of *Homoneura* van der Wulp. Insecta Matsumurana new series 46: 133–210.

Shatalkin AI (2000) Keys to the Palaearctic flies of the family Lauxaniidae (Diptera). Zoologicheskie Issledovania 5: 1–102.

Shi L, Gaimari SD, Yang D (2012) Notes on the *Homoneura* subgenera *Euhomoneura*, *Homoneura* and *Minettioides* from China (Diptera: Lauxaniidae). Zootaxa 3238: 1–22.

Shi L, Yang D (2014) Supplements to species groups of the subgenus *Homoneura* in China (Diptera: Lauxaniidae: *Homoneura*), with description of twenty new species. Zootaxa 3890 (1): 1–117. http://dx.doi.org/10.11646/zootaxa.3890.1.1

Wulp FM van der (1891) Eenige uitlandsche Diptera. Tijdschrift voor Entomologie 34: 193–218.

ZooKeys 725: 79–95 (2017)
doi: 10.3897/zookeys.725.19952
http://zookeys.pensoft.net

RESEARCH ARTICLE

A peer-reviewed open-access journal
ZooKeys
Launched to accelerate biodiversity research

Southern limits of distribution of the intertidal gobies *Chaenogobius annularis* and *C. gulosus* support the existence of a biogeographic boundary in southern Japan (Teleostei, Perciformes, Gobiidae)

Atsunobu Murase[1,2], Ryohei Miki[1,3], Hiroyuki Motomura[4]

1 *Nobeoka Marine Science Station, Field Science Center, University of Miyazaki, 376-6 Akamizu, Nobeoka, Miyazaki 889-0517, Japan* **2** *Department of Marine Biology and Environmental Sciences, Faculty of Agriculture, University of Miyazaki, Gakuen-Kibanadai-Nishi, Miyazaki 889-2192, Japan* **3** *Interdisciplinary Graduate School of Agriculture and Engineering, University of Miyazaki, 1-1 Gakuen-kibanadai-nishi, Miyazaki 889-2192, Japan* **4** *The Kagoshima University Museum, 1-21-30 Korimoto, Kagoshima 890-0065, Japan*

Corresponding author: *Atsunobu Murase* (nobi@cc.miyazaki-u.ac.jp)

Academic editor: *S. Kullander* | Received 1 August 2017 | Accepted 26 November 2017 | Published 29 December 2017

http://zoobank.org/EA691A0E-8BA9-4EC7-899F-BA1CEFAD801E

Citation: Murase A, Miki R, Motomura H (2017) Southern limits of distribution of the intertidal gobies *Chaenogobius annularis* and *C. gulosus* support the existence of a biogeographic boundary in southern Japan (Teleostei, Perciformes, Gobiidae). ZooKeys 725: 79–95. https://doi.org/10.3897/zookeys.725.19952

Abstract

Understanding the distributional patterns of individual animal groups with respect to coastal topology and the local physical environment provides essential foundational frameworks for marine zoogeography. In the northwestern Pacific waters of Japan, the distributional pattern of some cool-temperate species of marine fishes suggests the existence of a biogeographic boundary corresponding to a long sandy shore on the eastern coast of Kyushu, southern Japan. The existence of this hypothetical biogeographic boundary was tested by mapping the southern distributional limit of two species of cool-temperate intertidal gobies, *Chaenogobius annularis* and *C. gulosus*, which are endemic to East Asia and common in rock pools within their range in the Japanese Archipelago. Distribution and abundance were assessed by survey of museum collections from south-east Kyushu (i.e., the entire coasts of Kagoshima and Miyazaki prefectures); and a quantitative survey of the abundance of these gobies in rock pools at various sites around the hypothesized boundary on the eastern coast of Kyushu, including the subtropical Tanega-shima Island. The museum collection survey showed different distribution patterns between the two species: *C. annularis* was distributed along the entire coasts of south-east Kyushu including subtropical islands, whereas *C. gulosus* was distributed along these coasts, including one site on a subtropical island, except for an area

south of the hypothesized boundary on the eastern coast of Kyushu. The density and occurrence rates of *C. annularis* in rock pools decreased with latitude, it being absent from a subtropical island, and *C. gulosus* was not detected from sites south of the hypothesized boundary. The qualitative survey showed that the southernmost records of *C. annularis* and *C. gulosus* were the adjacent subtropical islands (Yaku-shima and Tanega-shima islands respectively), although the quantitative survey suggested that their normal range of distribution was limited to the southern part of the Kyushu mainland. A combination of qualitative and quantitative survey methods in the present study highlighted that the southernmost record of a certain species may not necessarily indicate the true limit of its distribution. The distribution of *C. gulosus* supports the existence of the hypothetical biogeographic boundary, and the different distribution patterns of the two species may be caused by differences in their early life histories.

Keywords
Distributional range, northwestern Pacific, rock pools

Introduction

The delineation and characterization of the marine fauna is one of the objectives of marine zoogeography (Briggs 1974) and understanding the distribution patterns of individual animal groups is essential for this work. When a species' distribution is considered on a geographical, habitat, or microhabitat scale, its limits may be surrounded by areas where the species cannot maintain a population due to adverse physical conditions or a lack of resources permitting survival (Cox and Moore 2005). Indeed, a strong link between species distribution and climatic areas is universally observed in the coastal zone (Briggs 1974, 1995, Nishimura 1992, Cox and Moore 2005, Briggs and Bowen 2012). According to these biogeographic foundations, the distribution of a certain species can be used to construct baseline information for delineating any biogeographic boundaries that correspond to topographic and/or climatic features. Accurate range limit data can reveal range boundary disequilibrium, where a species' distribution and its potential geographic distribution differ. Such discrepancies may reflect differences in dispersal, life history, recolonization history, or stochasticity (Sexton et al. 2009).

Intertidal organisms are generally easily accessible, and readily available to be sampled and used as ecological and biogeographic indicators (Raffaelli and Hawkins 1996). Biogeographic analyses using intertidal macrobenthic fauna have detected faunal similarities and relationships relating to coastal environments in the north-western Pacific region (Asakura and Suzuki 1987, Nakaoka et al. 2006, Kurihara 2007, Ohgaki 2011). Intertidal fishes are also likely to be useful indicator species for coastal biogeography in terms of their taxonomic arrangement and distribution information, which can lead to a biogeographic categorization for each species (Murase 2013, Okada et al. 2015).

The East Asian endemic genus *Chaenogobius* Gill, 1859, is composed of two species, *C. annularis* Gill, 1859, and *C. gulosus* (Sauvage, 1882) (Fig. 1), which are distributed along the temperate coasts of Japan and the Korean Peninsula (Stevenson 2002, Akihito et al. 2013, Kwun et al. 2017). Both species inhabit intertidal rocky shores and rock pools, and are common and/or the predominant species throughout the temper-

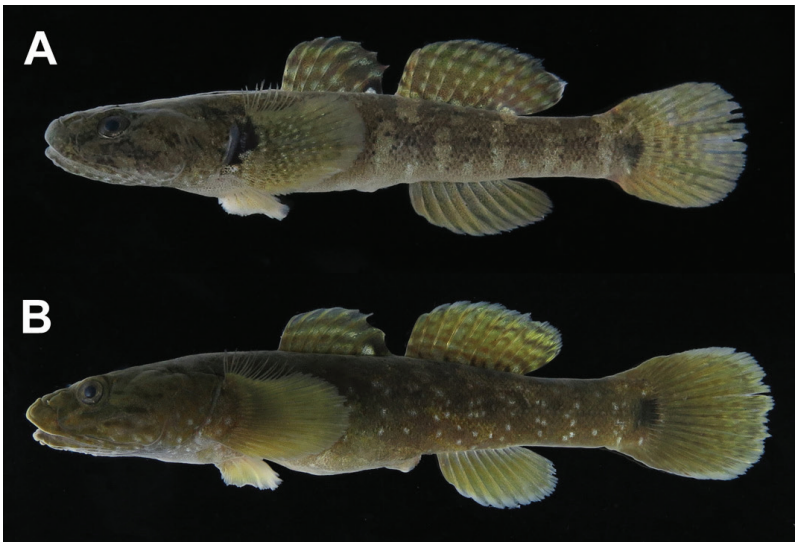

Figure 1. Fresh specimens of the two species of *Chaenogobius*: **A** *Chaenogobius annularis*, KPM-NI 42850 (photo number, KPM-NR 179153), 52.7 mm SL, Nobeoka City, Miyazaki Prefecture **B** *Chaenogobius gulosus*, KPM-NI 42951 (KPM-NR 179221), 73.0 mm SL, Kadogawa Bay, Miyazaki Prefecture. Photos by A. Murase.

ate region of the Japanese Archipelago (Sasaki and Hattori 1969, Nakamura 1970, Okamura and Amaoka 1997, Arakaki and Tokeshi 2006, Murase et al. 2010; Amaoka et al. 2011, Kohno 2011). Nakabo (2013), in assigning each Japanese fish species to its biogeographic affinity, classified the genus *Chaenogobius* as a category of "shallow rocky-reef fishes in the continental coast of cool-temperate water area (thereafter represented as "cool-temperate species" in this text)". This group occurs in the following areas: Tsugaru strait southward to southern Kyushu along the Sea of Japan coast, Aomori Prefecture to Miyazaki Prefecture along the Pacific coast, and the southern Korean Peninsula. In addition, according to fig. 2B of Nakabo (2013), the northern part of Miyazaki Prefecture is the southern distributional limit of this group on the Pacific coast. *Ditrema temminckii* Bleeker, 1853 (Embiotocidae), a species within this biogeographic group, has been reported from Kadogawa Bay in the northern part of Miyazaki Prefecture, representing its southern limit on the Pacific coast (Murase et al. 2017). Nakabo's results, and the known distribution of other members of cool-temperate species, suggest the existence of a biogeographic boundary between the northern and southern parts of the eastern coast of Kyushu. This hypothetical biogeographic boundary casts doubt on the previous understanding of the distribution of the two species of *Chaenogobius*. Akihito et al. (2013) summarized the species' distribution as the temperate region of the Japanese Archipelago including almost the entire coast of Kyushu: *C. annularis* ranging from Otaru, western Hokkaido, southward to Amakusa, Kumamoto Prefecture, along the Sea of Japan/East China Sea coast, Otsuchi, Iwate Prefecture to Yaku-shima Island along the Pacific coast, and the southern Korean Pen-

insula; and *C. gulosus* ranging from Yoichi Town, western Hokkaido, southward to Amakusa, Kumamoto Prefecture along the Sea of Japan/East China Sea coast, Kominato, Chiba Prefecture to Miyazaki City, Miyazaki Prefecture along the Pacific coast, and the southern Korean Peninsula (Fig. 2). The two species are common in Japanese waters and are likely to be important for biogeographic analyses, not only in comprehensive ichthyofaunal surveys but also as components of intertidal fish assemblages. In order to clarify the southernmost limit of distribution of the two species of *Chaenogobius* with regard to the abovementioned hypothetical biogeographic boundary on the eastern coast of Kyushu, the present study re-examines the distribution of these species in south-east Kyushu (Kagoshima and Miyazaki prefectures including subtropical adjacent islands (Fig. 2) on the basis of voucher specimens deposited in public museums. To further test the existence of this biogeographic boundary for cool-temperate species, we analysed also the results of rock pool surveys to estimate the occurrence and abundance of these gobies at various sites along the eastern coast of Kyushu.

Materials and methods

Qualitative survey

Laboratories of the Kagoshima University Museum and the Nobeoka Marine Science Station, University of Miyazaki, have collected specimens of fish species inhabiting coastal zones of Kagoshima and Miyazaki prefectures, south-east Kyushu. The specimens were deposited in fish collections of public museums, both the Kagoshima University Museum (KAUM–I.) and the Kanagawa Prefectural Museum of Natural History (KPM-NI). Curatorial procedures for those specimens followed Motomura and Ishikawa (2013). Specimens of the genus *Chaenogobius* were examined in the Kagoshima University Museum (KAUM–I.) and the Kanagawa Prefectural Museum of Natural History (KPM-NI), and re-identified following Akihito et al. (2013) and Harada (2014). Standard length (SL: distance from tip of snout to posterior edge of hypural plate) was measured on each specimen. Collecting localities were mapped as distribution records. Specimens examined are listed in Suppl. materials 1 and 2.

Study sites for quantitative survey

A long, sandy shore, measuring about 50 km in length from north to south, lies at the centre of the Miyazaki Prefecture coast (Fig. 2). The abovementioned southernmost limit of the cool-temperate fish species on the Pacific coast side of Kyushu is just north of the upper part of this sandy shore. We herein define the position of this sandy shore as a hypothetical biogeographic boundary (HBB) for members of the cool-

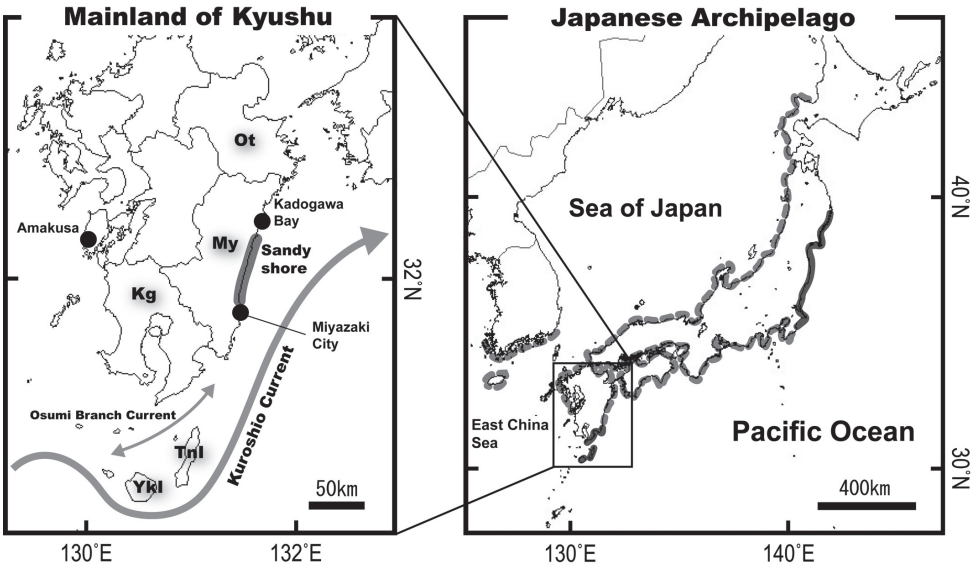

Figure 2. Conventional information on the distributional range of the two species of *Chaenogobius* (sensu Akihito et al. 2013 and Kwun et al. 2017) and a map of mainland Kyushu, southern Japan, showing the position of a long sandy shore on the eastern coast of Kyushu (a bold gray line on left-hand map). The grey-dash and solid lines on the Japanese Archipelago with adjacent areas (right-hand map) indicate the distributional range shared by the two species and that of only *C. annularis* respectively. Abbreviations for prefecture and island names mentioned in the text are as follows: **Ot** Oita Prefecture **My** Miyazaki Prefecture **Kg** Kagoshima Prefecture **Tnl** Tanega-shima Island **Ykl** Yaku-shima Island.

temperate fish species. In each of the northern and southern regions of the HBB, two rocky shore sampling sites were selected (total 4 sites), including the Osumi Islands, to examine the occurrence of the two species of *Chaenogobius* near the HBB (Fig. 3). Each site was separated by roughly the same distance (ca. 50–70 km). The sites were as follows: the northernmost site (33°09'53"N, 131°49'27"E) was in Shitanoe, Usuki City, Oita Prefecture (hereafter Oita) at the middle of the western coast of the Bungo Strait, northern part of eastern coast of Kyushu; the second site, on the Pacific coast of Kyushu (32°28'16"N, 131°40'58"E), was Kaneiso Beach, northern coast of Kadogawa Bay, Miyazaki Prefecture (hereafter N-Miyazaki), north of the HBB; the third site (31°47'40"N, 131°28'37"E) was Oryuzako, Miyazaki City, Miyazaki Prefecture (hereafter S-Miyazaki), located at the southern part of Pacific coast of Kyushu, south of the HBB; the southernmost sites (30°41'02"N, 130°57'10"E and 30°25'12"N, 130°51'49"E) were both on Tanega-shima Island (one of the Osumi Islands, hereafter Tanega-shima), located ca. 20 km southeast of the tip of Osumi Peninsula, Kagoshima Prefecture. Data from the two Tanega-shima sites were combined as one site. All the sites were selected to be as uniform as possible with respect to the physical environment (such as wave exposure).

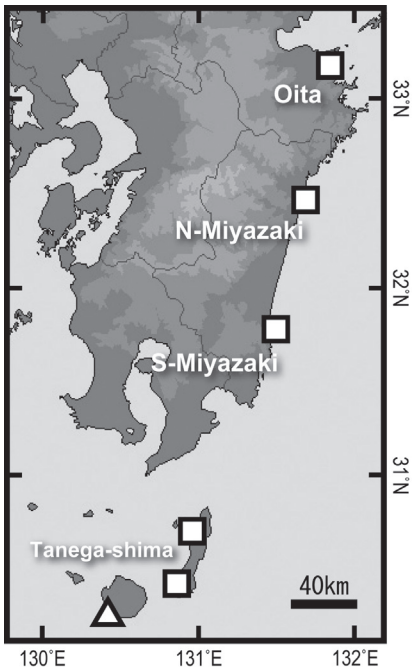

Figure 3. Map showing the sampling sites in the present study (squares) and the site of a previous study (triangle, Yaku-shima Island: Murase 2013, 2015) for the quantitative survey in rock pools along the eastern coast of Kyushu, southern Japan.

Methods for quantitative survey

Generally, five rock pools were sampled at each designated sampling site, except for the two sites on Tanega-shima Island, where 2–4 rock pools were sampled at each site. The total number of rock pools investigated during the seasons differed at each site, as the same pools were not sampled each time; some tide pools were inaccessible on certain sampling occasions due to costal weather conditions, such as high waves, and at these times, a neighbouring rock pool was selected. Across the sampling sites, tide pools were selected to be as similar as possible in mean size and elevation, following the methods of Castellanos-Galindo et al. (2005) for rock pool measurements and volume estimations. Rock pool samplings were conducted near the spring tide in Japanese spring (late March–May) and autumn (late September–October) 2016 at each site. These seasons were chosen because juveniles of *Chaenogobius* are abundant in spring on shallow rocky shores, and these gobies appear to settle by autumn (Harada 2014; Murase, pers. obs.). Therefore, these are the best seasons for comparing goby abundance between the sites in terms of both juvenile and mature individuals. Fish sampling was performed once at each rock pool in each season by completely emptying the rock pool with a bucket and a mug as in Murase (2013). Just after collection, the fishes were immediately placed in a plastic bag with ice and sea water, and transported to the laboratory. The specimens

were preserved in 70 % ethanol after fixation with 10 % formalin. Specimens were identified according to Akihito et al. (2013) and Harada (2014), and measured (SL). All specimens were deposited in KPM-NI as vouchers for the quantitative survey, and listed in Suppl. materials 3 and 4. Density (individuals per m^3) of each species at each rock pool was calculated using the number of individuals and the estimated volume of each rock pool. To ascertain the variation in fish density between the sites, one-way analysis of variance (ANOVA) and a Tukey's test or t-test were performed for each season after data were $\log_{10}(x + 1.0)$ transformed. Adding to this, the occurrence rates of the two species at each site for each season were calculated as the "frequency of occurrence in the species within a site (number of rock pools where the species was present)/ frequency of sampling event within the site (total number of rock pools investigated at the site) × 100 (%)".

Results

Geographical distribution obtained from museum specimens is shown in Fig. 4. *Chaenogobius annularis* is distributed along almost the entire coasts of Kagoshima and Miyazaki prefectures, south-east Kyushu including two of the Osumi Islands (Yaku-shima and Tanega-shima islands). Museum data also resulted in new records for the species on the East China Sea coasts, southern part of Satsuma Peninsula and Kinko Bay, Kagoshima Prefecture. The distribution of *C. gulosus* was also extended, from the coasts of the East China Sea to Kinko Bay in Kagoshima prefecture, but on the eastern coast of Kyushu it was restricted to the northern part of Miyazaki Prefecture (Kadogawa Bay and Nobeoka City), in the northern area of the HBB (Fig. 2). Two adult individuals of *C. gulosus* were recorded from the northwestern coast of Tanega-shima Island (Fig. 4, Suppl. material 2), representing the southernmost record of the species. We re-identified the specimen of *C. gulosus* reported from Miyaziki City by Akihito et al. (2013) (KAUM–I. 21427, Masahiro Aizawa personal communication) as *C. annularis*.

Rock pool volumes for the quantitative survey ranged from 0.06 to 0.76 m^3 (n = 5, mean ± SD: 0.47 ± 0.33 m^3), 0.31 to 1.01 m^3 (n = 5, 0.72 ± 0.32 m^3), 0.08 to 5.92 m^3 (n = 7, 1.73 ± 2.54 m^3), and 0.12 to 4.13 m^3 (n = 8, 1.14 ± 1.33 m^3) in Oita, N-Miyazaki, S-Miyazaki, and Tanega-shima respectively. Rock pool heights (pool surface height at low tide; see fig. 1 in Murase et al. 2010) ranged from 0.52 to 1.24 m (n = 5, mean ± SD = 0.79 ± 0.30 m), 0.60 to 1.41 m (n = 5, 0.95 ± 0.35 m), 0.69 to 1.08 m (n = 7, 0.90 ± 0.14 m), and 0.76 to 1.66 m (n = 8, 1.12 ± 0.28 m) in Oita, N-Miyazaki, S-Miyazaki, and Tanega-shima respectively. The quantitative survey revealed variation and a gradient of occurrence pattern in the two species of *Chaenogobius* along the eastern coast of Kyushu (Fig. 5). There were no individuals for each species in the following sites and seasons: *C. annularis* at S-Miyazaki in autumn and at Tanega-shima sites in any season; *C. gulosus* at N-Miyazaki in autumn, at S-Miyazaki and Tanega-shima sites in any season. Based on this, the values of non-individual sites were omitted from the descriptions of size range and statistical analyses. The density of *C. annularis*

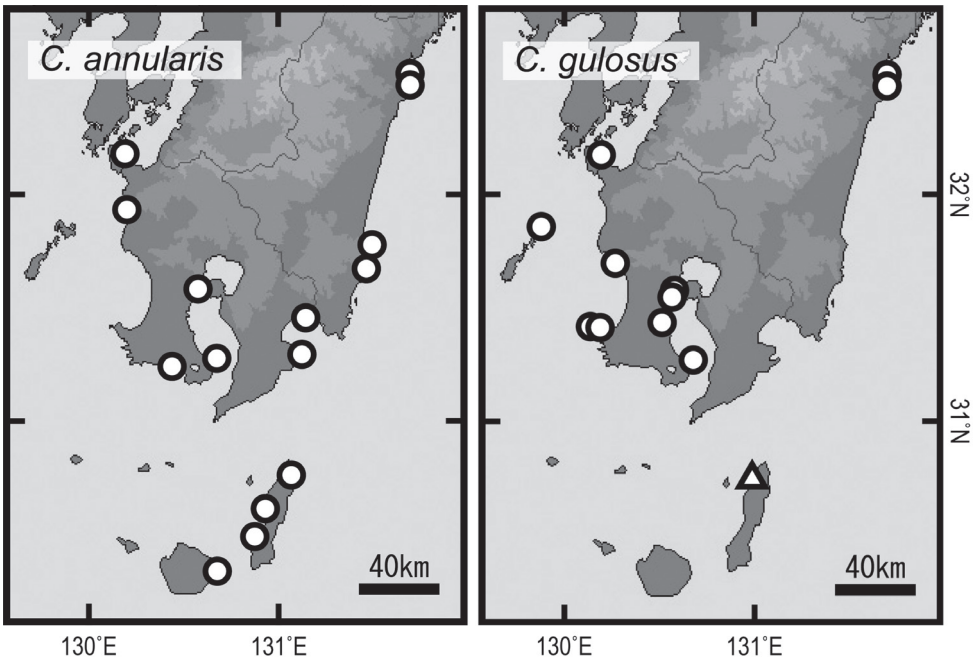

Figure 4. Records (circles and a triangle) of *Chaenogobius annularis* (left) and *C. gulosus* (right) in south-east Kyushu, southern Japan, based on the examination of museum specimens (qualitative survey). A triangle indicating occurrence of *C. gulosus* in Tanega-shima Island by possible human-induced transportation.

decreased from Oita to Tanega-shima in each season. In spring, the density at Oita (58.0 ± 16.4 per m^3 = average ± SE) was significantly higher than that at N-Miyazaki (8.5 ± 1.9 per m^3) and S-Miyazaki (11.6 ± 4.2 per m^3) (Tukey's test: $p < 0.05$ in each comparison). In autumn, the density at Oita (37.9 ± 24.4 per m^3) tended to be higher than that at N-Miyazaki (15.9 ± 8.6 per m^3) but no significant difference was detected (t-test: $p = 0.3663$). The occurrence rates of *C. annularis* increased with latitude from zero to 100 %, reflecting the density pattern in each season (Fig. 5). The density of *C. gulosus* did not significantly differ between Oita and N-Miyazaki in the spring (t-test: $p = 0.1375$) but only a single individual was collected at a single rock pool in N-Miyazaki by the quantitative method. Correspondingly, the occurrence rates of *C. gulosus* were higher in Oita (60 and 100 % in spring and autumn respectively) than in N-Miyazaki (20 % in spring).

Discussion

The qualitative and quantitative surveys showed different distribution patterns between the two species of *Chaenogobius*. The qualitative survey showed *C. annularis* to be distributed along almost the entire coasts of south-east Kyushu including Osumi Islands

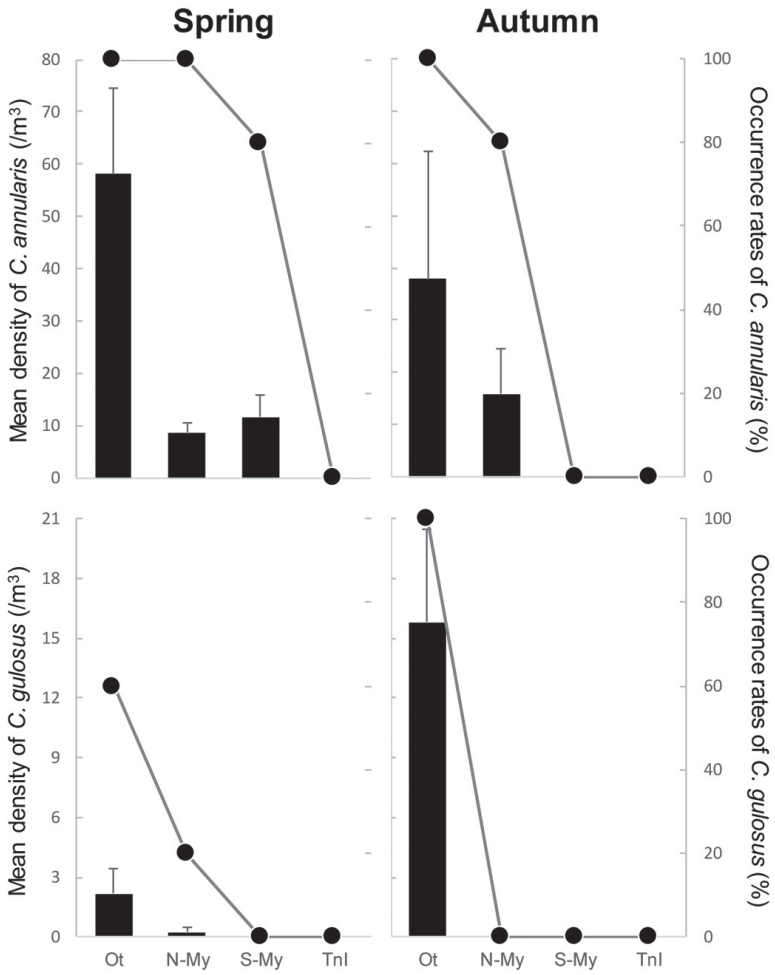

Figure 5. Results of quantitative samplings in rockpools at four sites on the eastern coast of Kyushu, southern Japan. Solid bars and plots show mean density (error bars indicating standard error) and occurrence rates of each species of *Chaenogobius* (upper, *C. annularis*; lower, *C. gulosus*) at each site in the two seasons (left, spring; right, autumn) respectively. Abbreviations of the sites on the x-axis are as follows: Ot, Oita; N-My, N-Miyazaki, S-My, S-Miyazaki; TnI, Tanega-shima (these locality names correspond to those used in Fig. 3). Sample sizes, n = 5, except for Tanega-shima in autumn (n = 8).

(both Yaku-shima and Tanega-shima islands), whereas the distribution of *C. gulosus* on the eastern coast of Kyushu was restricted to a northern area around Kadogawa Bay, north of the HBB, and among Osumi Islands; this species was recorded from only a single site at Tanega-shima Island (Fig. 4). The quantitative surveys supported these distribution patterns, with *C. annularis* detected from the three sites of the eastern coast of Kyushu, but *C. gulosus* was detected only from north of the HBB on the eastern coast of Kyushu (Fig. 5). This distribution pattern of *C. gulosus* corresponds well with that of the cool-temperate species in Nakabo's (2013) fig. 2B and suggests a range

boundary disequilibrium (sensu Sexton et al. 2009) on the coast of Kyushu: the species is present on the western side of Kyushu while being absent from the eastern side even at the same latitude. The coastal environment of Miyazaki Prefecture is characterized by two main features, which the western coast of Kyushu does not have: a long sandy shore, oriented north to south, located in the mid-prefecture; and located at the upper reaches of the Kuroshio Current in a domestic temperate region (Fig. 2). Furthermore, the average surface temperature in 2016 was significantly lower in Kadogawa Bay than in Miyazaki City (n = 51, paired t-test, $p < 0.0001$: Hydrographic and Oceanographic Department 2017). The long sandy shore provides a non-reef environment where reef fishes cannot settle and inhabit, and the warm strong Kuroshio Current may construct the latitudinal temperature gradient along the coasts of Miyazaki Prefecture. This combination of environmental factors can be a biogeographic barrier for cool-temperate fish species to move from north to south. On the other hand, no such barrier effect on *C. annularis* was detected in terms of its distributional pattern. Observed differences in the distributional pattern of the two species may be caused by their early life history. *C. annularis* occurred in rock pools as juvenile stages prior to settlement (10–20 mm in body length), whereas *C. gulosus* occurred in rock pools as larger individuals after settlement (> 20 mm in body length) (Fig. 6, Suppl. materials 1–4, Sasaki and Hattori 1969). Juveniles of *C. gulosus* have generally been observed out of rock pools, such as in inner zones of fishing ports and near beaches of inner small bays of both eastern and western coasts of Kyushu (Murase unpublished data; Fig. 6B, C). The rock pool environment is physically regulated by the tidal cycle and is unstable depending on its vertical position and size (Metaxas and Scheibling 1993, Raffaelli and Hawkins 1996). These facts might mean that juveniles of *C. gulosus* have a lower tolerance for intertidal environments than *C. annularis*, especially with respect to variation of water temperature. If so, the multiplier effects of a long sandy shore and a high-temperature current may explain the range boundary disequilibrium for *C. gulosus* on the coasts of Kyushu. In addition to this difference among the species of *Chaenogobius*, records of *C. annularis* decreased from Oita to Tanega-shima, and no individuals were detected at S-Miyazaki in autumn during the quantitative survey (Fig. 5); this might indicate an inverse negative relationship with latitudinal environmental gradients for this species. Detailed information on the different physical tolerances of the two species, and the effects of the physical environment on them, is needed for understanding the relationships between these intertidal gobies and the coastal environment.

Senou et al. (2006) were the first to compare the composition of coastal fish faunas along the Kuroshio Current region of Japan by analysing data from 12 sites. Their results revealed two clusters: the Ryukyu Islands and the temperate mainland of Japan including the Ogasawara Islands. The fact that the fish fauna of Tanega-shima Island shares some temperate species with mainland Japan indicates that Tanega-shima Island is clustered with temperate mainland Japan whereas Yaku-shima Island, one of the Osumi Islands, does not share those temperate species and should be clustered with the tropical Ryukyu Islands (Motomura et al. 2010, Motomura 2015, Motomura and Harazaki 2017). The qualitative survey of the present study supports these clusters on the basis

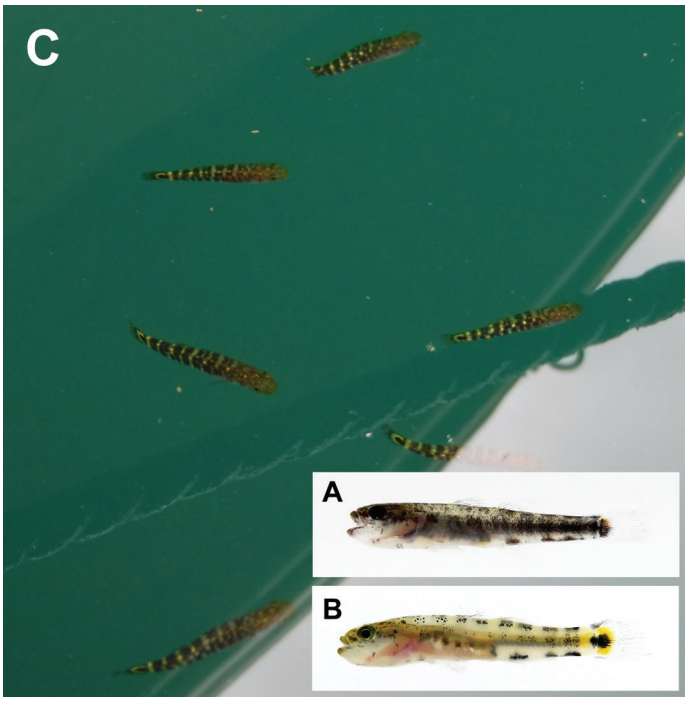

Figure 6. Images of juveniles of the two species of *Chaenogobius* on the coasts of Kyushu, southern Japan: **A** *Chaenogobius annularis*, fresh specimen, KPM-NI 42964 (photo number KPM-NR 179226), 17.6 mm SL, collected at rockpool environment in Usuki City, Oita Prefecture **B** *Chaenogobius gulosus*, fresh specimen, un-catalogued specimen (personal collection number, UMNB-I 3941), 19.2 mm SL, collected with seine net at a small beach in Totoro Port, Nobeoka City, Miyazaki Prefecture, April 2017 **C** *Chaenogobius gulosus*, swimming individuals in Tomioka Port, Reihoku Town, Amakusa, Kumamoto Prefecture, May 2017. Photos by A. Murase.

of the presence of *C. gulosus* in Tanega-shima and the absence of the species from Yaku-shima Island, although *C. annularis* was present at both islands. However, the present study compared the abundance of certain coastal-fish species on the mainland of Kyushu with the subtropical Osumi Islands located southward from the mainland, and detected no species of *Chaenogobius* at Tanega-shima. Furthermore, a year-round quantitative survey on Yaku-shima Island did not record any species of *Chaenogobius* (Murase 2013, 2015) although individuals of the genus were recorded at all three sites on mainland Kyushu (Fig. 5) in the present study. These facts indicate that the occurrence of species of *Chaenogobius* in the Osumi Islands is occasional and that these subtropical islands are a non-preferred region for these cool-temperate species. The reason for their occurrence at the Osumi Islands could be physical or human-induced transportation. Because *C. annularis* is distributed on the coasts of the Osumi Peninsula, the southernmost part of Kyushu, this species can be transported from the southern part of Kyushu to the Osumi Islands by the Osumi Branch Current, which flows irregularly and bi-directionally between those islands and the southernmost area of Kagoshima Prefecture

(Fig. 2; Motomura et al. 2010). However, the occurrence of *C. gulosus* in Tanega-shima does not correspond to the above biogeographic interpretation regarding species distribution and the currents around the southern coast of Kyushu because *C. gulosus* is not distributed in any area associated with the Osumi Branch Current (i.e., the coasts of the Osumi Peninsula). Some Japanese gobiid fish species are known to have been transported overseas via ship ballast water (Okiyama, 1985), and numerous large ferries ply the waters between Kagoshima City and Nishino-omote City on the northwestern part of Tanega-shima Island every week (e.g., Ferry Hibiscus, http://www.yakushimaferry.com/). Because *C. gulosus* is usually present in port areas as juveniles (Fig. 6C), and is distributed on the coasts of Kagoshima City, ballast water may be a more reasonable explanation for its occurrence at Tanega-shima. A combination of qualitative and quantitative survey methods in the present study highlighted that the southernmost record of a certain species may not necessarily mean the true limit of its distributional range.

The distribution patterns and proportion of occurrence in the two species of *Chaenogobius* reported in this study indicate the difference of distribution range of the two species at their southernmost limit, even though they are both categorized as cool-temperate species, and provided implications for the different effects of a biogeographic barrier to each species. In addition to a species/genus level test, comprehensive ichthyofaunal surveys along the coast of Kyushu using qualitative and quantitative methods could clarify the effects of the biogeographic barrier suggested here, and as well as further define variation in physical factors along the Kuroshio Current that influence the formation of coastal fish communities.

Acknowledgements

The authors would like to express sincere thanks to members of Miyazaki City Fishermen's Cooperative, Fisheries Cooperative Association of Iorigawa and Usuki Branch of Oita Fishermen's Cooperative for permitting field surveys, members of KAUM for their help in examining museum specimens, Yukiya Ogata (University of Miyazaki) for field sampling efforts, Hiroshi Senou (KPM) for his help in depositing specimens and photos, Masahiro Aizawa (Biological Laboratory, Imperial Household Agency) for providing voucher information on a past study, and the staff of the Hydrographic and Oceanographic Department of the 10th Regional Coast Guard Headquarters (Kagoshima, Japan) who provided tidal information for the study sites. We also sincerely thank Gordon Yearsley (Ellipsis Editing, Australia) for the English revision of an early draft, anonymous reviewers and Sven Kullander for their valuable comments on the manuscript. This research was partly supported by JSPS KAKENHI Grant Number 15H06514, Fujiwara Natural History Foundation, and the Sasakawa Scientific Research Grant from The Japan Science Society (Grant Number: 29-737), and performed as a part of the project "Research for understanding coastal fish diversity and ecology of the crested murrelet in Kadogawa Town, northern part of Miyazaki Prefecture" supported by Kadogawa Town.

References

Akihito Sakamoto K, Ikeda Y, Aizawa M (2013) Gobioidei. In: Nakabo T (Ed.) Fishes of Japan with pictorial keys to the species, third edition. Tokai University Press, Hadano, 1347–1608, 2109–2211. [in Japanese]

Amaoka K, Nakaya K, Yabe M (2011) Fishes of Hokkaido. Hokkaido Shinbun-sya, Sapporo, 482 pp. [in Japanese]

Arakaki S, Tokeshi M (2006) Short-term dynamics of tidepool fish community: diel and seasonal variation. Environmental Biology of Fishes 76: 221–235. https://doi.org/10.1007/s10641-006-9024-5

Asakura A, Suzuki H (1987) Zoogeographical aspects of rocky-intertidal molluscan fauna of the Pacific coasts of Japan. Marine Biology 95: 75–81. https://doi.org/10.1007/BF00447487

Briggs JC (1974) Marine zoogeography. McGraw-Hill, New York, 475 pp.

Briggs JC (1995) Global biogeography. Elsevier, Amsterdam, 452 pp.

Briggs JC, Bowen BW (2012) A realignment of marine biogeographic provinces with particular reference to fish distributions. Journal of Biogeography 39: 12–30. https://doi.org/10.1111/j.1365-2699.2011.02613.x.

Castellanos-Galindo GA, Giraldo A, Rubio EA (2005) Community structure of an assemblage of tidepool fishes on a tropical eastern Pacific rocky shore, Colombia. Journal of Fish Biology 67: 392–408. https://doi.org/10.1111/j.0022-1112.2005.00735.x

Cox CB, Moore PD (2005) Biogeography: an ecological and evolutionary approach, seventh edition. Blackwell Publishing, Oxford, 428 pp.

Harada S (2014) Genus *Chaenogobius*. In: Okiyama M (Ed.) An atlas of early stage fishes in Japan. Tokai University Press , Hadano, 1269–1271. [in Japanese]

Hydrographic and Oceanographic Department 10th Regional Coast Guard Headquaters (2017) Information on surface water temperature [original title in Japanese: Hyomen Suion Jyoho]. http://www1.kaiho.mlit.go.jp/KAN10/kaisyo/suion/suion.html [accessed 29 May 2017]

Kohno H (2011) A photographic guide to the fishes in Tokyo Bay. Heibonsha, Tokyo, 374 pp. [in Japanese]

Kurihara T (2007) Spatiotemporal variations in rocky intertidal malacofauna throughout Japan in the 1970s and 1980s. Marine Biology 153: 61–70. https://doi.org/10.1007/s00227-007-0784-z

Kwun HJ, Park J, Kim HS, Bae H (2017) Preliminary report on fish diversity in the tidal pools of Jeju Island, Korea. Marine Biodiversity 47: 957–963. https://doi.org/10.1007/s12526-016-0589-8

Metaxas A, Scheibling RE (1993) Community structure and organization of tidepools. Marine Ecology Progress Series 98: 187–198. https://doi.org/10.3354/meps098187

Motomura H (2015) Fish species diversity in the Ryukyu Islands [original title in Japanese: Ryukyu-retto no Gyorui Tayosei] In: Ecological Society Japan (Ed.) Biodiversity, Formation history, and conservation in the Nansei Islands [original title in Japanese: Nansei-syoto no Seibutsu-tayosei, Sono Seiritsu to Hozen]. Nanposhinsha, Kagoshima, 56–63. [in Japanese]

Motomura H, Harazaki S (2017) Annotated checklist of marine and freshwater fishes of Yakushima island in the Osumi Islands, Kagoshima, southern Japan, with 129 new records. Bulletin of the Kagoshima University Museum 9: 1–183.

Motomura H, Ishikawa S (2013) Fish Collection Building and Procedures Manual. English Edition. Kagoshima University Museum, Kagoshima; Research Institute for Humanity and Nature, Kyoto, 69 pp. http://www.museum.kagoshima-u.ac.jp/staff/motomura/dl_en.html

Motomura H, Kuriiwa K, Katayama E, Senou H, Ogihara G, Meguro M, Matsunuma M, Takata Y, Yoshida T, Yamashita M, Kimura S, Endo H, Murase A, Iwatsuki Y, Sakurai Y, Harazaki S, Hidaka K, Izumi H, Matsuura K (2010) Annotated checklist of marine and estuarine fishes of Yaku-shima island, Kagoshima, southern Japan. In: Motomura H, Matsuura K (Eds) Fishes of Yaku-shima island—a World Heritage island in the Osumi Group, Kagoshima Prefecture, southern Japan. National Museum of Nature and Science, Tokyo, 65–247.

Murase A (2013) Community structure and short temporal stability of a rockpool fish assemblage at Yaku-shima island, southern Japan, northwestern Pacific. Ichthyological Research 60: 312–326. https://doi.org/10.1007/s10228-013-0351-1

Murase A (2015) Ichthyofaunal diversity and vertical distribution patterns in the rock pools of the southwestern coast of Yaku-shima island, southern Japan. Check List: the journal of biodiversity data 11(4): 1682. https://doi.org/10.15560/11.4.1682

Murase A, Miki R, Wada M (2017) Range extension of an embiotocid surfperch, *Ditrema temminckii temminckii* (Teleostei: Perciformes), based on specimens from Kadogawa Bay, Pacific coast of Kyushu, southern Japan. Bulletin of the Biogeographical Society of Japan 71: 167–172. [in Japanese with English abstract]

Murase A, Miyazaki Y, Okuyama G, Kaiga J, Tazaki Y, Sunobe T (2010) A preliminary study of rockpool fish assemblage structure in Tateyama Bay, Boso Peninsula, Chiba, central Japan. Bulletin of the Biogeographical Society of Japan 65: 141–149. [in Japanese with English abstract]

Nakabo T (2013) Biogeography of East Asian fishes. In: Nakabo T (Ed.) Fishes of Japan with pictorial keys to the species, third edition. Tokai University Press, Hadano, 2289–2338. [in Japanese]

Nakamura K (1970) The tidal fish fauna of Sagami Bay and its adjacent waters. Research Report of the Kanagawa Prefectural Museum Natural History 1: 1–33. [in Japanese]

Nakaoka M, Ito N, Yamamoto T, Okuda T, Noda T (2006) Similarity of rocky intertidal assemblages along the Pacific coast of Japan: effects of spatial scales and geographic distance. Ecological Research 21: 425–435. https://doi.org/10.1007/s11284-005-0138-6

Nishimura S (1992) Distribution of marine organisms around Japanese waters [original title in Japanese: Nihon-kinkai ni Okeru Dobutsu-bunpu]. In: Nishimura S (Ed.) Guide to Seashore Animals of Japan with Color Pictures and Keys, Vol I. Hoikusha, Osaka, 25 pp. [in Japanese]

Ohgaki S (2011) A regional biogeography of shore molluscs: Influence of the Kuroshio Current and the two capes. Zoological Science 28: 268–275. https://doi.org/10.2108/zsj.28.268

Okada T, Ishihara K, Murase A, Hino T (2015) A latitudinal gradient in the biogeographic compositions of rock pool fish assemblages on the Pacific coast of central Japan: an examination of the influence of the Kuroshio Current. Biogeography 17: 1–11.

Okamura O, Amaoka K (1997) Sea Fishes of Japan. Yama-Kei Publishers, Tokyo, 783 pp. [in Japanese]

Okiyama M (1985) Community disturbance [original title in Japanese: Gunshu no Kakuran]. In: Okiyama M, Suzuki K (Eds) Marine Organisms in Japan: Ecology of Invasion and Disturbance [original title in Japanese: Nihon no Kaiyoseibutsu—Shinryaku to Kakuran no Seitaigaku]. Tokai University Press, Tokyo, 151–160. [in Japanese]

Raffaelli D, Hawkins S (1996) Intertidal Ecology. Chapman & Hall, London, 356 pp.

Sasaki T, Hattori J (1969) Comparative ecology of two closely related sympatric gobiid fishes living in tide pools. Japanese Journal of Ichthyology 15: 143–155. [In Japanese with English summary]

Senou H, Matsuura K, Shinohara G (2006) Checklist of fishes in the Sagami Sea with zoogeographical comments on shallow water fishes occurring along the coastlines under the influence of the Kuroshio Current. Memoirs of the National Science Museum 41: 390–542.

Sexton JP, McIntyre PJ, Angert AL, Rice KJ (2009) Evolution and ecology of species range limits. Annual Review of Ecology, Evolution, and Systematics 40: 415–436. https://doi.org/10.1146/annurev.ecolsys.110308.120317

Stevenson DE (2002) Systematics and distribution of fishes of the Asian goby genera *Chaenogobius* and *Gymnogobius* (Osteichthyes: Perciformes: Gobiidae), with the description of a new species. Species Diversity 7: 251–312.

Supplementary material 1

List of voucher specimens of *Chaenogobius annularis* for distribution records in south-east Kyushu by examination of museum collections

Authors: Atsunobu Murase, Ryohei Miki, Hiroyuki Motomura

Data type: PDF

Explanation note: Lots of specimens ordered according to longitude. Number of KPM-NR indicates photographs of fresh specimens deposited in KPM.

Link: https://doi.org/10.3897/zookeys.725.19952.suppl1

Supplementary material 2

List of voucher specimens of *Chaenogobius gulosus* for distribution records in south-east Kyushu by examination of museum collection

Authors: Atsunobu Murase, Ryohei Miki, Hiroyuki Motomura

Data type: PDF

Explanation note: Lots of specimen ordered according to longitude. Number of KPM-NR indicating photographs of fresh specimen deposited in KPM.

Link: https://doi.org/10.3897/zookeys.725.19952.suppl2

Supplementary material 3

List of voucher specimens of *Chaenogobius annularis* from quantitative surveys at rockpools on the eastern coasts of Kyushu

Authors: Atsunobu Murase, Ryohei Miki, Hiroyuki Motomura

Data type: PDF

Explanation note: KPM-NI and KPM-NR indicates the number of the specimen and its photograph respectively.

Link: https://doi.org/10.3897/zookeys.725.19952.suppl3

Supplementary material 4

List of voucher specimens of *Chaenogobius gulosus* from quantitative surveys at rockpools on the eastern coasts of Kyushu

Authors: Atsunobu Murase, Ryohei Miki, Hiroyuki Motomura

Data type: PDF

Explanation note: KPM-NI and KPM-NR indicates the number of the specimen and its photograph respectively.

Link: https://doi.org/10.3897/zookeys.725.19952.suppl4

ZooKeys 725: 97–122 (2017)
doi: 10.3897/zookeys.725.21006
http://zookeys.pensoft.net

RESEARCH ARTICLE

A peer-reviewed open-access journal
ZooKeys
Launched to accelerate biodiversity research

Three new species and the molecular phylogeny of *Antipathozoanthus* from the Indo-Pacific Ocean (Anthozoa, Hexacorallia, Zoantharia)

Hiroki Kise[1,2], Takuma Fujii[1,3], Giovanni Diego Masucci[1], Piera Biondi[1], James Davis Reimer[1,2,4]

1 *Molecular Invertebrate Systematics and Ecology Laboratory, Graduate School of Engineering and Science, University of the Ryukyus, 1 Senbaru, Nishihara, Okinawa 903-0213, Japan* **2** *Palau International Coral Reef Center, 1-M-Dock Road, Koror, Palau 96940* **3** *Research Center for Island Studies Amami Station, Kagoshima University, Naze-Yanagimachi 2-1, Amami, Kagoshima 894-0032, Japan* **4** *Tropical Biosphere Research Center, University of the Ryukyus, 1 Senbaru, Nishihara, Okinawa 903-0213, Japan*

Corresponding author: *Hiroki Kise* (hkm11sea@yahoo.co.jp)

Academic editor: *B. W. Hoeksema* | Received 15 September 2017 | Accepted 7 November 2017 | Published 29 December 2017

http://zoobank.org/E47535C1-21CF-417C-A212-F6E819080565

Citation: Kise H, Fujii T, Masucci GD, Biondi P, Reimer JD (2017) Three new species and the molecular phylogeny of *Antipathozoanthus* from the Indo-Pacific Ocean (Anthozoa, Hexacorallia, Zoantharia). ZooKeys 725: 97–122. https://doi.org/10.3897/zookeys.725.21006

Abstract

In this study, three new species of macrocnemic zoantharians (Hexacorallia, Zoantharia) are described from localities in the Indo-Pacific Ocean including the Red Sea, the Maldives, Palau, and southern Japan: *Antipathozoanthus obscurus* **sp. n.**, *A. remengesaui* **sp. n.**, and *A. cavernus* **sp. n.** Although the genus *Antipathozoanthus* is currently restricted to species living on antipatharians, *A. obscurus* **sp. n.** is not associated with any living substrate and instead is found on coral reef carbonate substrate within narrow caves or cracks. The two new species that have association with antipatharians, *A. remengesaui* **sp. n.** and *A. cavernus* **sp. n.**, can be distinguished by their relative coenenchyme development and the antipatharian species that each uses as substrate. Additionally, all new species described in this study have unique nuclear internal transcribed spacer region of ribosomal DNA (ITS-rDNA) sequences. Our results indicate that more phylogenetic studies focusing on increasing the numbers of species examined within each of the genera of Parazoanthidae are required in order to better understand the evolutionary history of substrate specificity within the family Parazoanthidae.

Keywords

antipatharian, cave-dwelling, diversity, evolution, new species, substrate specificity

Introduction

Zoantharia Rafinesque, 1815 is the third most speciose order within the subclass Hexacorallia Haeckel, 1896. Zoantharians can be found in a wide variety of marine environments from intertidal zones to deep-sea cold seeps (e.g., Reimer et al. 2007b), and are characterized by having two rows of tentacles and the unique bilateral arrangements of the mesenteries, with most species forming clonal colonies without hard structures such as skeletons of the order Scleractinia. Zoantharia is currently divided into two suborders; Brachycnemina Haddon & Shackleton, 1891, and Macrocnemina Haddon & Shackleton, 1891, based on differences in the fifth pair of mesenteries from the dorsal directive. Zoantharians within suborder Macrocnemina are distributed worldwide, and are usually found in associations with other invertebrates. Within Macrocnemina, the largest family is Parazoanthidae Delage & Hérouard, 1901, which currently contains 13 genera (Low et al. 2016). Most species of these genera live in association with other marine invertebrates, including antipatharians (Ocaña and Brito 2003; Sinniger et al. 2010), octocorals (Reimer et al. 2008; Bo et al. 2012; Sinniger et al. 2013), and sponges (Haddon and Shackleton 1891; Swain and Wulff 2007; Montenegro et al. 2015, 2016). Historically, establishing the taxonomic framework of Parazoanthidae was challenging due to relatively few diagnostic morphological characteristics (Sinniger et al. 2005; Montenegro et al. 2015), and the family was shown to be paraphyletic in initial molecular studies (Sinniger et al. 2005). Recently, however, studies based on molecular phylogeny combined with ecological data have greatly revised the taxonomy within the family Parazoanthidae (Sinniger et al. 2005, 2013; Sinniger and Häussermann 2009; Montenegro et al. 2015, 2016). As a consequence of these studies, nine genera within Parazoanthidae have been described since 2008 and another genus, *Bergia* Duchassaing & Michelotti, 1860, has been resurrected. Key to this new taxonomic framework is the idea initially proposed by Sinniger et al. (2005, 2010) that different parazoanthid genera share long evolutionary histories with the associated marine invertebrates they use as substrates.

One of these recently erected genera is *Antipathozoanthus* Sinniger, Reimer & Pawlowski, 2010. As the generic name indicates, species in this genus utilize antipatharians (Hexacorallia, Antipatharia) as their obligate substrate. The genus currently includes two valid species; *A. macaronesicus* (Ocaña & Brito, 2003) from the eastern Atlantic and *A. hickmani* Reimer & Fujii, 2010 from the Galapagos Islands. Additionally, several potentially undescribed species have been reported from the Red Sea (Reimer et al. 2014b), the South China Sea (Reimer et al. 2017), and Japan (Sinniger et al. 2010; Reimer et al. 2013, 2014a). However, the species diversity of *Antipathozoanthus* spp. in the Indo-Pacific Ocean remains generally unknown. In this study, three new *Antipathozoanthus* species are formally described based on specimens collected from a number of regions in the Indo-Pacific Ocean, and the genus is redescribed based on these findings.

Materials and methods

Specimen collection. *Antipathozoanthus* specimens were collected between 2009 to 2016 from three localities in the Red Sea, three localities in the Maldives, five localities in Japan, and two localities in Palau (Fig. 1), with one comparative specimen of *A. macaronesicus* collected from Pico Island, Azores, Portugal. All specimens were collected by SCUBA. Specimen images were taken *in situ* for gross external morphological analyses. Collected specimens were preserved in 99.5% ethanol (Table 1).

Molecular analyses. *Antipathozoanthus* DNA was extracted using the guanidine protocol following Sinniger et al. (2010). PCR was performed for three genetic markers: mitochondrial cytochrome oxidase subunit I (COI), mitochondrial 16S ribosomal DNA (16S-rDNA), and the nuclear internal transcribed spacer region of ribosomal DNA (ITS-rDNA) using a HotStarTaq Master Mix Kit (Qiagen, Tokyo, Japan). COI was amplified with the following primers: COIZoanF (5'-TGA TAA GGT TAG AAC TTT CTG CCC CGG AAC-3') (Reimer et al. 2007b) and COIantr (5'-GCC CAC ACA ATA AAG CCC AA TAY YCC AAT-3') (Sinniger et al. 2010). 16S-rDNA was amplified with the following primers: 16SarmL (5'-GGC CTC GAC TGT TTA CCA AA-3') (Fujii and Reimer 2011) and 16SbmoH (5'-CGA ACA GCC AAC CCT TGG-3') (Sinniger et al. 2005). The ITS-rDNA was amplified with the following primer pairs: either ITSf (5'-CTA GTA AGC GCG AGT CAT CAG C-3') and ITSr (5'-GGT AGC CTT GCC TGA TCT GA-3') (both Swain 2009) or Zoan-f (5'-CTT GAT CAT TTA GAG GGA GT-3') and Zoan-r (5'-CGG AGA TTT CAA ATT TGA GCT-3') (both Reimer et al. 2007a). The markers were amplified following the thermal cycle conditions: 5 min at 95 °C followed by 35 cycles of: 30 s at 94 °C, 1 min at 40 °C, and 1 min 30 s at 72 °C, and followed by a 7 min extension at 72 °C for COI; 5 min at 95 °C and then 35 cycles of: 1 min at 95 °C, 1 min at 52 °C, and 2 min at 72 °C, followed by a 7 min extension at 72 °C for 16S-rDNA; and 5 min at 95 °C then 35 cycles of: 1 min at 94 °C, 1 min at 50 °C, and 2 min at 72 °C, followed by a 10 min extension at 72 °C for ITS-rDNA. Amplified PCR products were checked by 1.5 % agarose gel and positive PCR products were sequenced in both directions by Fasmac (Kanagawa, Japan) after clean up using shrimp alkaline phosphatase (SAP) and Exonuclease I (Takara Bio Inc., Shiga, Japan).

Molecular phylogenetic analyses. Newly obtained sequences were inspected by eye and manually edited using Geneious v8.1 (Kearse et al. 2012, http://www.geneious.com) and deposited in GenBank (accession numbers MG384639–MG384705; Table 1). Nucleotide sequences of COI, 16S-rDNA and ITS-rDNA from specimens were aligned with previous study sequences from various parazoanthid genera (*Antipathozoanthus*, *Bergia*, *Bullagummizoanthus*, *Corallizoanthus*, *Hurlizoanthus*, *Kauluzoanthus*, *Kulamanamana*, *Mesozoanthus*, *Parazoanthus*, *Umimayanthus*, *Zibrowius*) using the Muscle algorithm (Geneious plug-in; Edgar 2004) (Suppl. material 1). Sequences of the genus *Epizoanthus* were selected as the outgroup for all three markers' alignments. The *A. hickmani* sequence from Reimer and Fujii (2010; EU333790) was not included

Table 1. List of examined specimens, and GenBank Accession Numbers.

Specimen ID	Genus	Species	Locality	Coordinates		Collecter	Sampling date	Depth (m)	Accession number (COI)	Accession number (16S–rDNA)	Accession number (ITS–rDNA)
				Latitude	Longitude						
AZCN	*Antipathozoanthus*	*macaronesicus*	Pico Island, Azores, Portugal	N38°28'3.8"	W28°24'0"	P Wirtz	13-May-16	43	MG384664	MG384684	MG384696
BISE1	*Antipathozoanthus*	*obscurus*	Bise, Motobu, Okinawa, Japan	N26°42'34.4"	E127°52'49.2"	JD Reimer, I Kawamura	14-Aug-14	5	MG384644	MG384685	MG384691
BISE3	*Antipathozoanthus*	*obscurus*	Bise, Motobu, Okinawa, Japan	N26°42'34.4"	E127°52'49.2"	JD Reimer, I Kawamura	14-Aug-14	5	–	–	MG384693
MAL46	*Antipathozoanthus*	*remengesaui*	Coral Garden, Maldives	N3°05'24.3"	E72°58'04.5"	JD Reimer	06-May-14	24	MG384658	MG384679	–
MAL82	*Antipathozoanthus*	*remengesaui*	Wall Street, Maldives	N3°07'14.2"	E72°58'46.5"	JD Reimer	07-May-14	9	MG384657	–	–
MAL83	*Antipathozoanthus*	*remengesaui*	Wall Street, Maldives	N3°07'14.2"	E72°58'46.5"	JD Reimer	07-May-14	9	MG384656	–	–
MAL84	*Antipathozoanthus*	*remengesaui*	Wall Street, Maldives	N3°07'14.2"	E72°58'46.5"	JD Reimer	07-May-14	9	MG384655	–	MG384702
MAL85	*Antipathozoanthus*	*remengesaui*	Wall Street, Maldives	N3°07'14.2"	E72°58'46.5"	JD Reimer	07-May-14	9	MG384654	MG384678	MG384701
MAL145	*Antipathozoanthus*	*remengesaui*	Wall Street, Maldives	N3°07'14.2"	E72°58'46.5"	JD Reimer	10-May-14	12	MG384653	MG384677	–
MAL147	*Antipathozoanthus*	*remengesaui*	Wall Street, Maldives	N3°07'14.2"	E72°58'46.5"	JD Reimer	10-May-14	10	MG384652	–	–
MAL2592601	*Antipathozoanthus*	*cavernus*	Capital Reef, Maldives	N3°02'55.8"	E72°53'21.2"	M Oliverio	16-May-14	19	MG384651	MG384676	MG384697
MAL2592602	*Antipathozoanthus*	*remengesaui*	Capital Reef, Maldives	N3°02'55.8"	E72°53'21.2"	M Oliverio	16-May-14	19	–	MG384675	–
MAL261	*Antipathozoanthus*	*remengesaui*	Wall Street, Maldives	N3°07'14.2"	E72°58'46.5"	JD Reimer	17-May-14	9	MG384650	MG384674	–
KINKO1	*Antipathozoanthus*	*cavernus*	Sakurajima, Kagoshima, Japan	N31°35'23.5"	E130°35.27.8"	JD Reimer	20-Sep-15	21	MG384660	MG384681	MG384699
KINKO2	*Antipathozoanthus*	*remengesaui*	Sakurajima, Kagoshima, Japan	N31°35'23.5"	E130°35'27.8"	JD Reimer	20-Sep-15	21	MG384659	MG384680	–
PALAU2	*Antipathozoanthus*	*remengesaui*	Blue Hole, Palau	N7°8'29.4"	E134°13'23.3"	JD Reimer	15-Sep-14	23	MG384649	MG384673	MG384703
PALAU3	*Antipathozoanthus*	*remengesaui*	Siaes Tunnel. Palau	N7°18'54.8"	E134°13'13.3"	JD Reimer	15-Sep-14	37	MG384648	–	–
PALAU4	*Antipathozoanthus*	*remengesaui*	Blue Hole, Palau	N7°8'29.4"	E134°13'23.3"	JD Reimer	12-Sep-14	28	MG384647	MG384672	–
PALAU5	*Antipathozoanthus*	*cavernus*	Siaes Tunnel. Palau	N7°18'54.8"	E134°13'13.3"	JD Reimer	15-Sep-14	39	–	–	MG384698
HK70	*Antipathozoanthus*	*remengesaui*	Siaes Tunnel. Palau	N7°18'54.8"	E134°13'13.3"	H Kise	12-Sep-14	NA	MG384663	MG384683	–
HK90	*Antipathozoanthus*	*remengesaui*	Blue Hole, Palau	N7°8'29.4"	E134°13'23.3"	H Kise	15-Sep-14	22	MG384662	–	–

Specimen ID	Genus	Species	Locality	Coordinates		Collecter	Sampling date	Depth (m)	Accession number (COI)	Accession number (16S–rDNA)	Accession number (ITS–rDNA)
				Latitude	Longitude						
TF54	*Antipathozoanthus*	*obscurus*	Cape Zanpa, Yomitan, Okinawa, Japan	N26°26'26.5"	E127°42'43.7"	T Fujii	06-Apr-09	3	MG384641	–	MG384689
TF78	*Antipathozoanthus*	*obscurus*	Cape Manza, Onna, Okinawa, Japan	N26°30'18.3"	E127°51'02.3"	T Fujii	02-Oct-09	5	MG384640	MG384668	MG384687
TF102	*Antipathozoanthus*	*remengesaui*	Sakurajima, Kagoshima, Japan	N31°35'23.5"	E130°35'27.8"	T Fujii	26-Jul-11	20	MG384646	–	MG384704
TF103	*Antipathozoanthus*	*remengesaui*	Sakurajima, Kagoshima, Japan	N31°35'23.5"	E130°35'27.8"	T Fujii	26-Jul-11	40	MG384645	–	MG384705
TF148	*Antipathozoanthus*	*obscurus*	Cape Manza, Yomitan, Okinawa, Japan	N26°30'18.3"	E127°51'02.3"	T Fujii	22-Oct-12	10	MG384642	MG384669	MG384688
TF173	*Antipathozoanthus*	*remengesaui*	Onna, Okinawa, Japan	N26°26'20.9"	E127°47'7.2"	T Fujii	27-Jun-14	15	–	–	–
JDR190	*Antipathozoanthus*	*obscurus*	Al Wajh Shaybarah, Saudi Arabia	N25°21'	E36°54'	JD Reimer	03-Oct-13	3	–	MG384667	MG384692
JDR191	*Antipathozoanthus*	*obscurus*	Al Wajh Shaybarah, Saudi Arabia	N25°21'	E36°54'	JD Reimer	03-Oct-13	3	–	MG384666	MG384694
JDR192	*Antipathozoanthus*	*obscurus*	Al Wajh Shaybarah, Saudi Arabia	N25°21'	E36°54'	JD Reimer	03-Oct-13	3	MG384643	MG384665	MG384695
JDR209	*Antipathozoanthus*	*remengesaui*	Yanbu , Saudi Arabia	N24°26'	E37°14'	JD Reimer	04-Oct-13	11	–	–	MG384700
JDR211	*Antipathozoanthus*	*remengesaui*	Yanbu , Saudi Arabia	N24°26'	E37°14'	JD Reimer	04-Oct-13	12	–	MG384682	–
JDR214	*Antipathozoanthus*	*remengesaui*	Yanbu , Saudi Arabia	N24°26'	E37°14'	JD Reimer	04-Oct-13	12	MG384661	–	–
JDR279	*Antipathozoanthus*	*obscurus*	Shib Nazar, Saudi Arabia	N22°19'	E38°51'	JD Reimer	10-Oct-13	4	–	MG384671	MG384690
KU1	*Antipathozoanthus*	*obscurus*	Ara, Kumejima Island, Okinawa, Japan	N26°19'15.0"	E126°45'21.3"	T Fujii	20-Nov-09	15	MG384639	MG384670	MG384686

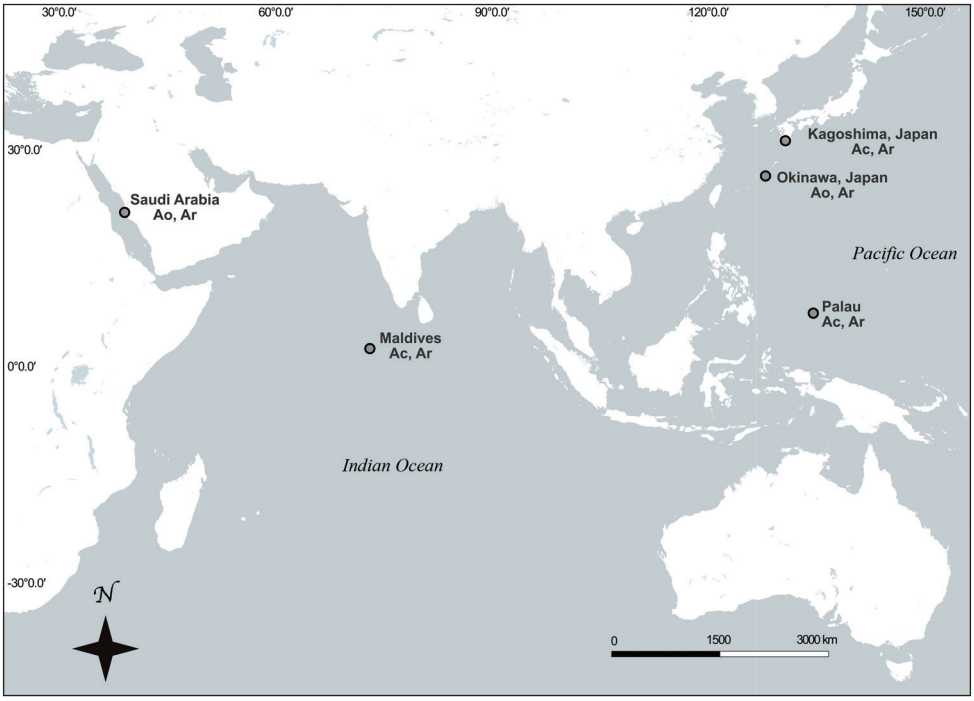

Figure 1. Sampling location in the Indian Ocean and Pacific Ocean of specimens used in this study. Location of specimens collected in this study represented by closed symbols. Species abbreviations after locations: Ao, *Antipathozoanthus obscurus* sp. n.; Ar, *A. remengesaui* sp. n.; Ac, *A. cavernus* sp. n.

in the COI phylogenetic tree in this study due to its short length (280 bp). The 16S-rDNA and ITS-rDNA indels were aligned following previous studies (Sinniger et al. 2010; Montenegro et al. 2016). Three alignment datasets were generated; 430 sites of 48 sequences for COI; 589 sites of 57 sequences for 16S-rDNA and 938 sites of 48 sequences for ITS-rDNA. The alignment data are available as electronic supplementary material (Suppl. material 1–4).

The generated alignments of each marker were used to construct a concatenated alignment. All missing data, including gaps, were replaced with "N". All specimens of *Antipathozoanthus* included in the concatenated alignment included at least ITS-rDNA sequences. The concatenated alignment consisted of 1957 positions and 54 sequences. Phylogenetic analyses of the concatenated alignment were performed using maximum likelihood (ML) and Bayesian inference (BI), with gene partitions set for ML in RAxML v8 (Stamatakis 2014), and gene partitions for BI as indicated by jModelTest version 0.0.1 (Posada 2008) per each marker in MrBayes v3.2.2 (Huelsenbeck and Ronquist 2001) as shown below. Phylogeny reconstructions were performed for each marker using neighbor joining (NJ), ML and BI.

The NJ phylogeny reconstruction was performed using Geneious v8.1 (Kearse et al. 2012, http://www.geneious.com) with the Hasegawa-Kishino-Yano genetic dis-

tance model (HKY) (Hasegawa et al. 1985) and 1000 replicates of bootstrapping. The best-fitting models for ML phylogeny reconstruction were performed by jModelTest under Akaike Information Criterion (AIC). The following models were suggested by jModelTest: TrN+I for the COI dataset; K80+G for the 16S-rDNA dataset; HKY+I+G for ITS-rDNA dataset. ML phylogenetic trees were constructed with PhyML (Guindon and Gascuel 2003) for each marker independently. PhyML was performed using an input tree generated by BIONJ with the models suggested by jModelTest, with 8 gamma-categories of substitution rates. Bootstrap replicates (1000) were conducted using the same parameters. The best fitting models for BI phylogeny reconstruction was performed by jModelTest under Bayesian Information Criterion (BIC). The following models were suggested by jModelTest: K80+G for the COI dataset; K80+G for the 16S-rDNA dataset; and HKY+I+G for the ITS-rDNA dataset. BI phylogenetic trees were constructed with the program MrBayes as a plug-in in Geneious with the models suggested by jModelTest. One cold and three heated Markov chain Monte Carlo (MCMC) chains with default temperature were run for 20,000,000 generations, subsampling frequency of 1000 and a burn in length of 3,000,000 (15%) for all alignments. Average Standard Deviation of Split Frequency (ASDOSF) values were <0.01 for all three Bayesian datasets.

Morphological analyses. Numbers of tentacles, polyp coloration, oral disk coloration, relative tentacle lengths, and polyp dimensions (oral disk diameter/polyp height) were examined using *in situ* images. Additionally, the relative development of the coenenchyme was examined using a dissecting microscope. Coenenchyme development was classified as 1) “highly developed coenenchyme" when polyps covered the antipatharian substrate completely, or 2) “poorly developed coenenchyme" when polyps did not completely cover the antipatharian substrate and the antipatharians were clearly visible. For internal morphological analyses, we observed mesentery arrangement and numbers, and location and shape of marginal muscle. Histological sections of 8 μm thickness were made and stained with hematoxylin and eosin after decalcification with Bouin’s fluid for 24h.

Cnidae analyses. Cnidae analyses were conducted using undischarged cnidocysts from tentacles, column, actinopharynx, and mesenteries filaments of holotype polyps (n = 6) for all new species under a Nikon Eclipse80i stereomicroscope (Nikon, Tokyo). Cnidae sizes were measured using ImageJ v1.45s (Rasband 2012). Although cnidae classification basically followed England (1991) and Ryland and Lancaster (2004), basitrichs and microbasic mastigophores were considered as the same type of nematocyst based on studies by Schmidt (1974), Hidaka et al. (1987), and Hidaka (1992), and therefore these two types were pooled together in this study.

Abbreviations used

NSMT National Science Museum, Tsukuba, Ibaraki, Japan
RMNH Naturalis Biodiversity Center, Leiden, Netherlands

RUMF Ryukyu University Museum, Fujukan, University of the Ryukyus, Nishihara, Okinawa, Japan

MISE Molecular Invertebrate Systematics and Ecology Laboratory, University of the Ryukyus, Nishihara, Okinawa, Japan

Results

Systematics

Phylum Cnidaria Hatschek, 1888
Class Anthozoa Ehrenberg, 1831
Subclass Hexacorallia Haeckel, 1896
Order Zoantharia Rafinesque, 1815
Suborder Macrocnemina Haddon & Shackleton, 1891
Family Parazoanthidae Delage & Hérouard, 1901

Antipathozoanthus Sinniger, Reimer & Pawlowski, 2010

Type species. *Antipathozoanthus macaronesicus* (Ocaña & Brito, 2003)

Diagnosis. Macrocinemic zoantharians with cteniform endodermal muscle or endo-meso transitional sphincter muscle (Swain et al. 2015). Substrate consists of either antipatharians or coral carbonate (reef). Genetic distance of mitochondrial COI sequences and insertion/deletion patterns in 16S-rDNA sequences are significantly different from those in other parazoanthid genera (Sinniger et al. 2005, 2010).

Remarks. Four of five formally described species grow mainly on antipatharians, but this character is not exclusive to all species in the genus as *A. obscurus* sp. n. is not associated with any host organism. Results of the current study showed that *A. obscurus* sp. n. is clearly placed within this genus according to COI and 16S-rDNA sequence analyses. Thus, these non-associated species/specimens are within the genus based on their phylogenetic position but do not fit the original definition of the genus by Sinniger et al. (2010).

Antipathozoanthus obscurus sp. n.

http://zoobank.org/2CE5BEAD-1772-4CB6-A7DA-EEA2FB480F87
Fig. 2a, b

Antipathozoanthus sp. 3 *sensu* Reimer and Fujii 2017, 394, fig. 14.4e.

Material examined. *Holotype*: NSMT-Co1602 (MISE-BISE1), collected from the wall of a shallow cave in a coral reef. Preserved polyps are approximately 3.0–4.5 mm in diameter, and approximately 3.0–8.0 mm in height from the coenenchyme.

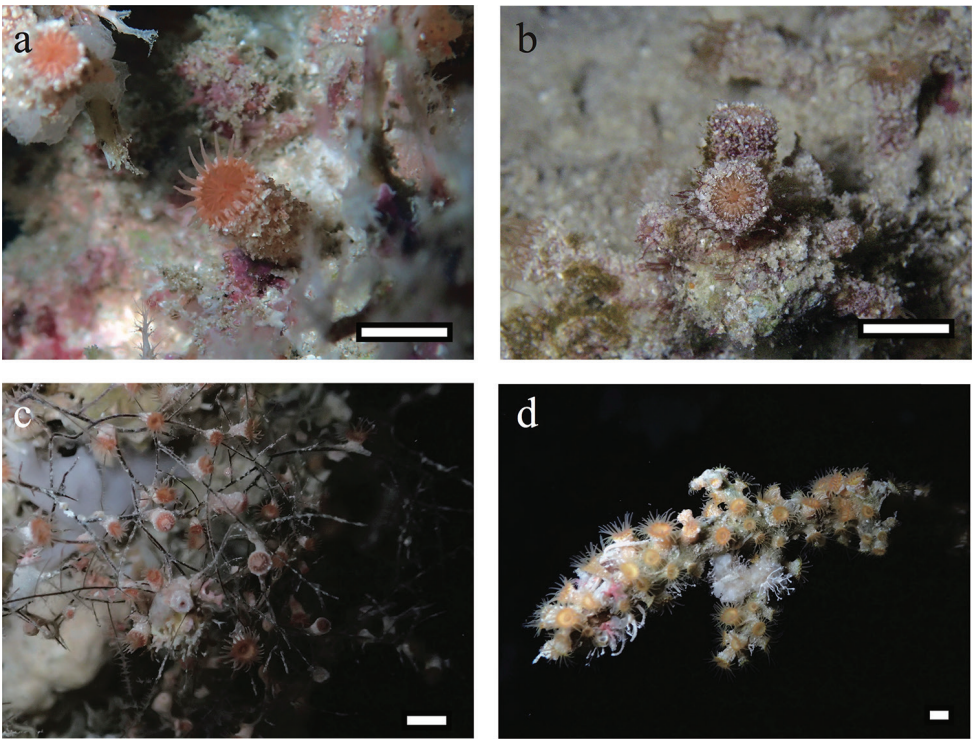

Figure 2. Polyp images of *Antipathozoanthus obscurus* sp. n., *A. remengesaui* sp. n. and *A. cavernus* sp. n. *in situ*. **a** *A. obscurus* sp. n. . NSMT-Co1602 (MISE-BISE1), Collected from Cape Bise, Motobu, Okinawa-jima Island, Japan (26°42'34.4"N, 127°52'49.2"E) at a depth of 5 m by JDR, 14 August 2014. **b** *A. obscurus* sp. n., closed polyp with heavy encrustion by various fine sand particles. MISE-TF54, collected from Cape Zanpa, Yomitan, Okinawa-jima Island, Japan (26°26'26.5"N, 127°42'43.7"E) at a depth of 3 m by TF, 6 April 2009. **c** *A. remengesaui* sp. n., colony connected by poorly developed coenenchyme with white polyps on *Antipathes* sp. NSMT-Co1603 (MISE-PALAU2) collected from Blue Hole, Palau (7°8'29.4"N, 134°13'23.3"E) at a depth of 23 m by JDR, 15 September 2014 **d** *A. cavernus* sp. n., polyp connected by highly developed coenenchyme with orange ring around oral disk. RMNH.Coel.42322 (MISE-PALAU5) collected from Siaes Tunnel, Palau (7°18'54.8"N, 134°13'13.3"E) at a depth of 39 m by JDR, 1 September 2014.

Approximately 15–20 polyps connected by a stolon form a mesh network, with additional solitary polyps close by (n = 6). Polyps and coenenchyme are heavily encrusted by various fine sand particles. External color light orange when alive, light beige when fixed. Collected from Cape Bise, Motobu, Okinawa-jima Island, Japan (26°42'34.4"N, 127°52'49.2"E) at a depth of 5 m by James Davis Reimer (JDR), 14 August 2014.

Paratypes: RUMF-ZG-4390 (MISE-JDR190), collected from Al Wajh Shaybarah, Saudi Arabia, (25°21'N, 36°54'E) at a depth of 3 m by JDR, 3 October 2013; RUMF-ZG-4391 (MISE-JDR191), collected from Al Wajh Shaybarah, Saudi Arabia, (25°21'N, 36°54'E) at a depth of 3 m by JDR, 3 October 2013; RUMF-ZG-4392

(MISE-JDR192), collected from Al Wajh Shaybarah, Saudi Arabia, (25°21'N, 36°54'E) at a depth of 3 m by JDR, 3 October 2013; RUMF-ZG-4393 (MISE-JDR279), collected from Shib Nazar, Saudi Arabia, (22°19'N, 38°51'E) at a depth of 3 m by JDR, 3 October 2013; RUMF-ZG-4394 (MISE-KU1), collected from Kume-jima Island, Okinawa, Japan (26°19'15.0"N, 126°45'21.3"E) at a depth of 15 m by Takuma Fujii (TF), 20 November 2009; RUMF-ZG-4395 (MISE-TF54), collected from Cape Zanpa, Yomitan, Okinawa-jima Island, Japan (26°26'26.5"N, 127°42'43.7"E) at a depth of 3 m by TF, 6 April 2009, divided into two pieces, one portion fixed in 99.5% ethanol, and other in 5–10% saltwater formalin; RUMF-ZG-4396 (MISE-TF78), collected from Cape Manza, Onna, Okinawa-jima Island, Japan (26°30'18.3"N, 127°51'02.3"E) at a depth of 5 m by TF, 2 October 2009, divided into two pieces, one portion fixed in 99.5% ethanol, and other in 5–10% saltwater formalin; RMNH. Coel.42320 (MISE-TF148), collected from Cape Manza, Onna, Okinawa-jima Island, Japan (26°30'18.3"N, 127°51'02.3"E) at a depth of 10 m by TF, 22 October 2012.

Other materials examined: MISE-BISE3, collected from Cape Bise, Motobu, Okinawa-jima Island, Japan (26°42'34.4"N, 127°52'49.2"E) at a depth of 5 m by JDR, 14 August 2014.

Diagnosis. *External morphology*: Open oral disks are approximately 5–10 mm in diameter, and polyps approximately 5–10 mm in height when open (Fig. 2). Polyps of a single colony are usually connected by a stolon forming a mesh-like network. *Antipathozoanthus obscurus* sp. n. has approximately 26–32 bright brown and/or orange tentacles that are as long as or longer than oral disk diameter. Polyps and coenenchyme have a heavily encrusted ectoderm including numerous various sand particles (usually 1 to 8 mm in size). Capitular ridges (= number of complete mesenteries) are slightly visible on tops (= capitulum) of closed polyps.

Internal morphology: Azooxanthellate. Fine sand particles and silica heavily encrusted into ectoderm and mesoglea. We could not obtain cross-sections or images to observe internal morphology such as mesenterial arrangement, marginal muscle or siphonoglyph due to heavy sand and silica encrustation.

Cnidae: Holotrichs (large), basitrichs and microbasic p-mastigophores (usually difficult to distinguish), spirocysts (Fig. 3; Table 2).

Habitat and distribution. *Antipathozoanthus obscurus* sp. n. is found in low-light environments such as within crevasses of reef slopes and reef floors, and coral reef caves. Specimens were found from 3 to 15 m. This species has been found from the Red Sea and Okinawa.

Differential diagnosis. *Antipathozoanthus obscurus* sp. n. is easily distinguished from all other *Antipathozoanthus* species, including the two other new species in this study, which all have associations with antipatharians. *A. obscurus* sp. n. is not associated with antipatharians and instead is found on coral reef carbonate substrate within caves or cracks. Additionally, the cnidome of *A. obscurus* sp. n. is different from all other known *Antipathozoanthus* species, including the other new species in this study, as there are no medium holotrichs in any tissue of *A. obscurus* sp. n., and instead only large holotrichs are found in all tissues.

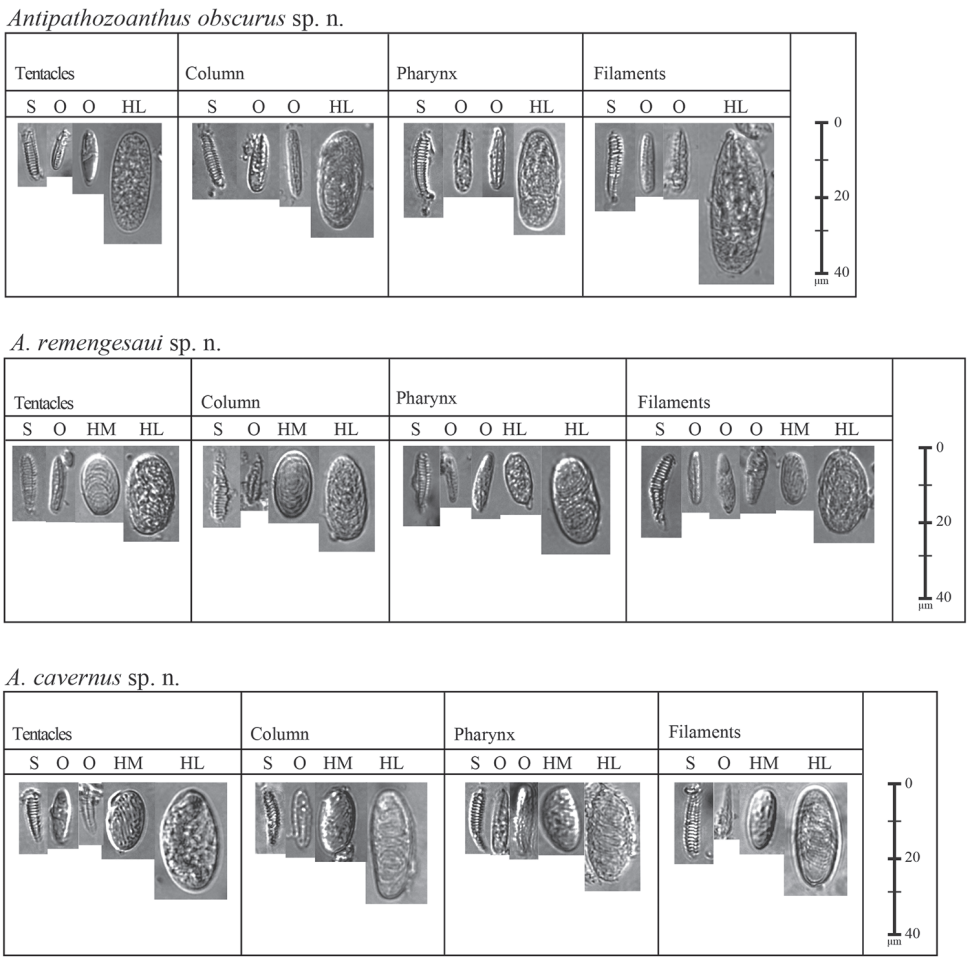

Figure 3. Cnidae in the tentacles, column, pharynx, and filament of *Antipathozoanthus obscurus* sp. n., *A. remengesaui* sp. n. and *A. cavernus* sp. n., respectively. Abbreviations: HL: holotrich large, HM: holotrich medium, O: bastrichs or mastigophores, S: spriocysts.

Although *A. obscurus* sp. n. is not associated with antipatharians, phylogenetic data indicate that *A. obscurus* sp. n. is very closely related to other *Antipathozoanthus* species associated with antipatharians, with identical COI and 16S-rDNA sequences to those of *A. macronesicus* (EU591618).

Remarks. The samples of *Antipathozoanthus obscurus* sp. n. in the present study contain two morphotypes; one with bright brown tentacles that are longer than the oral disk (MISE-TF54); and the other morphotype with orange tentacles that are only as long as the oral disk (MISE-BISE1, MISE-BISE3, MISE-JDR190, MISE-JDR191, MISE-JDR192, MISE-JDR279, MISE-KU1, MISE-TF78, MISE-TF148). However, the sequences of all specimens formed a monophyletic clade and therefore we have described *A. obscurus* sp. n. in this study as containing two morphotypes. Genetic vari-

Table 2. Cnidae types and sizes observed in three new Antipathozoanthus species. Frequency: relative abundance of cnidae type in decreasing order; numerous, common, occasional, rare (n = number of cnidae).

		Antipathozoanthus obscurus sp. n.				*A. remengesaui* sp. n.				*A. cavernus* sp. n.			
		Length (min-max, average)	**Width (min-max, average)**	**n**	**Frequency**	**Length (min-max, average)**	**Width (min-max, average)**	**n**	**Frequency**	**Length (min-max, average)**	**Width (min-max, average)**	**n**	**Frequency**
Tentacles	Spirocysts	11–20, 16.3	2–5, 3.1	48	Occasional	11–25, 18.0	2–7, 3.4	98	Numerous	14–25, 18.0	2–5, 2.9	137	Numerous
	Holotrichs (L)	21–33, 28.1	10–15, 11.9	39	Occasional	20–29, 21.8	7–14, 10.1	27	Occasional	20–31, 22.7	9–17, 11.4	28	Occasional
	Holotrichs (M)	–	–	–	–	10–19, 17.0	5–17, 9.9	105	Numerous	14–19, 17.9	7–14, 10.0	95	Numerous
	Bastrichs and Mastigophores	–	–	–	–	10–23, 16.3	2–6, 4.2	31	Occasional	15–19, 16.7	4–6, 4.7	7	Rare
Column	Spirocysts	12–22, 18.2	2–5, 3.1	57	Numerous	17–25, 19.7	2–4, 3.1	20	Occasional	11–28, 17.5	2–16, 5.6	44	Numerous
	Holotrichs (L)	22–34, 28.2	9–15, 11.8	78	Numerous	20–29, 25.1	9–17, 12.5	40	Occasional	20–32, 25.6	9–16, 11.2	24	Occasional
	Holotrichs (M)	–	–	–		11–19, 17.0	8–12, 9.9	21	Occasional	12–19, 16.5	5–13, 8.8	40	Occasional
	Bastrichs and Mastigophores	12–25, 18.2	2–5, 3.6	29	Occasional	14–18, 15.9	4–8, 5.9	16	Common	2	5	1	Rare
Pharynx	Spirocysts	13–25. 16.5	2–5, 3.0	69	Numerous	11–24, 17.7	2–6, 3.4	65	Numerous	13–23, 18.2	2–5, 3.2	101	Numerous
	Holotrichs (L)	20–34, 28.5	8–15, 11.5	76	Numerous	20–31, 23.4	7–18, 11.7	35	Occasional	20–31, 22.7	9–15, 12.0	33	Occasional
	Holotrichs (M)	–	–	–		10–19, 16.8	6–13, 9.5	76	Numerous	13–19, 17.6	6–13, 10.0	85	Numerous
	Bastrichs and Mastigophores	13–18, 16.1	3–6, 3.4	18	Common	13–21, 16.5	2–8, 4.5	52	Numerous	12–21, 16.9	2–5, 3.4	37	Occasional
Mesenteries	Spirocysts	13–21, 17.4	2–6, 3.4	64	Numerous	13–25, 17.9	2–6, 3.3	60	Numerous	3–26, 18.0	2–5, 3.1	61	Numerous
	Holotrichs (L)	23–38, 28.2	7–14, 11.5	27	Occasional	20–34, 24.3	8–15, 10.8	31	Occasional	20–36, 27.6	10–15, 11.8	52	Numerous
	Holotrichs (M)	–	–	–		10–19, 16.5	4–15, 9.4	86	Numerous	12–19, 16.2	6–13, 8.3	61	Numerous
	Bastrichs and Mastigophores	13–18, 16.0	3–5, 3.8	16	Common	13–22, 16.9	3–9, 4.6	71	Numerous	10–18, 14.6	2–5, 2.7	21	Occasional

ation in all three genetic markers in the samples of *A. obscurus* sp. n. was observed, and the possibility remains that *A. obscurus* sp. n. may contain cryptic species. Thus, we have excluded specimen MISE-BISE3 from the type series, although it was tentatively identified as *A. obscurus* sp. n. Further specimens and fine-scale genetic analyses are required to better understand if there is any cryptic diversity within this species.

Etymology. *Antipathozoanthus obscurus* sp. n. is named from the Latin "obscura" meaning "dark", as this species can be found in dark environments.

Common name. Tsuno-nashi-sunaginchaku (new Japanese name).

***Antipathozoanthus remengesaui* sp. n.**

http://zoobank.org/758A60AA-6D66-441A-8D54-2181F5ACF48D
Fig. 2c

Antipathozoanthus sp. sensu Reimer et al. 2014a, 2, fig. 1d
Antipathozoanthus sp. 1 sensu Reimer and Fujii 2017, 304, fig. 14.4c.

Material examined. *Holotype*: NSMT-Co1603 (MISE-PALAU2), colony of approximately 70 polyps connected by poorly developed white coenenchyme on genus *Antipathes* antipatharian (Hexacorallia: Antipatharia: Antipathidae). Preserved polyps approximately 1.5–3.0 mm in diameter, and approximately 1.5–2.0 mm in height from coenenchyme. Collected from Blue Hole, Palau (7°8'29.4"N, 134°13'23.3"E) at a depth of 23 m by JDR, 15 September 2014.

Paratypes: RMNH.Coel.42321 (MISE-MAL84), collected from Wall Street, Maldives (3°07'14.2"N, 72°58'46.5"E) at a depth of 9 m by JDR, 7 May 2014; RUMF-ZG-4397 (MISE-MAL85), collected from Wall Street, Maldives (3°07'14.2"N, 72°58'46.5"E) at a depth of 9 m by JDR, 7 May 2014; RUMF-ZG-4398 (MISE-JDR209), collected from Yanbu, Saudi Arabia, (24°26'N, 37°14'E) at a depth of 11 m by JDR, 4 October 2013; RUMF-ZG-4399 (MISE-TF102), collected from Okogashima Island, Kagoshima, Japan (31°33'58.75"N, 130°35'32.01"E) at a depth of 20 m by TF, 26 July 2011; RUMF-ZG-4400 (MISE-TF103), collected from Okoga-shima Island, Kagoshima, Japan (31°33'58.75"N, 130°35'32.01"E) at a depth of 40 m by TF, 26 July 2011.

Other materials examined: MISE-PALAU3, collected from Siaes Tunnel, Palau (7°18'54.8"N, 134°13'13.3"E) at a depth of 37 m by JDR, 15 September 2014; MISE-PALAU4, collected from Blue Hole, Palau (7°8'29.4"N, 134°13'23.3"E) at a depth of 28 m by JDR, 12 September 2014; MISE-KINKO2, collected from Hakamagoshi, Sakurajima, Kagoshima, Japan (31°35'23.5"N, 130.35.27.8"E) at a depth of 21 m by JDR, 20 September 2015; MISE-TF173, collected from Onna, Okinawa, Japan (26°26'20.9"N, 127°47'7.22"N) at depth of 15 m by TF, 27 June 2014; MISE-MAL46, collected from Coral Garden, Maldives (3°05'24.3"N, 72°58'04.5"E) at a depth of 24 m by JDR, 6 May 2014; MISE-MAL82, collected from Wall Street, Maldives (3°07'14.2"N, 72°58'46.5"E) at a depth of 9 m by JDR, 7 May 2014; MISE-MAL83,

collected from Wall Street, Maldives (3°07'14.2"N, 72°58'46.5"E) at a depth of 9 m by JDR, 7 May 2014; MISE-MAL2502602, collected from Capital Reef, Maldives (3° 02'55.8"N, 72°53'21.2"E) at a depth of 19 m by Marco Oliverio, 16 May 2014; MISE-MAL145, collected from Wall Street, Maldives (3°07'14.2"N, 72°58'46.5"E) at a depth of 12 m by JDR, 10 May 2014; MISE-MAL147, collected from Wall Street, Maldives (3°07'14.2"N, 72°58'46.5"E) at a depth of 10 m by JDR, 10 May 2014; MISE-MAL261, collected from Wall Street, Maldives (3°07'14.2"N, 72°58'46.5"E) at a depth of 9 m by JDR, 17 May 2014; MISE-HK70, collected from Siaes Tunnel, Palau (7°18'54.8"N, 134°13'13.3"E) by Hiroki Kise (HK), 12 September 2014, depth not available; MISE-HK90, collected from Blue Hole, Palau (7°8'29.4"N, 134°13'23.3"E) at a depth of 22 m by HK, 15 September 2014; MISE-JDR211, collected from Yanbu, Saudi Arabia, (24°26'N, 37°14'E) at a depth of 12 m by JDR, 4 October 2013; MISE-JDR214, collected from Yanbu, Saudi Arabia, (24°26'N, 37°14'E) at a depth of 12 m by JDR, 4 October 2013.

Diagnosis. *External morphology*: Polyps *in situ* are approximately 4–8 mm in diameter, and approximately 3–8 mm in height *in situ* when oral disks expanded (Figure 2). Colonial zoantharian, white or off-white polyps that may be solitary or connected by a white and poorly developed coenenchyme on *Antipathes* substrate. *Antipathozoanthus remengesaui* sp. n. has approximately 40–42 tentacles that are pinkish or/and translucent. Tentacles are usually as long as open oral disk diameter. Oral disk is pink or bright brown in color, and the capitulum is also pinkish or bright brown in color when polyps are closed. Polyps encrusted with visible sand particles (1–3 mm) in their coenenchyme and ectodermal tissue. Colonies attached on axis from proximal extremity to base of *Antipathes*.

Internal morphology: Cteniform endodermal marginal muscle sensu Swain et al. 2015 (Fig. 4). Azooxanthellate. The large scattered lacunae in ectoderm and mesogleal are present due to their encrustations.

Cnidae: Holotrichs (large and medium), basitrichs and microbasic p-mastigophores (usually difficult to distinguish), spirocysts (Fig. 3; Table 2).

Habitat and distribution. *Antipathozoanthus remengesaui* sp. n. has been found on the sides and/or floors of cave entrance, and always on *Antipathes*. Specimens were collected from depths of 9 to 40 m. This species is known from Palau, Kagoshima in Japan, the Maldives, and the Red Sea.

Differential diagnosis. In the Pacific, *Antipathozoanthus remengesaui* sp. n. can be distinguished from *A. hickmani* by the development of the coenenchyme and in part by polyp size; the larger polyps (4–12 mm in diameter and 4–15 mm in height) of *A. hickmani* are connected by a well-developed coenenchyme on *Antipathes galapagensis*, while the slightly smaller polyps (4–8 mm in diameter and 3–8 mm in height *in situ*) of *A. remengesaui* sp. n. are either connected by a poorly developed coenenchyme or may even be solitary on *Antipathes*. Additionally, the cnidomes of these species are different; *A. hickmani* does not have spirocysts in the column, while *A. remengesaui* sp. n. has spirocysts in the column.

Remarks. The *Antipathozoanthus remengesaui* sp. n. specimens found in Kagoshima, Japan have different morphological features compared to the specimens found in all other regions. Specimens collected from Kagoshima have relatively large polyps (6–8 mm in diameter, and approximately 5–8 mm in height *in situ*) compared to specimens from other regions. The coloration of oral disks is also different between Kagoshima and other regions; *A. remengesaui* sp. n. from Kagoshima has a bright brown oral disk, while those from other regions have pink oral disks. However, sequences of these specimens collected from all regions formed a monophyletic clade for all genetic markers including ITS-rDNA. In terms of substrate organisms, *A. remengesaui* sp. n. collected from all regions in this study was associated with black corals of the genus *Antipathes*. Here, we have described this group as a single species, *A. remengesaui* sp. n., based on phylogeny and substrate specificity, although we have excluded some specimens for which we could not amplify ITS-rDNA successfully from the type series.

Etymology. *Antipathozoanthus remengesaui* sp. n. is named after Tommy Esang Remengesau, Jr., the current president of the Republic of Palau, who has greatly contributed to marine research and conservation in Palau.

Common name. Momoiro-mame-tsuno-sunaginchaku (new Japanese name).

***Antipathozoanthus cavernus* sp. n.**

http://zoobank.org/CC4A5D45-FC91-4E8F-B496-184DDA7C1AC1

Fig. 2d

Material examined. *Holotype*: NSMT-Co1604 (MISE-KINKO1), colony of approximately 125 polyps connected by a highly developed coenenchyme on genus *Myripathes* (Antipatharia: Myriopathidae). Preserved polyps approximately 2.0–5.0 mm in diameter, and approximately 2.0–5.0 mm in height from coenenchyme. Collected from Sakurajima, Kagoshima, Japan (31°35'23.5"N, 130.35.27.8"E) at a depth of 21 m by JDR, 20 September 2015.

Paratypes: RUMF-ZG-4401 (MISE-MAL2592601), collected from Capital Reef, Maldives (3° 02'55.8"N, 72°53'21.2"E) at a depth of 19 m by Marco Oliverio, 16 May 2014; RMNH.Coel.42322 (MISE-PALAU5), collected from Siaes Tunnel, Palau (7°18'54.8"N, 134°13'13.3"E) at a depth of 39 m by JDR, 15 September 2014.

Diagnosis. *External morphology*: Polyps *in situ* are approximately 4–15 mm in diameter when oral disk is expanded, and approximately 3–10 mm in height (Figure 2). Colonial zoantharian with polyps connected by highly developed coenenchyme on *Myripathes*. *Antipathozoanthus cavernus* sp. n. has approximately 32–40 translucent tentacles of approximately 1 to 5 mm in length. Tentacle lengths are either as long as or slightly shorter than expanded oral disk diameter. Polyps have orange oral disk with orange or light orange ring around oral disk. When polyps are closed, capitular ridges are present and observed clearly, numbering approximately 16–20. The capitulum is orange or light orange in color. Polyps encrusted with visible sand particles (1–8 mm)

in their coenenchyme and ectodermal tissue. Polyps usually much more encrusted than coenenchyme. Colonies attached on axis from proximal extremity to base of *Myripathes.*

Internal morphology: Cteniform endodermal arrangement marginal muscle sensu Swain et al. (2015) in longitudinal section (Fig. 4). Azooxanthellate. Large scattered lacunae in ectoderm and mesogleal are present due to their encrustations.

Cnidae: Holotrichs (large and medium), basitrichs and microbasic p-mastigophores (usually difficult to distinguish from each other), spirocysts (Fig. 3; Table 2).

Habitat and distribution. *Antipathozoanthus cavernus* sp. n. is found on the sides and/or floor of cave entrances, and on steep slopes, and always on *Myripathes*. Specimens were collected from depths of 19 to 39 m.

Differential diagnosis. *Antipathozoanthus cavernus* sp. n. occurs in similar environments as *A. remengesaui* sp. n., but these species can be distinguished by their coenenchyme development and by the generic identity of the antipatharian host. *A. remengesaui* sp. n. is associated with genus *Antipathes* (family Antipathidae) covered by a poorly developed coenenchyme, while *A. cavernus* sp. n. is associated with genus *Myripathes* (family Myripathidae) covered by a highly developed coenenchyme. *A. cavernus* sp. n. can be distinguished from *A. hickmani* by a different coloration and by its antipatharian association; *A. cavernus* sp. n. does not have red or cream colored polyps as seen in *A. hickmani*. Additionally, *A. hickmani* is associated with *Antipathes galapagensis*, while *A. cavernus* sp. n. is associated with genus *Myripathes*. *A. macaronesicus* is easily distinguishable from *A. cavernus* sp. n. by their polyp coloration (orange and light orange versus pinkish and yellowish, and their antipatharian host (genus *Antipathes* versus genus *Myripathes*). Finally, all species above have unique ITS-rDNA sequences.

Etymology. *Antipathozoanthus cavernus* sp. n. is named from the Latin “caverna" meaning “cave", as this species is found in caves.

Common name. Hana-tsuno-sunaginchaku (new Japanese name).

Phylogenetic analyses

Concatenated alignment. All *Antipathozoanthus* species together formed a large monophyletic clade within the Parazoanthidae with complete support (ML = 100%, BI = 1) in the concatenated (COI+16S-rDNA+ITS-rDNA) alignment phylogeny (Fig. 5). Within the *Antipathozoanthus* clade, the various *Antipathozoanthus* species were divided into two subclades, an ‘associated’ subclade consisting of species associated with antipatharians, and a ‘non-associated’ subclade consisting only of *A. obscurus* sp. n. found directly on non-biotic substrates. The associated subclade consisted of *A. macaronesicus*, *A. hickmani*, *A. remengesaui* sp. n. and *A. cavernus* sp. n. and had very strong support (ML = 95%, BI = 0.99), while the non-associated subclade of *A. obscurus* sp. n. had complete support (ML = 100%, BI = 1). Within the associated clade, *A. hickmani* and *A. cavernus* sp. n. were sister to each other (ML = 59%, BI = 0.96). *A. remengesaui* sp. n. was basal to a poorly nodal supported clade (ML ≤ 50%, BI ≤0.95) containing other associated *Antipathozoanthus* spp. (*A. macaronesicus*,

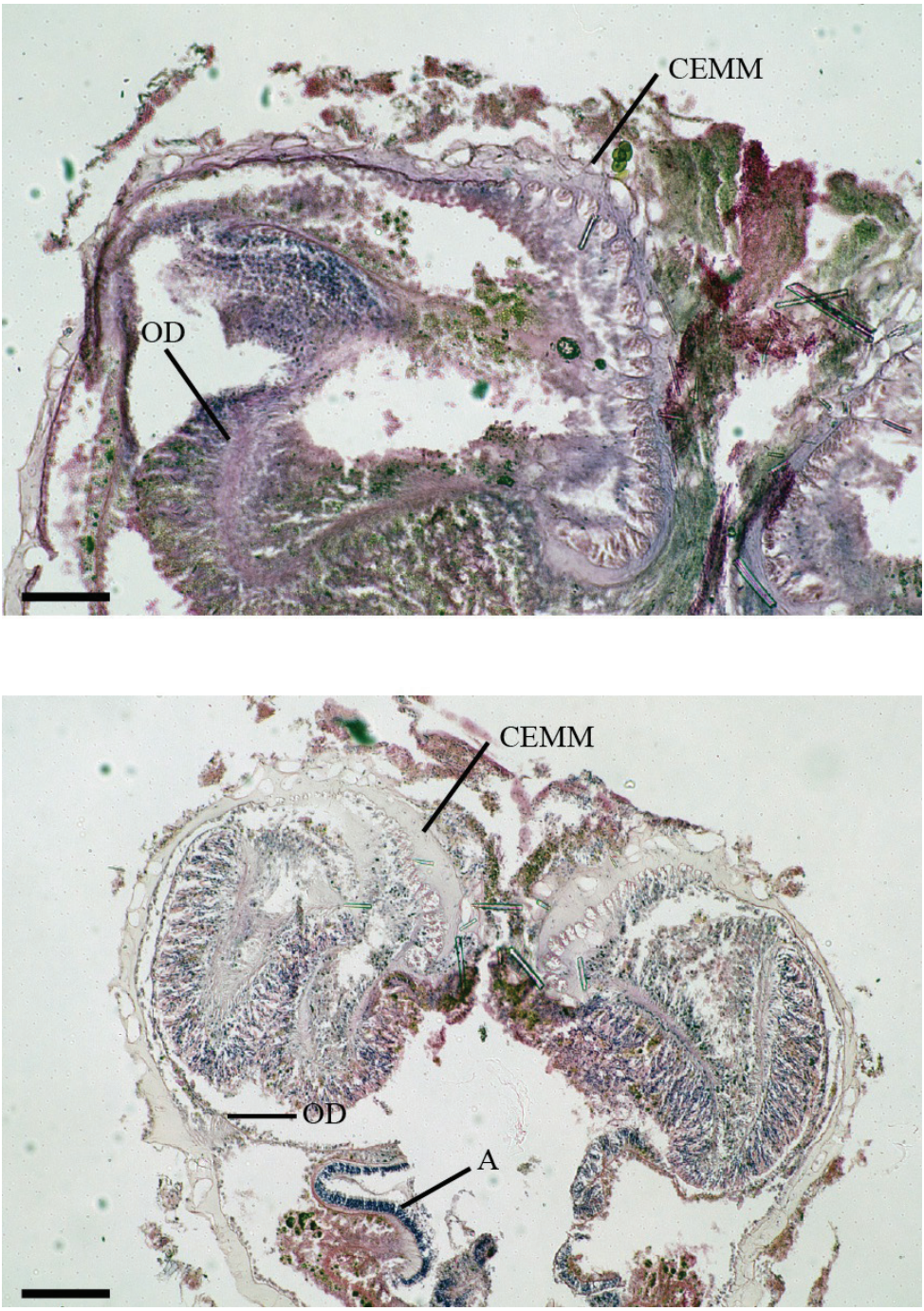

Figure 4. Images of histological section of *Antipathozoanthus* species. **a** longitudinal section of *A. remengesaui* sp. n. **b** longitudinal section of *A. cavernus* sp. n.. Abbreviations: (CEMM) cteniform endodermal marginal muscle, (OD) oral disk, (A) actinopharynx. Scale bars: **a** 200 μm, **b** 50 μm.

Figure 5. Maximum likelihood (ML) tree based on concatenated alignments of 16S-rDNA, COI and ITS-rDNA. Numbers on nodes represent ML bootstrap values (> 50% are shown). Bold branches indicate high supports of Bayesian posterior probabilities (> 0.95).

A. hickmani and *A. cavernus* sp. n.). *A. macaronesicus* formed a subclade with very strong support (ML = 97%, BI = 1).

COI. All *Antipathozoanthus* species formed a large monophyletic clade within the Paraozoanthidae with a very strong support (NJ = 99%, ML = 99%, BI = 1) in the COI phylogeny (Suppl. material 2). Within the clade, *Antipathozoanthus* species were divided into two subclades (associated subclade + non-associated subclade). The topology within the large monophyletic associated subclade was very similar to that as seen in the 16Sr-DNA phylogeny. Both the associated subclade (NJ =77%, ML = 66%) and the non-associated subclade had moderate support (NJ = 86%, ML = 85%, BI = 0.99). Sequences of *Antipathozoanthus* species within each of the subclades showed no differences in sequences. The difference in sequences between the associated subclade and the non-associated subclade was 3 bp (0.69%).

16S-rDNA. All *Antipathozoanthus* species formed a large monophyletic clade within the Parazoanthidae with generally high support (NJ = 99%; ML = 85%; BI = 1) in the

16Sr-DNA phylogeny (Suppl. material 3). Within this large clade, *Antipathozoanthus* species were divided into two subclades; an associated subclade (*A. macaronesicus*, *A. hickmani*, *A. remengesaui* sp. n., and *A. cavernus* sp. n.); and the other subclade not associated with antipatharians (*A. obscurus.* sp. n.; 'non-associated subclade'). The associated subclade formed only in NJ phylogenetic tree with moderate support in the 16S-rDNA tree (NJ = 78%), while the non-associated subclade had strong support in each phylogeny (NJ = 97%; ML = 95%; BI = 0.96). Sequences of *Antipathozoanthus* species within the associated subclade were identical with the exception of *A. hickmani* (EU333757), which differed by one base substitution, while within the non-associated subclade there were a few small sequence differences (maximum difference 3 bp). Differences of sequences between the associated and the non-associated subclades were 4–6 bp (0.67 to 1.01%).

ITS-rDNA. All *Antipathozoanthus* species formed a large monophyletic clade within the Parazoanthidae with complete support (NJ = 100%, ML = 100%, BI = 1) in the ITS-rDNA phylogeny (Suppl. material 4). Within the *Antipathozoanthus* clade there were again two subclades, corresponding to the associated subclade and the non-associated subclade, as seen in both the mitochondrial COI and 16S-rDNA phylogenies. The associated subclade had moderate support (NJ = 100%, ML = 69%, BI = 0.96), while the non-associated subclade had very strong support (NJ = 96%, ML = 100%, BI = 1). Within the associated subclade, all four species had different sequences; *A. macaronesicus* formed a monophyletic grouping with very strong support (NJ = 99%, ML = 90%, BI = 0.99), while *A. remengesaui* sp. n., *A. cavernus* sp. n., and *A. hickmani* each formed monophyletic groupings with moderate support (NJ = 95%, ML = 69%, BI = 0.62; NJ = 86%, ML = 62%, BI = 0.96; NJ = 79%; ML = 84%, BI = 0.96, respectively). *A. obscurus* sp. n. formed a monophyletic clade with very strong support (NJ = 96%; ML = 100%; BI = 1).

Discussion

Distribution of *Antipathozoanthus* species in the Indo-Pacific Ocean. *Antipathozoanthus hickmani* is found in only the Galapagos with *A.* cf. *hickmani* reported from the coast of Ecuador (Bo et al. 2012), suggesting an East Pacific distribution. On the other hand, *A. remengesaui* sp. n. was found in the Red Sea, the Maldives, Palau, and mainland Japan and Okinawa, Japan, while *A. cavernus* sp. n. was found in the Maldives, Palau, and mainland Japan, and *A. obscurus* sp. n. was found in the Red Sea and Okinawa, Japan. Additionally, unidentified *Antipathozoanthus* species have been previously reported from the central Indo-Pacific Ocean (Reimer et al. 2014a), the South China Sea (Reimer et al. 2017), and mainland Japan (Reimer et al. 2013). These results indicate that the three new *Antipathozoanthus* species described herein are likely widely distributed across the Indo-Pacific Ocean, and also that *Antipathozoanthus* species diversity is higher than has been previously known.

Evolution of macrocnemic zoantharians in caves. *Antipathozoanthus obscurus* sp. n. without host was found in similar environments as the 'associated' *Antipathozoanthus*

species, but this species does not associate with antipatharians and is instead directly attached to coral reef carbonate. Ocaña and Brito (2003) explained the relationship between *Antipathozoanthus* and antipatharians as a case of facultative parasitism, although this association still requires further research. It has been revealed that some macrocnemic species gain an advantage in plankton feeding by utilizing substrate organisms that filter feed in environments where plankton organisms are scarce (e.g., *Hydrozoanthus* species on oligotrophic coral reefs; Di Camillo et al. 2010), and this could be one reason that most *Antipathozoanthus* spp. utilize antipatharians as substrate. However, moderate currents conducive to plankton feeding may occur in coral reef caves by inflow of tidal currents or terrestrial runoff (Iliffe and Kornicker 2009), and it may be unnecessary to have an association with antipatharians for obtaining sufficient plankton in such environments. Additionally, in marine caves, there are fewer predators of zoantharians, such as fishes (e.g., Bussotti et al. 2002), and perhaps fewer competitors for substrate space. Such environments may promote the speciation of 'non-associated' zoantharian species as seen here with *A. obscurus* sp. n.

All new species in the present study are azooxanthellate, and this trait is common within macrocnemic zoantharians to the exception of some species such as *Bergia cutressi* (West, 1979) and *Nanozoanthus harenaceus* Fujii & Reimer, 2013. Irei et al. (2015) suggested that cave-dwelling *Palythoa* species within Brachycnemina lost their zooxanthellae to adapt to environments in caves and cracks. On the other hand, macrocnemic cave-dwelling species may originally have lacked zooxanthellae rather than undergone a loss of zooxanthellae. However, more investigations are needed to evaluate the species diversity of zoantharians in caves to more comprehensively understand the evolution of these zoantharian species.

Substrate specificity within *Antipathozoanthus*. Within the family Parazoanthidae, different generic lineages likely have long evolutionary histories associated with their substrate organisms, based on the fact that many parazoanthid genera form monophyletic clades in accord to their substrates (Sinniger et al. 2005, 2010, 2013; Montenegro et al. 2015). In this study, we found two different subclades within *Antipathozoanthus* (Fig. 5, Suppl. Materials 2–4) that corresponded to substrate differences. The genetic distances between the associated subclade (*A. hickmani*, *A. macaronesicus*, *A. remengesaui* sp. n., *A. cavernus* sp. n.) and the non-associated subclade of *A. obscurus* sp. n. were 0.60% (COI) to 1.01% (16S-rDNA). Additionally, we observed characteristic insertions and deletions in the 16S-rDNA between the associated and non-associated subclades. Although the two clades formed in accordance to their substrate (antipatharians, coral reef carbonate), we consider the genetic distances between the two clades as intra-generic based on previous comparisons of genetic distances (Sinniger et al. 2010). While many taxonomic and molecular studies focusing on the family Parazoanthidae have been conducted using various genetic markers (e.g., Sinniger et al. 2005, 2010; Reimer et al. 2008; Montenegro et al. 2015), little research has been conducted focusing on the phylogenetic relations within different parazoanthid genera, except for studies examining *Bergia, Parazoanthus*, and *Umimayanthus*, which are all associated with sponges (Sinniger et al. 2005; Montenegro et al. 2015, 2016;

Carreiro-Silva et al. 2017). There is a need for more phylogenetic studies focusing on increasing the numbers of species examined within each of the genera of Parazoanthidae in order to better understand the evolutionary history of substrate specificity and other traits within the family Parazoanthidae (Swain et al. 2015, 2016).

Acknowledgements

We thank the following people and institutions for supporting fieldwork and logistics; in Okinawa, all members of the Molecular Invertebrate Systematics and Ecology Laboratory (MISE) at the University of Ryukyus (UR), the KUMEJIMA 2009 expedition organized by the Transdisciplinary Research Organization for Subtropical and Island Studies of the University of the Ryukyus, the Center for Marine Bioscience & Biotechnology of the National Taiwan Ocean University, National University of Singapore, and the Biodiversity Research Center of the Academia Sinica; in Kagoshima, S. Dewa (Diving Service Umiannai), M. Matsuoka, R. Terada (both Kagoshima University) and D. Probizanski; in Palau, G. Mereb and A. Merep at the Palau International Coral Reef Center (PICRC) supported by the SATREPS P-CoRIE Project "Sustainable management of coral reef and island ecosystem: responding to the threat of climate change", funded by the Japan Science and Technology Agency (JST) and the Japan International Cooperation Agency (JICA) in cooperation with PICRC and Palau Community College. H. Takaoka (Okinawa Churaumi Aquarium, Okinawa) is acknowledged for identification of antipatharians. We also thank the University of Milano-Bicocca Marine Research and High Education Centre in Magoodhoo, the Ministry of Fisheries and Agriculture, Republic of Maldives and the community of Maghoodhoo, Faafu Atoll, for field work in the Maldives, and M.L. Berumen at the King Abdullah University of Science and Technology (KAUST), Saudi Arabia for Red Sea field work. The second author was partially supported by the "Establishment of Research and Education Network on Biodiversity and Its Conservation in the Satsunan Islands" project of Kagoshima University adopted by the Ministry of Education, Culture, Sports, Science and Technology, Japan and JSPS KAKENHI Grant numbers 17K15198 and 17H01913. Comments by Dr. S. Stampar and the editor improved the manuscript.

References

Bo M, Lavorato A, Di Camillo CG, Poliseno A, Baquero A, Bavestrello G, Irei Y, Reimer JD (2012) Black coral assemblages from Machalilla National Park (Ecuador). Pacific Science 66(1): 63–81. https://doi.org/10.2984/66.1.4

Bussotti S, Denitto F, Guindetti P, Belmonte G (2002) Fish assemblages in shallow marine caves in the Salento Peninsula (southern Apulia, SE Italy). PSZN: Marine Ecology 23: 11–20. https://doi.org/10.1111/j.1439-0485.2002.tb00004.x

Carreiro-Silva M, Ocaña O, Stanković D, Sampaio Í, Porteiro FM, Fabri M-C, Stefanni S (2017) Zoantharians (Hexacorallia: Zoantharia) associated with cold-water corals in the Azores Region: new species and associations in the deep sea. Frontiers in Marine Science 4: 88. https://doi.org/10.3389/fmars.2017.00088

Di Camillo CG, Bo M, Puce S, Bavestrello G (2010) Association between *Dentitheca habereri* (Cnidaria: Hydrozoa) and two zoanthids. Italian Journal of Zoology 77(1): 81–91. https://doi.org/10.1080/11250000902740962

Edgar RC (2004) MUSCLE: multiple sequence alignment with high accuracy and high throughput. Nucleic Acids Research 32(5): 1792–1797. https://doi.org/10.1093/nar/gkh340

England KW (1991) Nematocysts of sea anemones (Actiniaria, Ceriantharia and Corallimorpharia: Cnidaria): nomenclature. Hydrobiologia 216/217: 691–697. https://doi.org/10.1007/BF00026532

Fujii T, Reimer JD (2011) Phylogeny of the highly divergent zoanthid family Microzoanthidae (Anthozoa, Hexacorallia) from the Pacific. Zoologica Scripta 40: 418–431. https://doi.org/10.1111/j.1463-6409.2011.00479.x

Guindon S, Gascuel O (2003) A simple, fast, and accurate algorithm to estimate large phylogenies by maximum likelihood. Systematic Biology 52(5): 696–704. https://doi.org/10.1080/10635150390235520

Haddon AC, Shackleton AM (1891) Actiniae: I. Zoantheae. In Reports on the Zoological collections made in the Torres Straits by Professor A.C. Haddon, 1888–1889. Scientific Transactions of the Royal Dublin Society (2) 4(13): 673–658.

Hasegawa M, Kishino H, Yano T (1985) Dating of the human-ape splitting by a molecular clock of mitochondrial DNA. Journal of Molecular Evolution 22(2): 160–174. https://doi.org/10.1007/BF02101694

Hidaka M (1992) Use of nematocyst morphology for taxonomy of some related species of scleractinian corals. Galaxea 11: 21–28.

Hidaka M, Miyazaki I, Yamazato K (1987) Nematocysts characteristic of the sweeper tentacles of the coral *Galaxea fascicularis* (Linnaeus). Galaxea 6: 195–207.

Huelsenbeck JP, Ronquist F (2001) MRBAYES: Bayesian inference of phylogenetic trees. Bioinformatics 17(8): 754–755. https://doi.org/10.1093/bioinformatics/17.8.754

Irei Y, Sinniger F, Reimer JD (2015) Description of two azooxanthellate *Palythoa* species (Subclass Hexacorallia, Order Zoantharia) from the Ryukyu Archipelago, southern Japan. ZooKeys 478: 1–26. https://doi.org/10.3897/zookeys.478.8512

Iliffe TM, Kornicker LS (2009) Worldwide diving discoveries of living fossil animals from the depths of anchialine and marine caves. Smithsonian Contributions to the Marine Science 38: 269–280.

Kearse M, Moir R, Wilson A, Stones-Havas S, Cheung M, Sturrock S, Buxton S, Cooper A, Markowitz S, Duran C, Thierer T, Ashton B, Meintjes P, Drummond A (2012) Geneious Basic: an integrated and extendable desktop software platform for the organization and analysis of sequence data. Bioinformatics 28(12): 1647–1649. https://doi.org/10.1093/bioinformatics/bts199

Low MEY, Sinniger F, Reimer JD (2016) The order Zoantharia Rafinesque, 1815 (Cnidaria, Anthozoa, Hexacorallia): supraspecific classification and nomenclature. ZooKeys 641: 1–80. https://doi.org/10.3897/zookeys.641.10346

Montenegro J, Sinniger F, Reimer JD (2015) Unexpected diversity and new species in the sponge-Parazoanthidae association in southern Japan. Molecular Phylogenetics and Evolution 89: 73–90. https://doi.org/10.1016/j.ympev.2015.04.002

Montenegro J, Low ME, Reimer JD (2016) The resurrection of the genus *Bergia* (Anthozoa, Zoantharia, Parazoanthidae). Systematics and Biodiversity 14(1): 63–73. https://doi.org/10.1080/14772000.2015.1101028

Ocaña O, Brito A (2003) A review of Gerardiidae (Anthozoa: Zoantharia) from the Macaronesian islands and the Mediterranean Sea with the description of a new species. Revista de La Academia Canaria de Ciencias 15: 159–189.

Posada D (2008) jModelTest: phylogenetic model averaging. Molecular Biology and Evolution 25(7): 1253–1256. https://doi.org/10.1093/molbev/msn083

Rasband WS (2012) ImageJ: Image processing and analysis in Java. Astrophysics Source Code Library 1: 6013.

Reimer JD, Fujii T (2010) Four new species and one new genus of zoanthids (Cnidaria, Hexacorallia) from the Galápagos Islands. ZooKeys 42: 1–36. https://doi.org/10.3897/zookeys.42.378

Reimer J D, Fujii T (2017) Zoantharia (Cnidaria: Anthozoa: Hexacorallia) Diversity Research in Japan: Current State and Future Trends. In: Motokawa M, Kajihara H (Eds) Species Diversity of Animals in Japan. Springer Japan, Tokyo, 383–399. https://doi.org/10.1007/978-4-431-56432-4_14

Reimer JD, Takishita K, Ono S, Tsukahara J, Maruyama T (2007a) Molecular evidence suggesting interspecific hybridization in *Zoanthus* spp. (Anthozoa: Hexacorallia). Zoological Science 24(4): 346–359. https://doi.org/10.2108/zsj.24.346

Reimer JD, Sinniger F, Fujiwara Y, Hirano S, Maruyama T (2007b) Morphological and molecular characterisation of *Abyssoanthus nankaiensis*, a new family, new genus and new species of deep-sea zoanthid (Anthozoa: Hexacorallia: Zoantharia) from a north-west Pacific methane cold seep. Invertebrate Systematics 21(3): 255–262. https://doi.org/10.1071/IS06008

Reimer JD, Nonaka M, Sinniger F, Iwase F (2008) Morphological and molecular characterization of a new genus and new species of parazoanthid (Anthozoa: Hexacorallia: Zoantharia) associated with Japanese Red Coral. Coral Reefs 27(4): 935–949. https://doi.org/10.1007/s00338-008-0389-0

Reimer JD, Sinniger F, Irei Y (2013) Preliminary list of macrocnemic zoanthids diversity (Anthozoa: Hexacorallia: Zoantharia) from southern Shikoku, Japan. Kuroshio Biosphere 9: 1–12.

Reimer JD, Poliseno A, Hoeksema BW (2014a) Shallow-water zoantharians (Cnidaria, Hexacorallia) from the Central Indo-Pacific. ZooKeys 444: 1–57. https://doi.org/10.3897/zookeys.444.7537

Reimer JD, Uyeno D, Berumen ML (2014b) First records of Parazoanthidae and Microzoanthidae (Anthozoa: Hexacorallia: Zoantharia) from the Red Sea. Marine Biodiversity Records 7: 1–3. https://doi.org/10.1017/S175526721400002

Reimer JD, Santos MEA, Kise H, Neo ML, Chen CA, Soong K (2017) Diversity of Zoantharia (Anthozoa: Hexacorallia) at Dongsha Atoll in the South China Sea. Regional Studies in Marine Science 12: 49–57. https://doi.org/10.1016/j.rsma.2017.02.006

Ryland JS, Lancaster JE (2004) A review of zoanthid nematocyst types and their population structure. Hydrobiologia 530(1/3): 179–187. https://doi.org/10.1007/s10750-004-2685-1

Schmidt H (1974) On evolution in the Anthozoa. Proceedings of the 2nd International Coral Reef Symposium, Brisbane 1: 533–560.

Sinniger F, Häussermann V (2009) Zoanthids (Cnidaria: Hexacorallia: Zoantharia) from shallow waters of the southern Chilean fjord region, with descriptions of a new genus and two new species. Organisms Diversity & Evolution 9(1): 23–36. https://doi.org/10.1016/j.ode.2008.10.003

Sinniger F, Montoya-Burgos JI, Chevaldonné P, Pawlowski J (2005) Phylogeny of the order Zoantharia (Anthozoa, Hexacorallia) based on the mitochondrial ribosomal genes. Marine Biology 147(5): 1121–1128. https://doi.org/10.1007/s00227-005-0016-3

Sinniger F, Reimer JD, Pawlowski J (2010) The Parazoanthidae (Hexacorallia: Zoantharia) DNA taxonomy: description of two new genera. Marine Biodiversity 40(1): 57–70. https://doi.org/10.1007/s12526-009-0034-3

Sinniger F, Ocana OV, Baco AR (2013) Diversity of zoanthids (Anthozoa: Hexacorallia) on Hawaiian seamounts: description of the Hawaiian gold coral and additional zoanthids. PloS ONE 8(1): e52607. http://dx.doi.org/10.1371/journal.pone.0052607

Stamatakis A (2014) RAxML version 8: a tool for phylogenetic analysis and post-analysis of large phylogenies. Bioinformatics 30: 1312–1313. https://doi.org/10.1093/bioinformatics/ btu033

Swain TD (2009) Phylogeny-based species delimitations and the evolution of host associations in symbiotic zoanthids (Anthozoa, Zoanthidea) of the wider Caribbean region. Zoological Journal of the Linnean Society 156(2): 223–238. https://doi.org/10.1111/j.1096-3642.2008.00513.x

Swain TD (2010) Evolutionary transitions in symbioses: dramatic reductions in bathymetric and geographic ranges of Zoanthidea coincide with loss of symbioses with invertebrates. Molecular Ecology 19: 2587–2598. https://doi.org/10.1111/j.1365-294X.2010.04672.x

Swain TD, Wulff JL (2007) Diversity and specificity of Caribbean sponge–zoanthid symbioses: a foundation for understanding the adaptive significance of symbioses and generating hypotheses about higher-order systematics. Biological Journal of the Linnean Society 92: 695–711. https://doi.org/10.1111/j.1095-8312.2007.00861.x

Swain TD, Schellinger JL, Strimaitis AM, Reuter KE (2015) Evolution of anthozoan polyp retraction mechanisms: convergent functional morphology and evolutionary allometry of the marginal musculature in order Zoanthidea (Cnidaria: Anthozoa: Hexacorallia). BMC Evolutionary Biology 15: 123. https://doi.org/10.1186/s12862-015-0406-1

Swain TD, Strimaitis AM, Reuter KE, Boudreau W (2016) Towards integrative systematics of Anthozoa (Cnidaria): evolution of form in the order Zoanthidea. Zoologica Scripta 46: 227–244. https://doi.org/10.1111/zsc.12195

Supplementary material 1

List of GenBank accesion number

Authors: Hiroki Kise, Takuma Fujii, Giovanni Diego Masucci, Piera Biondi, James Davis Reimer

Data type: GenBank accession numbers

Explanation note: GenBank accession numbers, names and details of the sequences used in phylogenetic analyses of COI, 16S-rDNA and ITS-rDNA in this study. Sequences that were concatenated are indicated by bold text.

Link: https://doi.org/10.3897/zookeys.725.21006.suppl1

Supplementary material 2

Phylogenetic tree of COI

Authors: Hiroki Kise, Takuma Fujii, Giovanni Diego Masucci, Piera Biondi, James Davis Reimer

Data type: phylogenetic tree

Explanation note: Maximum likelihood (ML) tree based on cytochrome oxidase subunit I sequences. Numbers on nodes represent ML and neighbor-joining (NJ) bootstrap values (> 50% are shown). Bold branches indicate high supports of Bayesian posterior probabilities (> 0.95).

Link: https://doi.org/10.3897/zookeys.725.21006.suppl2

Supplementary material 3

Phylogenetic tree of 16S-rDNA

Authors: Hiroki Kise, Takuma Fujii, Giovanni Diego Masucci, Piera Biondi, James Davis Reimer

Data type: phylogenetic tree

Explanation note: Maximum likelihood (ML) tree based on mitochondrial 16S ribosomal DNA sequences. Numbers on nodes represent ML and neighbor-joining (NJ) bootstrap values (> 50% are shown). Bold branches indicate high supports of Bayesian posterior probabilities (> 0.95).

Link: https://doi.org/10.3897/zookeys.725.21006.suppl3

Supplementary material 4

Phylogenetic tree of ITS-rDNA

Authors: Hiroki Kise, Takuma Fujii, Giovanni Diego Masucci, Piera Biondi, James Davis Reimer

Data type: phylogenetic tree

Explanation note: Maximum likelihood (ML) tree based on internal transcribe spacer region of ribosomal DNA sequences. Numbers on nodes represent ML and neighbor-joining (NJ) bootstrap values (> 50% are shown). Bold branches indicate high supports of Bayesian posterior probabilities (> 0.95).

Link: https://doi.org/10.3897/zookeys.725.21006.suppl4

ZooKeys 725: 123–137 (2017)
doi: 10.3897/zookeys.725.22014
http://zookeys.pensoft.net

RESEARCH ARTICLE

A peer-reviewed open-access journal
ZooKeys
Launched to accelerate biodiversity research

A new species of *Trichopeltis* Pocock, 1894 from southern China, with a checklist and a distribution map of *Trichopeltis* species (Diplopoda, Polydesmida, Cryptodesmidae)

Natdanai Likhitrakarn[1], Sergei I. Golovatch[2], Ruttapon Srisonchai[3], Somsak Panha[3]

1 *Division of Plant Protection, Faculty of Agricultural Production, Maejo University, Chiang Mai, 50290, Thailand* **2** *Institute for Problems of Ecology and Evolution, Russian Academy of Sciences, Leninsky pr. 33, Moscow 119071, Russia* **3** *Animal Systematics Research Unit, Department of Biology, Faculty of Science, Chulalongkorn University, Bangkok, 10330, Thailand*

Corresponding author: *Somsak Panha* (somsak.pan@chula.ac.th)

Academic editor: *R. Mesibov* | Received 6 October 2017 | Accepted 24 November 2017 | Published 29 December 2017

http://zoobank.org/B8DFDD73-7C21-4735-B3AD-E31F5EFE79F6

Citation: Likhitrakarn N, Golovatch SI, Srisonchai R, Panha S (2017) A new species of *Trichopeltis* Pocock, 1894 from southern China, with a checklist and a distribution map of *Trichopeltis* species (Diplopoda, Polydesmida, Cryptodesmidae). ZooKeys 725: 123–137. https://doi.org/10.3897/zookeys.725.22014

Abstract

The millipede genus *Trichopeltis* Pocock, 1894 contains 12 described species including a new species from southern China described here. *Trichopeltis sutchariti* **sp. n.** can be distinguished from congeners by its gonopods that are strongly caudolaterally curved and have a prominent, high, curved, densely setose process on each coxa. An updated checklist and a distribution map are provided for all species of the genus.

Keywords

Millipede, *Trichopeltis*, new species, China, Cryptodesmidae

Introduction

Trichopeltis Pocock, 1894 is the largest genus within the mainly tropical family Cryptodesmidae which currently contains only 12 genera (mostly monotypic) and 39 species (Golovatch 2015, 2016; Golovatch and VandenSpiegel 2017; Liu et al. 2017).

Trichopeltis has recently been reviewed and a key provided (Liu et al. 2017). At present, this genus encompasses eleven species that range from the Himalayas of India (Assam and Darjeeling District) and Myanmar to southern China, Laos, Vietnam and Indonesia (Sumatra) (Fig. 5). Five of the species are presumed troglobites: one in Laos, the other four in southern China (Golovatch et al. 2010; Golovatch 2016; Golovatch and VandenSpiegel 2017; Liu et al. 2017). Below the description of one more new congener is presented, the first to be found epigeically in China. A catalogue to all presently known species is also provided, as well as a map showing their distributions.

Since a key to all hitherto known species of *Trichopeltis* is available (Liu et al. 2017), no update is needed.

Materials and methods

The material was collected from a limestone mountain area in Yunnan, southern China in October 2016. Photographs of live animals were taken in the laboratory using a Nikon 700D digital camera with a Nikon AF-S VR 105 mm macro lens. Specimens were preserved in 75% ethanol, and morphological investigations were carried out in the laboratory with the help of an Olympus SZX7 stereo microscope. Scanning electron micrographs (SEM) were taken with a JEOL, JSM–5410 LV microscope with no metallic coating, and the material returned from stubs to alcohol upon examination. Images of one holotype gonopod were taken in the laboratory and assembled using the "Cell^{D}" automontage software of the Olympus Soft Imaging Solution package. The holotype and most of the paratypes are housed in the Museum of Zoology, Chulalongkorn University (**CUMZ**), Bangkok, Thailand. A paratype has also been donated to the collection of the Zoological Museum, State University of Moscow, Russia (**ZMUM**), as indicated in the text.

The collecting site was located by GPS using the WGS84 datum.

In the catalogue sections, D stands for the original description and/or subsequent descriptive notes, K for the appearance in a key, L for the appearance in a species list, R for a new subsequent record, and M for a mere mention.

Results

Family Cryptodesmidae Karsch, 1880

Genus *Trichopeltis* Pocock, 1894

Trichopeltis Pocock, 1894: 374 (D).

Trichopeltis – Pocock 1895: 789 (K); Attems 1899: 301 (D, K); 1914: 167 (D); 1940: 218 (D, K); Hoffman 1961: 408 (M, K); Golovatch et al. 2010: 71 (D); Golovatch 2015:

156 (M); Golovatch and Akkari 2016: 1 (M); Golovatch and Wesener 2016: 35 (L), Golovatch and VandenSpiegel 2017: 762 (D, M); Liu et al. 2017: 2, 11 (M, D).

Otodesmus Cook 1896: 24 (D). Type species: *Trichopeltis watsoni* Pocock, 1895), synonymised by Golovatch et al. 2010: 71 (M).

Otodesmus – Attems 1899: 362 (D); Jeekel 1955: 415 (M); Hoffman 1961: 407 (M, K); 1973: 191 (M).

Description. Superficially, a typical genus of Cryptodesmidae, distinguished from other genera in the following combination of characters, the gonopodal ones being the most important.

Body small- to medium-sized (ca 8–21 mm long, ca. 1.7–5.5 mm wide), with 20 segments. Collum flabellate, much broader than head, fully covering it from above; eleven radii at collum's fore margin dividing it into 12 (sub)equal sectors; dorsal surface tuberculate to areate. Metaterga distinctly tuberculate to areate, usually setose, with at least two irregular transverse rows of tuberculations extending onto paraterga. The latter very short and very wide, subhorizontal, multilobulate at least at caudal and lateral margins. Ozopores highly variable, usually untraceable, when present then barely visible, located near base of paraterga either entirely dorsally or partly dorsally and mainly ventrally, or entirely ventrally. Only coxae 7 or both coxae 6 and 7 distinctly separated to accommodate tips of gonopods. Gonopod aperture usually subcordiform, edges with little or no elevation.

Gonopods ranging from rather simple to relatively complex (Fig. 4), small, usually foliate and held subparallel to each other; telopodites short to rather short, only slightly longer than coxae; the latter usually either bare or poorly setose, more rarely densely setose. Cannula usual, long, slender and falcate, normally not subtended by a median projection of coxa. Prefemoral (setose) part of telopodite making up 1/3–1/2 of the whole; acropodite either distinctly branched (usually with three branches, including an inconspicuous solenomere) or more or less deeply notched apically, seminal groove running entirely on mesal face to end on a more or less distinct caudo-apical solenomere.

Type species. *Cryptodesmus bicolor* Pocock, 1894, by original designation.

Other species included. *T. doriae* Pocock, 1895, *T. feae* Pocock, 1895, *T. watsoni* Pocock, 1895, *T. kometis* (Attems, 1938), *T. latellai* Golovatch, Geoffroy, Mauriès & VandenSpiegel, 2010, *T. cavernicola* Golovatch, 2016, *T. muratovi* Golovatch & VandenSpiegel, 2017, *T. bellus* Liu, Golovatch & Tian, 2017, *T. intricatus* Liu, Golovatch & Tian, 2017 and *T. reflexus* Liu, Golovatch & Tian, 2017.

Trichopeltis bicolor (Pocock, 1894)

Cryptodesmus bicolor Pocock, 1894: 373 (D).

Trichopeltis bicolor – Pocock 1895: 794 (M); Cook 1896: 25 (M); Attems 1899: 362 (L, K); 1914: 168 (L); 1940: 219 (D, K); Jeekel 1955: 414 (D, R); Hoffman 1961:

407 (M); 1973: 191 (M); Golovatch et al. 2010: 63 (M, K); Golovatch and VandenSpiegel 2017: 762 (L); Liu et al. 2017: 2, 12 (M, K).

Records from Indonesia. West Sumatra, Singkarah, 1,800 m a.s.l. (Pocock 1894; Jeekel 1955); Anai Cleft, 500 m a.s.l. (Jeekel 1955).

Trichopeltis doriae Pocock, 1895

Trichopeltis doriae Pocock, 1895: 792 (D).
Trichopeltis Doriae – Attems 1899: 362 (L, K); 1914: 168 (L).
Trichopeltis doriae – Attems 1936: 244 (R); 1940: 221 (D, K); Jeekel 1955: 415 (M); Hoffman 1973: 191 (M); Golovatch et al. 2010: 63 (M, K); Golovatch and VandenSpiegel 2017: 762 (L); Liu et al. 2017: 2, 12 (M, K).

Record from Myanmar. Yado, Carin Asciuii Cheba, 1,200–1,300 m a.s.l. (Pocock 1895; Attems 1936).

Trichopeltis feae Pocock, 1895

Trichopeltis feae Pocock, 1895: 793 (D).
Trichopeltis Feae – Attems 1899: 362 (L, K); 1914: 168 (L).
Trichopeltis feae – Attems 1936: 244 (R); 1940: 220 (D, K); Jeekel 1955: 415 (M); 1965; 124 (L); Hoffman 1973: 191 (M); Golovatch et al. 2010: 63 (M, K); Golovatch and VandenSpiegel 2017: 762 (L); Liu et al. 2017: 2, 12 (M, K).

Records from Myanmar. Village of Chiala, Carin Asciuii Ghecù, 1,200–1,600 m (Pocock 1895); Between Namkham and Kwangmu, 2,500 feet; Mule track between Hosi and Mio-Hsao, 3,700–4,400 feet; and North Shan States (Attems 1936).

Trichopeltis watsoni Pocock, 1895

Trichopeltis watsoni Pocock, 1895: 793 (D).
Trichopeltis watsoni – Cook 1896: 24 (M); Attems 1936: 244 (R); 1940: 219 (D, K); Jeekel 1955: 415 (M); Hoffman 1961: 408 (M); 1973: 191 (M); Golovatch et al. 2010: 63 (M, K); Shelley 2014: 5 (M); Golovatch and Wesener 2016: 35 (L); Golovatch and VandenSpiegel 2017: 762 (L); Liu et al. 2017: 2, 12 (M, K).
Otodesmus watsoni – Cook 1896: 25 (M); Attems 1899: 362 (L); Hoffman 1961: 408 (M).
Trichopeltis Watsoni – Attems 1899: 362 (L, K); 1914: 68 (L).
Trichodesmus (sic!) *watsoni* – Attems 1936: 244 (R); Rajulu 1970: 136 (L).

Records from Myanmar. Chin Hill (upper Burma) (Pocock 1895) and Waseru Choung River, south boundary of North Arakarn; India: Assam, Gauhati (Guwahati); Samagutung; Mangaldai district; Eastern Himalayas, Darjeeling district, Pashok; Bengal, Howrah opposite Calcutta (= Kolkata); Bangladesh: Chittagong Hills Tracts, Shishgk Valley (Attems 1936).

Trichopeltis kometis (Attems, 1938)

Niponielle (sic!) *kometis* Attems, 1938: 244 (D).
Onomatoplanus kometis – Attems 1940: 222 (D); 1953: 179 (R).
Pseudoniponiella kometis – Verhoeff 1942: 431 (D); Golovatch 2015: 156 (M).
Niponia kometis – Golovatch 1983: 180 (L); Enghoff et al. 2004: 41 (L); Likhitrakarn et al. 2014: 479 (L); 2015: 181 (L).
Trichopeltis deharvengi Golovatch et al., 2010: 64 (D); Golovatch 2015: 156 (M).
Trichopeltis kometis – Golovatch and Akkari 2016: 2 (D); Golovatch 2016: 33 (M), Golovatch and VandenSpiegel 2017: 757 (L); Liu et al. 2017: 2, 12 (M, K).

Records from Vietnam. Khanhhoa Province, Mt Hon Ba (Nhatrang); Lam Dong Province, Mt Diling, 1,000 m a.s.l. (S. Annam); Dalat (S. Annam), 1,500 m a.s.l.; Dalat, Camli, 1,500 m a.s.l.; Peak Langbian; Danang Province, Mt Bana, 1,400 m a.s.l. (Attems 1938); Lamdong Province, Peak Langbian; Dalat; Danang Province, Mt Bana, 1,500 m a.s.l.; Laocai Province, Mt. Fanxipan; Laichau Province, Laichau (Attems 1953); Lam Dong Province, Dalat, Peak Lang Bian, below summit (ca 2,030 m a.s.l.), (Golovatch et al. 2010); Laos: Xiang Khouang Province, Xieng Khouang; Luang Prabang Province, Luang Prabang; Sainyabuli Province, Paklay; Champasak Province, Bolaven Plateau; Cambodia: Kratie Province, Kratie (Mekong) (Attems 1953).

Trichopeltis latellai Golovatch, Geoffroy, Mauriès & VandenSpiegel, 2010

Trichopeltis latellai Golovatch et al., 2010: 66 (D).
Trichopeltis latellai – Golovatch and VandenSpiegel 2017: 762 (L); Liu et al. 2017: 2, 12 (M, K).

Records from China. Guizhou Province, Qianxi County, Hong Lin Town, Cave Chang Tu Dong; Cave Tiao Shuz Dong (Golovatch et al. 2010).

Trichopeltis cavernicola Golovatch, 2016

Trichopeltis cavernicola Golovatch, 2016: 34 (D).

Trichopeltis cavernicola – Golovatch and VandenSpiegel 2017: 765 (D, R); Liu et al. 2017: 2, 12 (M, K).

Records from Laos. Khammouane Province, Ban Naden, Cave Tham Namlat, 17.504969°N, 105.385598°E, ca. 180 m a.s.l. (Golovatch 2016) and ca. 65 km north of Thakaek, Cave Tham Nam Lod (Golovatch & VandenSpiegel, 2017).

Trichopeltis muratovi Golovatch & VandenSpiegel, 2017

Trichopeltis muratovi Golovatch & VandenSpiegel, 2017: 757 (D).
Trichopeltis muratovi – Liu et al. 2017: 2, 12 (M, K).

Record from Laos. Xieng Khoung Province, ca. 9 km northwest of Vieng Thong, secondary tropical forest, 20°08.466'N, 103°20.099'E, ca. 870–910 m a.s.l. (Golovatch and VandenSpiegel 2017).

Trichopeltis bellus Liu, Golovatch & Tian, 2017

Trichopeltis bellus Liu et al., 2017: 2, 12 (D).

Record from China. Yunnan Province, Qujing City, Luoping County, Machang village, Cave Shuiyuan Dong, 24°49'33"N, 104°21'48"E, 1,530 m a.s.l. (Liu et al. 2017).

Trichopeltis intricatus Liu, Golovatch & Tian, 2017

Trichopeltis intricatus Liu et al., 2017: 5, 12 (D).

Record from China. Yunnan Province, Kunming City, Shilin County, Guishan Town, Cave Haiyi I Dong, 24°38'50"N, 103°32'49"E, 1,890 m a.s.l. (Liu et al. 2017).

Trichopeltis reflexus Liu, Golovatch & Tian, 2017

Trichopeltis reflexus Liu et al., 2017: 8, 12 (D).

Record from China. Hunan Province, Chenzhou City, Linwu County, Xianghualing Town, Cave II Dong (Liu et al. 2017).

***Trichopeltis sutchariti* sp. n.**
http://zoobank.org/99801C98-30DD-4939-B346-4D279B80273F
Figs 1–5

Type material. Holotype ♂ (CUMZ), China, Yunnan Province, Xishuangbanna County, Mengla, 213 National Road, near Menglunzhen, Munlun village, 578 m a.s.l., 21°56'40"N, 101°13'45"E, 25.10.2016, leg. J. Sutcharit & S. Panha.

Paratypes. 2 ♂♂, 1 ♀ (CUMZ), 1 ♀ (ZMUM), same locality, together with holotype.

Name. Honours Jirasak Sutcharit (CUMZ), one of the collectors.

Differential dagnosis. This new species seems to be particularly similar to *T. bellus* Liu, Golovatch & Tian, 2017 and *T. intricatus* Liu, Golovatch & Tian, 2017, both from caves in southern China (Liu et al. 2017), since they all are distinguished by the presence of abundant long setae on the lateral face of the gonopodal coxae, and by highly complex gonopodal telopodites. However, *T. sutchariti* sp. n. differs from them,

Figure 1. Habitus, live colouration of *Trichopeltis sutchariti* sp. n., **A** ♀ paratype **B** ♂ holotype**.** Scale bar: 5 mm.

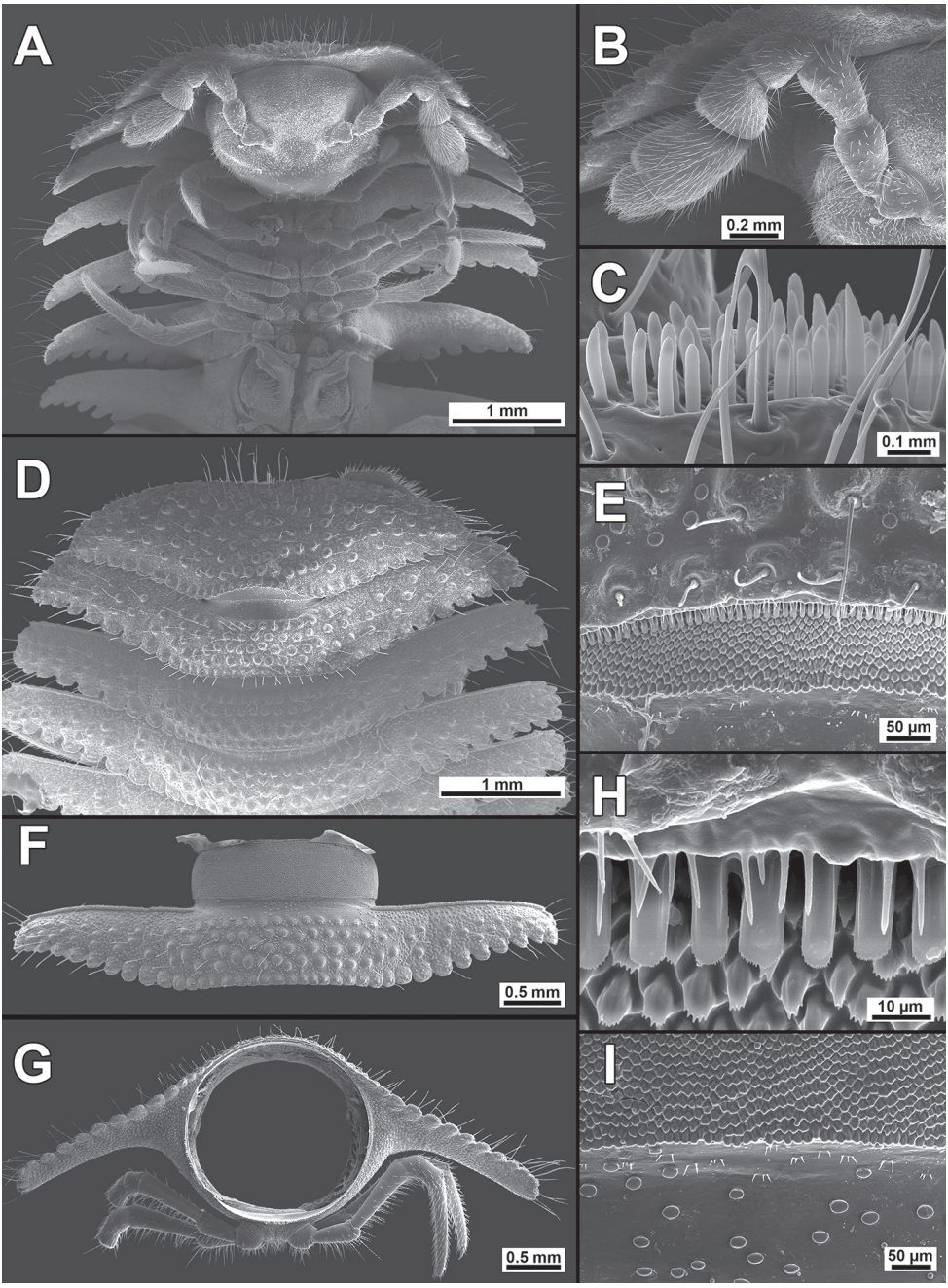

Figure 2. *Trichopeltis sutchariti* sp. n., ♂ paratype. **A, D** anterior part of body, ventral and dorsal views, respectively **B** antenna, ventral view **C** bacilliform sensilla on antennomere 5, lateral view **E** prozona of segment 2, dorsal view **H** limbus of collum, dorsal view **F** midbody segment, dorsal view **G** cross-section of a midbody segment, caudal view **I** enlarged prozona and stricture between pro- and metazona of a midbody segment, dorsal view.

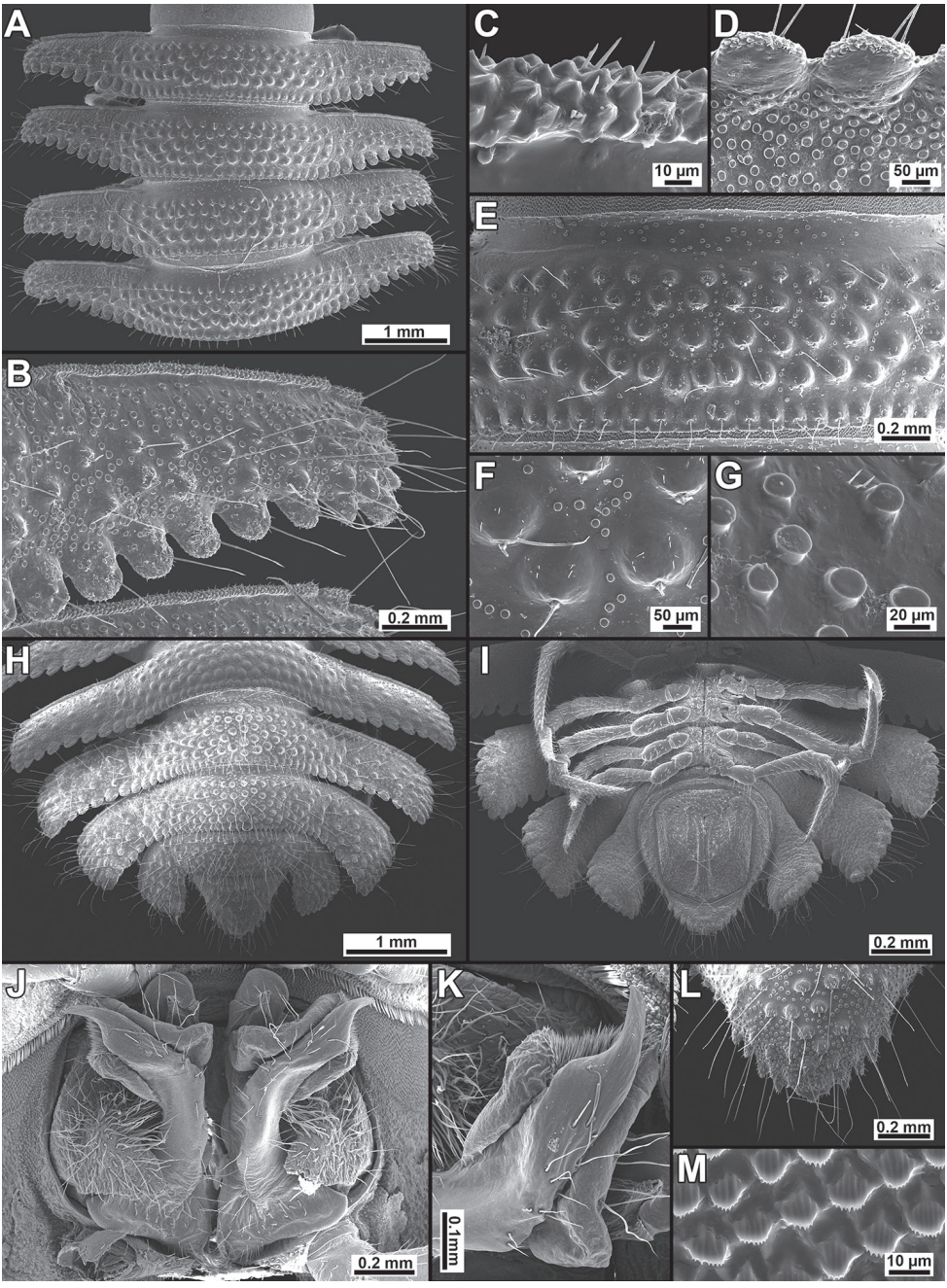

Figure 3. *Trichopeltis sutchariti* sp. n., ♂ paratype. **A** segments 9–12, dorsal view **B** paraterga of segment 10, dorsal view **C** anterior edge of paraterga, dorsal view **D** paraterga, lateral view **E** metaterga of segment 9, dorsal view **F** setigerous tuberculations on metaterga, dorsal view **G** spherical knobs on metaterga, dorsal view **H, I** posterior part of body, dorsal and ventral views, respectively **J, K** gonopod, ventral and sublateral views, respectively **L** enlarged epiproct, dorsal view **M** enlarged prozona, dorsal view. SEM without metallic coating.

as well from all other congeners in that its gonopodal telopodites are noticeably curved caudolaterad, and there is a strong, curved, laterally densely setose process (**cxp**) on each of the gonopodal coxae (Fig. 4).

Description. Length 13.9–15.2 (♂) or 14.2–14.5 mm (♀), width of midbody pro- and metazona 1.7–1.9 and 4.8–5.1 mm (♂) or 1.8–2.0 and 4.4–5.2 mm (♀), respectively.

Colouration of live animals uniformly whitish yellow (Fig. 1A), sometimes light red-brownish mid-dorsally (Fig. 1B); head, legs and venter whitish yellow to pallid, antennae light brown, increasingly infuscate distally; colouration in alcohol, after eight months of preservation, entirely pallid, only antennae still infuscate (brown) distally.

Clypeolabral region and vertex densely pilose, epicranial suture distinct. Antennae rather short and clavate (Figs 1B, 2A, B), reaching segment 3 (♂, ♀) when stretched laterally or ventrolaterally; in length, antennomere 6 > 3 > (4 = 2) > 5; antennomeres 5–7 each with a compact apicodorsal group of bacilliform sensilla (Fig. 2C). Body with 20 segments (Fig. 1A, B), composed of collum plus 17 podous and one apodous ring, plus telson. In width, head << collum < segment 2 <3 < 4 <5–17; thereafter body rapidly tapering towards telson (Fig. 3H).

Tegument dull, prozonae finely shagreened (Figs 2E, I, 3M); metaterga densely tuberculate and setose (Figs 2D, E, F, 3A, B, E, H). Fore and caudolateral margins of collum, as well as anterolateral, lateral and caudal margins of following paraterga evidently crenulate-lobulate, these lobulations being slightly larger at caudal margins of paraterga (Figs 2D, 3A, H).

Collum completely covering the head from above, regularly convex at fore margin, concave caudally, tuberculations arranged in 8–9 irregular transverse rows of evident setigerous knobs with abundant spherical granulations (Fig. 2D); caudal corner of paraterga narrowly rounded, declined ventrad, but not projecting beyond rear tergal margin (Fig. 2A).

Dorsum convex, postcollum paraterga flat, very broad and long, narrowly rounded laterally, evidently and regularly declivous and continuing the outline of dorsum; anterior edge straight, rib-shaped, forming a distinct shoulder, abundantly microgranulate and micropilose (Fig. 3C); tips of paraterga reaching level of venter, directed increasingly caudolaterad starting with segment 14, drawn behind rear tergal margin on segments 16–18 and strongly curved caudad on segment 19 (Fig. 3H); metatergal tuberculations arranged in 5–6 irregular transverse rows of small, round, setigerous knobs surrounded with abundant spherical granulations, these partly extending onto paraterga (Figs 2E, I, 3E, F, G); tergal setae rather short, slender and simple, mostly retained in caudal row on each metatergum (Fig. 2E), macrochaetae absent.

Limbus a row of simple, relatively short, tongue-shaped protuberances, abundantly microdenticulate apically (Fig. 2E, H). Ozopores invisible, pore formula untraceable. Pleurosternal carinae with complete crests only on segments 2 and 3 (♀) or with a sharp caudal tooth on segments 2 and 3, but segment 4 with a small rounded denticle (♂), thereafter absent.

Axial line absent. Stricture dividing pro- and metazonae broad, shallow and smooth, with abundant spherical granulations dorsally and microgranulate laterally (Fig. 3E).

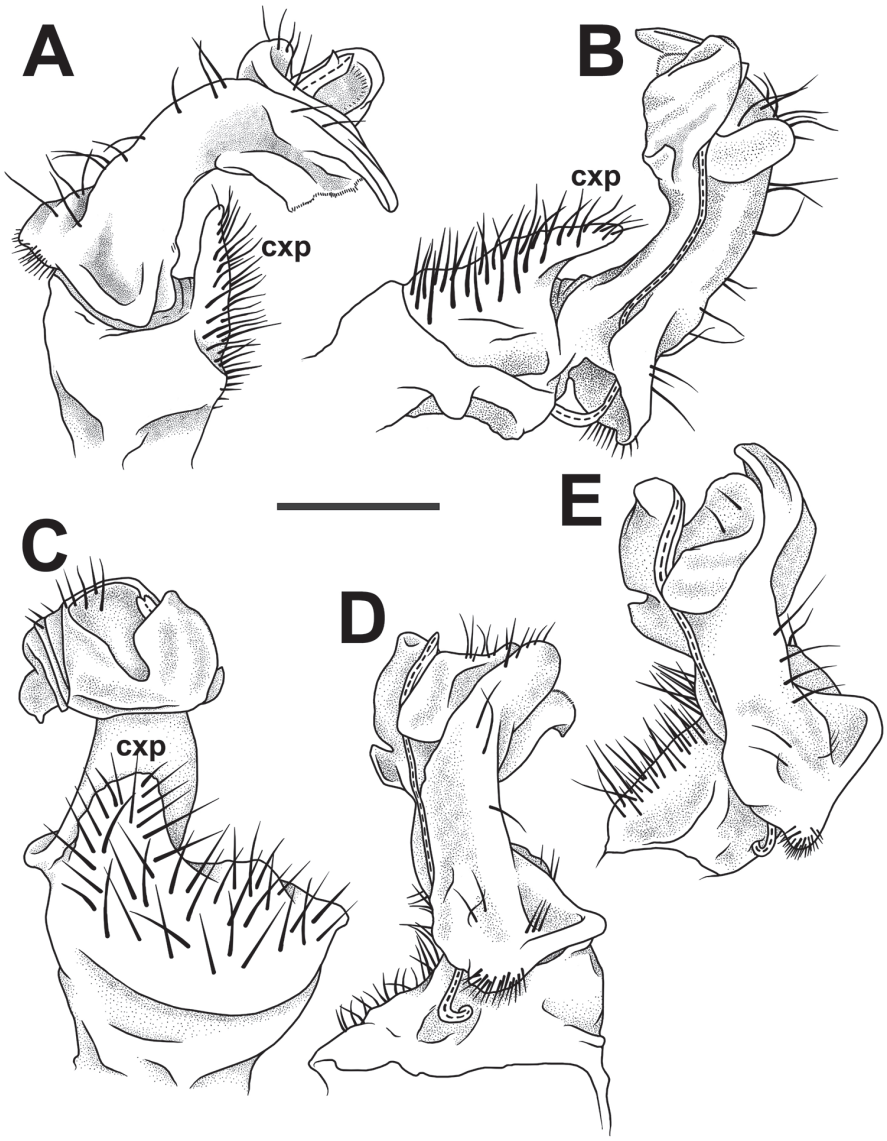

Figure 4. *Trichopeltis sutchariti* sp. n., ♂ holotype. **A–E** right gonopod, subfrontal, mesal (mirror image), sublateral, subcaudal and subfrontal views, respectively. Scale bar: 0.4 mm. Del. N. Likhitrakarn.

Epiproct (Fig. 3H, L) conical, flattened dorsoventrally, microtuberculate, with four strong apical papillae. Hypoproct roundly subtrapeziform (Fig. 3I), 1+1 caudal setae clearly separated, borne on small, but evident knobs.

Sterna usual, sparsely setose, without modifications, cross-impressions evident (Fig. 3I).

Legs very long and slender, without modifications (Figs 2G, 3I), ca. 1.3–1.4 times as long as paratergal width (♂, ♀) (Figs 1–3); in length, femora = tarsi >> prefemora

Figure 5. Distribution of 12 currently known species of *Trichopeltis*. Open diamonds: *T. watsoni* Pocock, 1895; crossed open square: *T. latellai* Golovatch, Geoffroy, Mauirès & VandenSpiegel, 2010; open triangle: *T. doriae* Pocock, 1895; filled circle: *T. feae* Pocock, 1895; inverted open triangle: *T. intricatus* Liu, Golovatch & Tian, 2017; filled diamond: *T. bellus* Liu, Golovatch & Tian, 2017; inverted filled triangle: *T. reflexus* Liu, Golovatch & Tian, 2017; filled triangle: *T. sutchariti* sp. n.; crossed open diamond: *T. muratovi* Golovatch & VandenSpiegel, 2017; filled squares: *T. cavernicola* Golovatch, 2016; open squares: *T. kometis* (Attems, 1938); asterisk: *T. bicolor* (Pocock, 1984).

> tibiae > coxae and postfemora (Fig. 2G); gonapophyses on ♂ coxae 2 small cones; neither adenostyles nor tarsal brushes present. Gonopod aperture transversely ovoid, caudal and lateral margins thin, only slightly elevated (Fig. 2A).

Gonopods (Figs 2A, 3J, K, 4) complex. Each coxa with a conspicuous, high, curved, laterally densely setose process (cxp). Telopodite stout, clearly curved caudolaterad (Fig. 3J), approximately twice as long as coxal process, divided by a notch, but compact apically (Fig. 4).

Remarks. All five specimens were taken from a rather large population found on limestone rocks, as well as on tree trunks during the rainy season. It seems noteworthy that the surface structures illustrated in the new species, such as the sculpture of the prozonae and the shape of the limbus (Fig. 2H, I), perfectly match the findings of Akkari and Enghoff (2011) in other genera/species of the same family.

Conclusions

At present, the genus *Trichopeltis* comprises 12 species ranging from the Himalayas of India (one species), through Bangladesh (one species), Myanmar (three species), to China (five species), Laos (three species), Vietnam, Cambodia and Indonesia (one species each) (Fig. 5).

Most of the species seem to be highly localised endemics, this being especially true of the five presumed troglobionts. There are only three congeners, all epigean, which are relatively widespread: *T. kometis*, found in Vietnam, Laos and Cambodia; *T. feae*, recorded from several localities in Myanmar; and *T. watsoni*, reported from Mynamar, Bangladesh and the Himalayas of India (Fig. 5).

Such a distribution pattern of *Trichopeltis* clearly suggests its Indo-Malayan (= Oriental) roots and there is little doubt that more new and interesting species will be discovered and additional localities recorded in future.

Acknowledgements

This project was partly funded through grants received from the Office of the Royal Development Projects Board (RDPB), while most of the financial support was obtained from The Thailand Research Fund, The TRF Senior Research Scholar RTA 5880002 (2015–2018) to SP. We thank the members of the Animal Systematics Research Unit for their invaluable assistance in the field. Last but not least, we extend our deep gratitude to Nathalie Yonow (U.K.) for polishing the English of the manuscript.

References

Akkari N, Enghoff H (2011) On some surface structures of potential taxonomic importance in families of the suborders Polydesmidea and Dalodesmidea (Polydesmida, Diplopoda). ZooKeys 156: 1–24. http://dx.doi.org/10.3897/zookeys.156.2134

Attems C (1899) System der Polydesmiden. II. Theil. Denkschriften der Akademie der Wissenschaften Wien, mathematisch-naturwissenschaftliche Classe 68: 251–436.

Attems C (1914) Die indo-australischen Myriopoden. Archiv für Naturgeschichte 80A: 1–398.

Attems C (1936) Diplopoda of India. Memoirs of the Indian Museum 11(4): 133–323.

Attems C (1938) Die von Dr. C. Dawydoff in Französisch Indochina gesammelten Myriopoden. Mémoires du Muséum national d'Histoire naturelle, NS 6(2): 187–353.

Attems C (1940) Myriapoda 3. Polydesmoidea III. Fam. Polydesmidae, Vanhoeffeniidae, Cryptodesmidae, Oniscodesmidae, Sphaerotrichopidae, Peridontodesmidae, Rhachidesmidae, Macellolophidae, Pandirodesmidae. Das Tierreich 70: 1–577.

Attems C (1953) Myriopoden von Indochina. Expedition von C. Dawydoff (1938–1939). Mémoires du Muséum national d'Histoire naturelle, Sér. A (Zoologie) 5(3): 133–230.

Cook OF (1896) *Cryptodesmus* and its allies. Brandtia 5: 19–28.

Enghoff H, Golovatch SI, Nguyen DA (2004) A review of the millipede fauna of Vietnam. Arthropoda Selecta 13(1/2): 29–43.

Golovatch SI (1983) [Millipedes (Diplopoda) in the fauna of Vietnam]. In: Sokolov VE (Ed.) Fauna i ekologiya zhivotnykh Vietnama [Fauna and animal ecology of Vietnam]. Nauka Publishers, Moscow, 178–186. [In Russian]

Golovatch SI (2015) Review of the millipede genus *Ophrydesmus* Cook, 1896, with the description of a new species from southern Vietnam (Diplopoda: Polydesmida: Cryptodesmidae). Tropical Natural History 15(2): 155–165.

Golovatch SI (2016) The millipede family Cryptodesmidae in Indochina (Diplopoda: Polydesmida). ZooKeys 578: 33–43. http://dx.doi.org/10.3897/zookeys.578.7994

Golovatch SI, Akkari N (2016) Identity of the millipede, *Pseudoniponiella kometis* (Attems, 1938) (Diplopoda: Polydesmida: Cryptodesmidae). Tropical Natural History 16(1): 1–6.

Golovatch SI, Geoffroy JJ, Mauriès JP, VandenSpiegel D (2010) Two new species of the millipede genus *Trichopeltis* Pocock, 1894 (Diplopoda: Polydesmida: Cryptodesmidae) from Vietnam and China. Arthropoda Selecta 19(2): 63–72.

Golovatch SI, VandenSpiegel D (2017) One new and two little-known species of the millipede family Cryptodesmidae from Indochina (Diplopoda, Polydesmida). Zoologicheskii zhurnal 96(7): 757–767.

Golovatch SI, Wesener T (2016) A species checklist of the millipedes (Myriapoda, Diplopoda) of India. Zootaxa 4129(1): 1–75. http://dx.doi.org/10.11646/zootaxa.4129.1.1

Hoffman RL (1961) An interesting new genus of cryptodesmoid Diplopoda from Borneo. Annals and Magazine of Natural History, Series 13(4): 401–409.

Hoffman RL (1973) A new milliped of the genus *Chonodesmus*, with a proposed reclassification of the family Cryptodesmidae (Diplopoda, Polydesmida). Studies on Neotropical Fauna and Environment 8: 179–193. https://doi.org/10.1080/01650527309360461

Jeekel CAW (1955) Milliped miscellany II. *Entomologische Berichten* 15: 412–417.

Jeekel CAW (1965) A revision of the South American Paradoxosomatidae in the Museo Civico di Storia Naturale di Genova (Diplopoda, Polydesmida). Annali del Museo Civico di Storia Naturale di Genova 75: 99–125.

Likhitrakarn N, Golovatch SI, Panha S (2014) A checklist of the millipedes (Diplopoda) of Laos. Zootaxa 3754(4): 473–482. http://dx.doi.org/10.11646/zootaxa.3754.4.8

Likhitrakarn N, Golovatch SI, Panha S (2015) A checklist of the millipedes (Diplopoda) of Cambodia. Zootaxa 3973(1): 175–184. http://dx.doi.org/10.11646/zootaxa.3754.4.8

Liu W, Golovatch SI, Tian M (2017) Three new cavernicolous species of the millipede genus *Trichopeltis* Pocock, 1894 (Diplopoda: Polydesmida: Cryptodesmidae) from southern China. ZooKeys 710: 1–14. https://doi.org/10.3897/zookeys.710.20025

Pocock RI (1894) Chilopoda, Symphyla and Diplopoda from the Malay Archipelago. In: Weber M (Ed.) Zoologische Ergebnisse einer Reise in Niederländisch Ost-Indien. Vol. 3, 307–404.

Pocock RI (1895) The Myriopoda of Burma, Pt. IV. Report upon the Polydesmoidea collected by Sig. L. Fea, Mr. E. W. Oates and others. Annali del Museo Civico di Storia Naturale di Genova, Serie 2, 16: 1–48.

Rajulu SG (1970) A catalogue of Myriapoda of India. (Part I). Journal of the Madras University, Series B, 1: 111–149.

Shelley RM (2014) A summary of the milliped faunas of Pakistan, Bangladesh, and Kashmir (Arthropoda: Diplopoda). Insecta Mundi 0368: 1–7.

Verhoeff KW (1942) Über eine neue Familie der Polydesmoideen und die peripheren Zweige der Hypocephalia. Archiv für Naturgeschichte, NF 10(4): 431–442.

ZooKeys 725: 139–141 (2017)
doi: 10.3897/zookeys.725.23022
http://zookeys.pensoft.net

CORRIGENDA

A peer-reviewed open-access journal
ZooKeys
Launched to accelerate biodiversity research

Corrigenda: Polyphyly of the traditional family Flabellinidae affects a major group of Nudibranchia: aeolidacean taxonomic reassessment with descriptions of several new families, genera, and species (Mollusca, Gastropoda). https://doi.org/10.3897/zookeys.717.21885

Tatiana Korshunova[1,2], Alexander Martynov[2], Torkild Bakken[3], Jussi Evertsen[3], Karin Fletcher[4], I Wayan Mudianta[5], Hiroshi Saito[6], Kennet Lundin[7,8], Michael Schrödl[9,10], Bernard Picton[11,12]

1 *Koltzov Institute of Developmental Biology, RAS, 26 Vavilova Str., 119334 Moscow, Russia* **2** *Zoological Museum, Moscow State University, Bolshaya Nikitskaya Str. 6, 125009 Moscow, Russia* **3** *NTNU University Museum, Norwegian University of Science and Technology, NO-7491 Trondheim, Norway* **4** *Port Orchard, Washington 98366, USA* **5** *Universitas Pendidikan Ganesha, Bali, 81116, Indonesia* **6** *National Museum of Nature and Science, Amakubo 4-1-1, Tsukuba, Japan* **7** *Gothenburg Natural History Museum, Box 7283, S-40235, Gothenburg, Sweden* **8** *Gothenburg Global Biodiversity Centre, Box 461, S-40530, Gothenburg, Sweden* **9** *Zoologische Staatssammlung München, Münchhausenstr. 21, D-81247 Munich, Germany* **10** *Biozentrum Ludwig Maximilians University and GeoBio-Center LMU Munich, Germany* **11** *National Museums Northern Ireland, Holywood, Northern Ireland, United Kingdom* **12** *Queen's University, Belfast, Northern Ireland, United Kingdom*

Corresponding author: *Alexander Martynov* (martynov@zmmu.msu.ru)

Academic editor: *N. Yonow* | Received 14 December 2017 | Accepted 19 December 2017 | Published 29 December 2017

http://zoobank.org/0A02E6D3-970D-45D7-AB36-1E6A31B81CCD

Citation: Korshunova T, Martynov A, Bakken T, Evertsen J, Fletcher K, Mudianta IW, Saito H, Lundin K, Schröd M, Picton B (2017) Corrigenda: Polyphyly of the traditional family Flabellinidae affects a major group of Nudibranchia: aeolidacean taxonomic reassessment with descriptions of several new families, genera, and species (Mollusca, Gastropoda). https://doi.org/10.3897/zookeys.717.21885. ZooKeys 725: 139–141. https://doi.org/10.3897/zookeys.725.23022

In our recently published study the traditional Flabellinidae underwent a major revision and 17 new genera were proposed. The Abstract should read "17 new genera".

Immediately after publication our attention was drawn to homonymy of three generic names: *Borealia*, *Occidentella*, and *Orientella* with *Borealia* Maksimova, 1977, an extinct trilobite, *Occidentella* Hoffmann, 1929, a junior synonym of *Onchidella*, a pulmonate slug, and *Orientella* Repina & Okuneva, 1969, another extinct trilobite. In

a stroke of irony the two trilobite names were published in little known Russian journals, with Russian descriptions. To avoid homonymy, throughout the text, figures, and all supplementary materials replacement names for these three genera are as follows: *Borealea* Korshunova et al., nom. n., *Occidenthella* Korshunova et al., nom. n., and *Orienthella* Korshunova et al., nom. n. We are grateful to Jimmy Gaudin for alerting us to this unfortunate circumstance. Other corrections are as follows:

On p. 14 "…the same region our…" should be "…the same region as our…"
On p. 16 "…additional rows of of small…" should be "…additional rows of small…"
On p. 17 In the diagnosis of *Paracoryphella ignicrystalla* should be "…rachidian tooth with up to 15 denticles..."
On p. 18 "…cusp of nealy 1/3 of the tooth…" should be "…cusp of nearly 1/3 of the tooth…"
On p. 19 "…*Coryphella polaris* Voldochenko, 1946…" should be "…*Coryphella polaris* Volodchenko, 1946…"; "…(Figs 7, 10H, I)…" should be "…(Figs 7, 11H, I)…"; "…(Fig. 10G)…" should be "…(Fig. 11G)…"
On p. 26 Table 1. In fifth column: minimum uncorrected p-distances between *Coryphella verrucosa* and *Itaxia falklandica* should be 17.2%.
On p. 27 "…original description in Verril, 1880…" should be "…original description in Verrill, 1880…"; "…detailed redescripton in Kuzirian…" should be "…detailed redescription in Kuzirian…"
On p. 31 In the diagnosis of *Fjordia chriskaugei* should be "...orange-brown to reddish brown, sometimes blackish…"
On p. 33 In the diagnosis of *Fjordia lineata* should be: "…orange-brown to salmon, bright red, and dark brown, sometimes almost black..."
On p. 35 In the diagnosis of *Gulenia monicae* should be "...delineated from central cusp..."
On p. 37 In the diagnosis of *Gulenia orjani* should be "…delineated from central cusp..."
On p. 52 "…inclusion of *F. funeka* and *F. ishitana* is not…" should be "…inclusion of *F. funeka* and *F. ischitana* is not…"; "…and "*Piseinotecus" gabienerei* must be…" should be "…and "*Piseinotecus" gabinierei* must be…"
On p. 53 "…related to *Paraflabellina ishitana*…" should be "…related to *Paraflabellina ischitana*…"
On p. 54 "… (pleuroproctic in higher acleiproctic position)..." should be "…(pleuroproctic in higher acleioproctic position)…"
On p. 57 "…on distinct elonagate elevations…" should be "…on distinct elongate elevations..."; "… (pleuroproctic in higher cleiproctic position)…" should be "…(pleuroproctic in higher acleioproctic position)…"
On p. 58 In the diagnosis of *U. nihonrossija* should be "….apical parts of cerata without white pigment... rachidian tooth with up to seven denticles, central cusp without small denticles, double proximal receptaculum seminis…".
On p. 66 "…due to the lack of the morphlogical description…" should be "…due to the lack of a morphological description…"

On p. 68 "…always posses oral glands…" should be "…always possess oral glands…"
On p. 74 "…reduction of the triserial radula into a unserial one…" should be "reduction of the triserial radula into a uniserial one…"
On p. 79 Figure 3. Should be *Chlamylla borealis borealis* Bergh, 1886
On p. 91 "(Cothouy, 1839)" should be "(Couthouy, 1838)"

Supplementary material 2. *Chlamylla atypica* should read *Chlamylla borealis borealis* Bergh, 1886. Localities for *Himatina trophina* (Bergh, 1890) GQ292023 and *Microchlamylla amabilis* (Hirano & Kuzirian, 1991) GQ292022 should be "WA, USA".

References

Hoffman H (1929) Zur Kenntnis der Oncidiien (Gastrop. pulmon.) Ein Beitragzur geographischen Verbreitung, Phylogenie und Systematik dieser Familie. Zoologische Jahrbücher Abteilung für Systematik, Ökologie und Geographie der Tiere, Jena 57: 253–302.

Maksimova ZA (1977) Devonian trilobites from Novaya Zemlya and other regions of Soviet Arctica. Ezhegodnik vsesoyuznogo paleontologicheskogo obshestva [Yearbook of paleontological society of USSR] 20: 140–190. [In Russian]

Korshunova TA, Martynov AV, Bakken T, Evertsen J, Fletcher K, Mudianta W, Saito H, Lundin K, Schrödl M, Picton B (2017) Polyphyly of the traditional family Flabellinidae affects a major group of Nudibranchia: aeolidacean taxonomic reassessment with descriptions of several new families, genera, and species (Mollusca, Gastropoda). ZooKeys 717: 1–139. https://doi.org/10.3897/zookeys.717.21885

Repina LN, Okuneva OG (1969) Cambrian arthropods of Primorie. Paleontologichesky Zhurnal [Paleontological Journal] 1: 106–114. [In Russian]